THESIS FOR THE DEGREE OF DOCTOR OF PHILOSOPHY

Simulation model of a ship's energy performance and transportation costs

Fabian Tillig

Department of Mechanics and Maritime Sciences
CHALMERS UNIVERSITY OF TECHNOLOGY
Gothenburg, Sweden 2020

Simulation model of a ship's energy performance and transportation costs

FABIAN TILLIG

ISBN 978-91-7905-283-6

Doktorsavhandlingar vid Chalmers tekniska högskola
Ny serie nr 4750
ISSN 0346-718X

Department of Mechanics and Maritime Sciences
Division of Marine Technology
Chalmers University of Technology
SE-412 96, Gothenburg
Sweden
Telephone: + 46 (0)31-772 1000

Printed by Chalmers Reproservice
Gothenburg, Sweden 2020

Simulation model of a ship's energy performance and transportation costs

FABIAN TILLIG
Department of Mechanics and Maritime Sciences
Division of Marine Technology

Abstract

Society faces a major challenge to reduce greenhouse gas emissions to limit the effects and propagation of climate change. As the main contributor to global trade, the shipping industry adds significantly to global greenhouse gas emissions and must actively work towards reducing, or eliminating, emissions in a short period. This thesis contributes by developing a generic model for quick and accurate prediction of the fuel consumption of existing ships or newbuilds in operational conditions. The aim is to be able to predict the potential of fuel-saving measures, e.g., design features, retrofitting, alternative propulsion, and operational improvements, and evaluate the impact of such measures both, logistically and technically.

A novel energy systems model called "ShipCLEAN" was developed, which provides the opportunity to predict the propulsion power, fuel consumption, and daily costs and income of ships in realistic operational conditions, i.e., a wide variety of drafts, speeds, and environmental conditions. ShipCLEAN is a unique coupling of a generic power prediction model and a marine transport economics model. Aside from a calm-water power prediction based on empirical and standard series methods, the power prediction model includes simulating alternative propulsion methods (i.e., wind-assisted propulsion), respects all environmental loads acting on a ship at sea (e.g., wind, waves, current), is valid for multiple operational conditions (i.e., speed and draft of the ship), and balances the forces and moments in four degrees of freedom. Validation studies using five example ships (a container ship, a tanker, a cruise ferry, and two RoRo ships) show good agreement of the predicted propulsion power with both model tests in the design condition and full-scale measurements in variable operational conditions. A detailed uncertainty analysis provides an overview of how to further increase the prediction accuracy.

Special focus of the study is put on evaluating measures to decrease the emissions of ships through operational optimization, i.e., speed optimization, alternative propulsion concepts, and new design of zero-emission concepts. ShipCLEAN includes novel methods to evaluate the aerodynamic interaction effects of Flettner rotors on a ship (in between the rotors and between the rotors and the ship), to control the rpm of each rotor in an array on a ship and to evaluate the hydrodynamic forces acting on a ship sailing at a drift angle.

Results from application studies show that fuel savings of around 3% are achievable by optimizing the speed profile of a ship in operation. Wind-assisted propulsion shows the potential to save up to 30% of fuel if applied to a tanker on a Pacific Ocean trade. It is concluded that flexible power prediction models requiring limited input data help to identify and quantify potential fuel savings and to identify motivators for ship owners and operators to apply fuel-saving measures. Further, it is concluded that four degrees of freedom analysis and methods to respect aero- and hydrodynamic interaction effects are crucial to accurately predict the performance of wind-assisted propulsion.

Keywords: energy efficiency, energy systems model, performance prediction, ship design, speed optimization, wind-assisted propulsion.

Preface

This thesis presents research work carried out from 2014-2020 at the Division of Marine Technology, Department of Mechanics and Marine Sciences at Chalmers University of Technology. The work was partly funded by the Swedish Ship Owners' Association (through the Swedish Maritime Competence Center Lighthouse, 2016-2017) and the Swedish Energy Agency by the two projects "Energy efficient marine transport through energy systems analysis of ships" (2014-2015) and "ShipCLEAN - Energy efficient marine transport through optimization of coupled transportation logistics and energy systems analyses" (2017-2020).

I want to thank all partners in the ShipCLEAN project, for their contribution, for their input, and for fruitful meetings. Thanks also to my colleagues at the Division of Marine Technology for making it a nice place to work and for the discussions about shipping-related topics, skiing, sailing, and all the other relevant topics in life.

Special thanks to my supervisor Jonas W. Ringsberg for all the time spent on this thesis, the underlying work, and each of the publications. Thanks also for all the nice (and long) discussions about life in general. Your attention to detail and your will to help people, to motivate and to bring our division forward, are much appreciated, impressive, and much needed.

Finally, thanks to my family, especially Ronja and Pontus, for making my life as enjoyable and fun as it could be.

Gothenburg, May 2020

Fabian Tillig

Table of Contents

List of appended papers

Each of the five appended papers presents the development and application of the energy systems model "ShipCLEAN", a model designed, developed, and implemented by the author of this thesis. The contributions of the authors to each paper are specified below in the list of papers.

Paper A F. Tillig, J.W. Ringsberg, W. Mao and B. Ramne (2017). A generic energy systems model for efficient ship design and operation. *IMechE, Part M, Journal of Engineering for the Maritime Environment*, 231(2): 649-666.

Paper B F. Tillig, J.W. Ringsberg, W. Mao and B. Ramne (2018). Analysis of uncertainties in the prediction of ship's fuel consumption - from early design to operation conditions. *Ships and Offshore Structures*, 13(sup1): 13-24.

Paper C F. Tillig and J.W. Ringsberg (2019). A 4 DOF simulation model developed for fuel consumption prediction of ships at sea. *Ships and Offshore Structures*, 14(S1): 112-120.

Paper D F. Tillig, J.W. Ringsberg, H.N. Psaraftis and T. Zis (2020). Reduced environmental impact of marine transport through speed reduction and wind assisted propulsion. Submitted for publication in *Transportation Research Part D: Transport and Environment* (accepted for publication 2020-05-01).

Paper E F. Tillig and J.W. Ringsberg (2020). Design, operation and analysis of wind assisted cargo ships. Submitted for publication in *Ocean Engineering* (under review).

Authors' contributions (CRediT):

Fabian Tillig: Conceptualization, Methodology, Software, Validation, Formal analysis, Investigation, Resources, Writing - Original Draft, Writing - Review & Editing, Visualization, Project administration.

Jonas W. Ringsberg: Conceptualization, Resources, Writing - Review & Editing, Writing - Original Draft (papers A-D), Supervision, Project administration, Funding acquisition.

Bengt Ramne (papers A and B): Writing - Review & Editing, Supervision.

Wengang Mao (papers A and B): Writing - Review & Editing, Supervision.

Harilaos N. Psaraftis (Paper C): Writing - Review & Editing, Methodology (Transport economics).

Thalis Zis (Paper C): Writing - Review & Editing, Methodology (Transport economics).

List of other published papers by the author

For papers I and II listed below, the author of this thesis contributed to the ideas presented, planned the papers with the co-authors, performed the numerical simulations, and wrote most of the manuscript. Paper II presents the development of the energy systems model ShipCLEAN, a model developed and implemented by the author of this thesis.

For Paper III, the author of this thesis contributed with numerical simulations of the fuel consumption using ShipCLEAN.

Paper IV presents an extension of the ShipCLEAN model applicable to zero-emission ships. The author contributed with numerical simulation, ideas, and planned the paper with the co-authors.

Paper I F. Tillig, J.W. Ringsberg, W. Mao and B. Ramne (2015). Holistic ship energy systems modelling for efficient ship design and operation. *Proceedings of The RINA International Conference on Energy Efficient Ships.* 4 November, Rotterdam, The Netherlands. pp. 7-16.

Paper II F. Tillig, J.W. Ringsberg, H.N. Psaraftis and T. Zis (2019). ShipCLEAN - An integrated model for transport efficiency, economics and CO2 emissions in shipping. Editors: G. Theotokatos and A. Coraddu. *Proceedings of The 2nd International Conference on Modelling and Optimisation of Ship Energy Systems (MOSES2019)*. 8-10 May, Glasgow, Scotland UK. pp. 189-198 (MOSES2019-02013).

Paper III T. Zis, H.N. Psaraftis, F. Tillig and J.W. Ringsberg (2020). Decarbonizing maritime transport: A Ro-Pax case study. Submitted for publication in *Journal of Transport Geography* (under review).

Paper IV E. Luis, F. Tillig and J.W. Ringsberg (2020). Concept design and performance evaluation of a fossil free operated cargo ship with unlimited range. Accepted for the *International INNOV'SAIL2020* conference, 15-17 June, Gothenburg, Sweden.

Symbols and abbreviations

AP	Aft Perpendicular	[-]
AR	Aspect ratio	[-]
A_R	Rudder area	[m^2]
AR_E	Efficient aspect ratio	[-]
A_{Rotor}	Projected area of the rotor	[m^2]
AWA	Apparent wind angle	[deg.]
AWS	Apparent wind speed	[m/s]
B	Beam	[m]
c_B	Block coefficient	[-]
c_D	Drag coefficient	[-]
c_{DI}	Induced drag coefficient	[-]
CFD	Computational fluid dynamics	[-]
c_L	Lift coefficient	[-]
c_M	Main frame area coefficient	[-]
c_R	Residual resistance coefficient	[-]
c_P	Power coefficient	[-]
c_S	Side force coefficient	[-]
c_T	Thrust coefficient	[-]
c_{TH}	Propeller thrust coefficient	[-]
D	Drag force	[N]
D_h	Deck height	[m]
D_P	Propeller diameter	[m]
DOF	Degrees of freedom	[-]
F	Force	[N]
FP	Forward perpendicular	[-]
GM_0	Metacentric height	[m]
h	Height	[m]
H_S	Significant wave height	[m]
k	Ratio between AR_E and AR	[-]
k’	Cross flow drag coefficient	[-]
L	Lift force	[N]
L_E	Length of waterline entrance	[m]
L_{oa}	Length over all	[m]
L_{PP}	Length between perpendicular	[m]
L_{pr}	Bulbous bow length	[m]
L_{wl}	Waterline length	[m]
N_v	Linear part of the yaw moment coefficient	[-]
N_{vv}	Nonlinear part of the yaw moment coefficient	[-]
P	Power	[kW]
pdf	Probability density function	[-]
r	Radius	[m]
R_c	Radius of the vortex	[m]
R_R	Radius of the rotor	[m]
SR	Spin ratio	[-]
T	Thrust force	[N]
T_D	Draft	[m]
TWA	True wind angle	[deg.]
TWS	True wind speed	[m/s]
u_A	Wind speed	[m/s]
v	Speed	[m/s]
v_{des}	Design speed	[kn]
v_S	Ship speed	[kn]
$v_{Service}$	Service speed	[kn]
v_T	Tangential speed	[m/s]
β	Drift angle	[deg.]
Γ	Circulation	[m^2/s]
γ_R	Flow straightening coefficient	[-]
Δ	Displacement	[t]
δ	Rudder angle	[deg.]
ρ_{Air}	Air density	[kg/m^3]
ρ_{Water}	Water density	[kg/m^3]
φ	Heel angle	[deg.]
ω	Angular speed	[1/s]

1 Introduction

Society faces a major challenge to reduce the emission of greenhouse gases to limit the effects and propagation of climate change. As the main contributor to global trade, the shipping industry significantly contributes to global greenhouse gas emissions and must actively work towards reducing, or eliminating, emissions in a short period. This thesis contributes by developing a generic model for quick and accurate prediction of the fuel consumption of commercial ships at sea (both existing ships and newbuilds) and to evaluate the potential of fuel-saving measures, economically and technically. Special focus is put on accurately evaluating the impact of wind-assisted propulsion on the ship and the fuel consumption. Novel methods to capture the aero- and hydrodynamic interaction effects on a wind-assisted propelled ship are presented. The model is validated against full- and model-scale data from five ships: a tanker, a container ship, a cruise ferry, and two RoRo ships.

1.1 Background and motivation

The International Maritime Organization (IMO) defined the goal of halving greenhouse gas (GHG) emissions generated from shipping by the year 2050, compared to the levels of 2008 (IMO (2018)). To understand the impact of this target, it must be put in context of the annual growth of marine trade and the typical age of ships. As presented in Figure 1, between 2008 and 2019, marine trade has grown from about 40 000 billion ton-miles to more than 60 000 billion ton-miles, a growth of about 50% (UNCTAD (2019)). Regardless that the annual growth slowed down to less than 3% in 2019, marine trade is not expected to decrease in the next few years (UNCTAD (2019)).

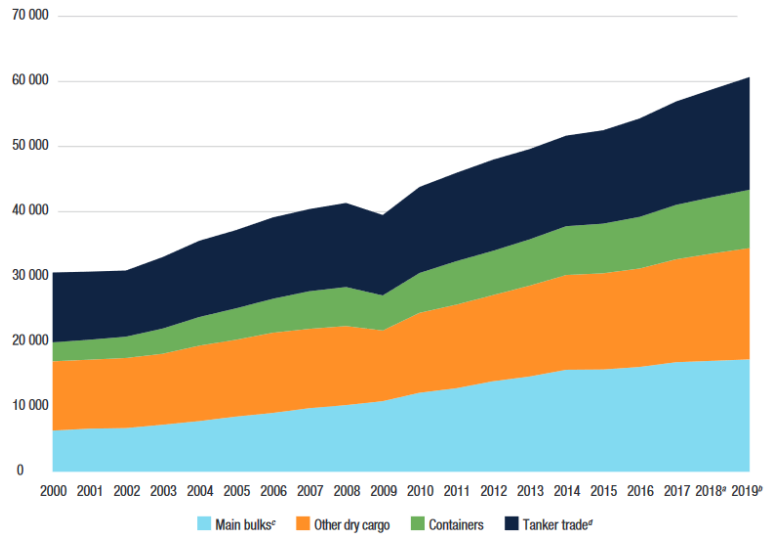

Figure 1: International maritime trade in cargo ton-miles (UNCTAD (2019)).

With a 50% growth of transported cargo (ton-miles) and a targeted reduction of fleets' GHG emission by 50%, a 66% reduction of emitted GHG per ton-mile must be achieved, even without any further growth of the maritime transport volume until 2050. Considering the average age of ships of about 21 years (UNCTAD (2019)), many ships built in or before 2019, which miss the targeted GHG emission reduction by a big margin, will still be operating in 2050. Thus, future newbuilds must far exceed the reduction of GHG emissions of 66% per ton-mile, preferably approaching zero emissions.

Such a decrease in GHG emissions is not achievable through classic design optimization, i.e., resistance, propulsion, and engine optimization. Instead, it is crucial to, apart from the classic design optimization, improve the performance of marine transport globally. Improvements can include alternative fuels for existing ships and newbuilds, e.g., synthetic or renewable fuels (Hansson et al. (2019)), alternative propulsion methods, e.g., wind propulsion (papers C, D, E, Viola et al. (2015), van Kolk (2019)) and wave propulsion (Bøckmann (2015)), as well as improvements of marine transport logistics, e.g., speed optimizations (papers A and D) and maximizing use (Varelas et al. (2013)). However, achieving the necessary reduction of GHG emissions while keeping the transport volume constant requires a radical change in ship design, operation, and marine transport logistics.

To predict potential GHG emission reductions by technical or logistical measures, models representing ships' energy systems are crucial. Such models must include modules for influences from ship design and operation, alternative propulsion, and environmental conditions. To face upcoming challenges, emissions from shipping and the effect of emission-reduction measures must be predictable for all ships in realistic conditions. However, for most cargo ships, detailed information is not publicly available; it is often not even available to the ships' owners and operators. Thus, models suitable for the upcoming challenges, i.e., a significant reduction of GHG emissions, must be quick, easy to use, accurate and applicable to a wide range of ships without adjustments or tuning, and without requiring detailed information about the ship. Further, such models must respect real-life environmental conditions, be able to model alternative propulsion methods, and must include marine transport logistics. This thesis presents a novel ship energy systems model, ShipCLEAN, fulfilling all the above requirements and thus providing a workbench to investigate potential emission and fuel consumption reduction from both technical and logistical measures.

1.2 Ship performance models

A ship is a complex energy system that is highly influenced by environmental conditions, especially wind and waves. An overview of the parts of a ship's energy system and the interaction in-between the parts is provided in Figure 2.

There is a wide range of ship performance models available, both commercially and academically, which aim to model the parts and interactions presented in Figure 2 to provide a prediction of the fuel consumption of a ship in realistic operational conditions. Generally, those models can be divided into two groups: (i) engineering-based models (white box), which aim to model the system's physics (for example Calleya (2014), Mermeris et al. (2011)), and (ii) machine learning models (black box), which rely on measurement data (for example Aldous (2015), Bialystocki and Konovessis (2016), Vinther-Hansen (2011)). While black-box models are limited to performance analysis because they require measurement data from the ship, white box models can also be applied in the design, re-design, or retrofitting of ships and propulsion systems. Alternative propulsion, as well as early design and fleet logistics optimization, are especially of interest to achieve the necessary GHG emission reduction (see Section 1.1). Thus, the further categorization and discussion only consider white-box models.

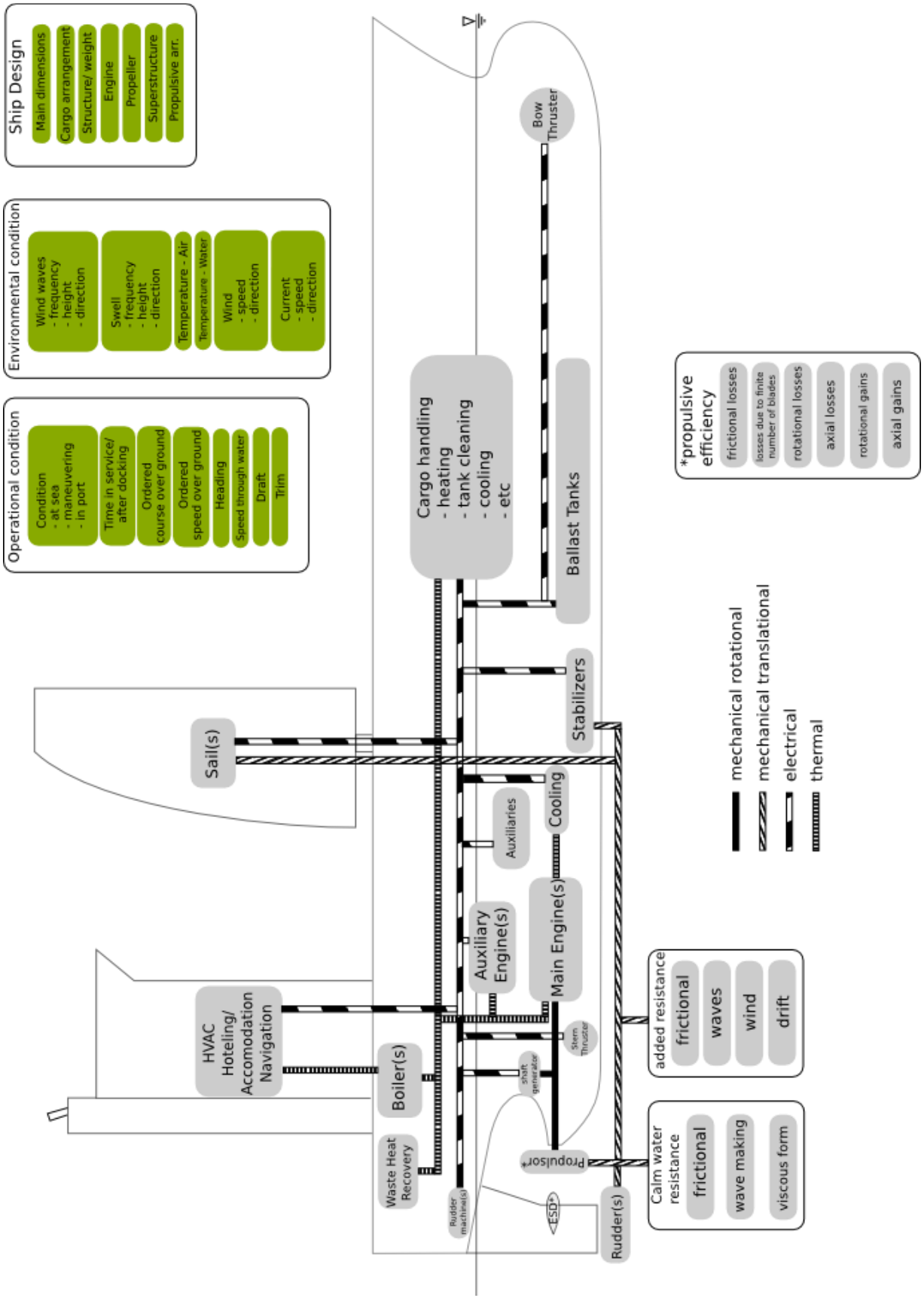

Figure 2: Parts and interaction of the parts of a ship's energy system (see Paper A).

To understand the difference and possible applications of existing white-box models, the following categorizations can be made to clarify their features: (i) the necessary input data to perform a simulation (e.g., ship dimensions, model test results, etc.), (ii) the considered degrees of freedom (DOF) (i.e., only thrust/resistance or even considering drift, yaw, etc.), and (iii) the dynamic effects that are considered (i.e., static, quasi-static or dynamic). Naturally, there are couplings between the different categorizations.

Category (i) – necessary input data

Table 1 presents four stages of models, which are defined using the necessary input data. Obviously, the achievable prediction accuracy of a white-box model depends on the Stage the model is developed for. While a Stage I model, for example, must include various methods to estimate missing dimensions and rely on empirical or standard series methods, a Stage IV model can be based on the ship's design using all available model test and CFD results, as well as possible full-scale measurements. This imposes different challenges in the model's development.

Table 1: Stages of available information for performance prediction models.

Stage	**Available information**
Stage I	Main dimensions (Loa, B, T, Δ, rpm, ship type, v_{design})
Stage II	Hull and propeller design
Stage III	Calm water model tests (resistance and propulsion)
Stage IV	Complete design information, including superstructure

The model presented in Calleya (2014) is reported to qualify as a Stage I model. However, it is based on standard ships where only small changes should be applied. The model presented in Mermeris et al. (2011) is a Stage II or III model, as it requires more information about the hull and propeller (to provide accurate predictions it even requires CFD or model test results). Over the past few years, virtual twin models have become popular, e.g., van Os (2018). Those models provide accurate predictions of the performance but require a huge amount of detailed information about the ship. Thus, all virtual twin models are Stage IV models.

With the increase in available information from Stage I to Stage IV and the applicability of more sophisticated prediction methods (e.g., model tests, CFD) once ship design details are known, naturally the prediction uncertainties decrease, i.e., the prediction accuracy increases. However, even Stage IV models have uncertainties in the prediction as a result of measurement and modeling uncertainties in model tests or CFD computations.

For the new design of ships, e.g., when details of the ship are not decided, only Stage I models are applicable. During the design process, when more information becomes available, more detailed models (Stage II to IV) can be used. However, the highest flexibility in the design of the ship is during the start of a project, where only Stage I models can be applied. Retrofitting of existing ships with energy-saving devices or alternative propulsion requires that the model can predict the effect of such measures on the ship's performance. Such methods can, in theory, be implemented in any type of white-box model.

Category (ii) – degrees of freedom

Performance prediction and analysis models for ships are often only considering 1 DOF (e.g., Calleya (2014), Mermeris et al. (2011), and Lu et al. (2015)), the surge direction. In Paper C, 1 DOF and 4 DOF methods are compared, showing that drift forces and yaw moments are considerable for high windage ships (e.g., PCTC or container ships) and especially when applying wind-assisted propulsion. Consequently, models developed to predict the effect of wind-assisted propulsion respect 4 DOF, e.g., van der Kolk et al. (2019), Viola et al. (2015).

Category (iii) – static, quasi-static or dynamic consideration

Most performance prediction and analysis models are quasi-static, i.e., the models capture the consequences of changes in the environment or operation of the ship but only evaluate the steady-state condition (e.g., Mermeris et al. (2011), Calleya (2014), van der Kolk et al. (2019), Viola et al. (2015)). These models neglect maneuvering, acceleration, and dynamic (i.e., ship motion) effects that occur during operation, for example in waves, but offer a robust and fast prediction and analysis of the performance of ships on a route or a longer period. Fully dynamic models require much shorter time steps and thus higher computational effort but give more detailed information about the system's behavior, for example, about the engine performance, e.g., as presented in Taskar et al. (2016).

Different objectives of existing white-box models

The different models in the literature emphasize on different objectives. As examples, Mermeris et al. (2011) focus on the hotel loads, Vinther-Hansen (2011) on performance analysis, van der Kolk et al. (2019) on the effect of wind-assisted propulsion, and Taskar et al. (2016) on the dynamics of the propeller and engine system on a ship in waves. However, the presented performance models do not include any logistical or economic models to evaluate the effects on the profit of a ship in service. Economy-focused discussions, as in van der Kolk et al. (2019), are limited to single cases.

1.3 Objectives and goals

Drastic measures (technically and logistically) must be taken to reduce GHG emissions from shipping. Performance models, as presented in Section 1.2, can contribute to reducing the emissions by providing the opportunity to evaluate the impact of measures taken on the fuel consumption and emissions from a ship or a fleet of ships. However, to achieve the targeted reduction of emissions, measures and the evaluation of possibilities cannot be limited to single ships with detailed information available. Instead, a suitable model must be able to evaluate the impact of emission reduction measures on the ship without requiring detailed information, measurement data or extensive modeling and calibration. From the discussion in Section 1.2, it can be concluded there is no Stage I model available today that includes all parts of ships' energy system, is flexible enough to apply to all cargo ships, combines performance modeling with economical modeling, and can accurately model the effects of alternative propulsion, e.g., wind-assisted propulsion. This thesis presents a ship performance and economics model targeted at filling this gap.

The main objective of the research presented in this thesis has been developing a quick, accurate, and easy-to-use Stage I power and fuel consumption prediction model, valid for commercial cargo ships with conventional propulsion with the possibility to model alternative propulsion methods, i.e., wind-assisted propulsion. A Stage I model is chosen because, as

discussed above, the necessary input information must be limited to provide the opportunity to evaluate fuel-saving measures on a broad range of ships or a fleet of ships. A suitable Stage I model shall not require calibration or modeling effort before providing an evaluation of the fuel consumption of ships in realistic conditions. However, the model must be flexible enough to provide the opportunity to use any data available to increase the prediction accuracy. Thus, the model must be engineering-based and a white-box model. Additionally, the model must be able to reflect the performance of ships in realistic operational conditions. Thus, it must predict the performance at a wide range of environmental and operational conditions (e.g., wind speed, wave height, ship speed, draft).

Another goal is that the model should be adapted to capture wind-assisted propulsion and model transport economics to present and evaluate measures (both technical and logistical) to reduce the environmental impact of shipping. Wind-assisted propulsion is seen as a promising, zero-emission, alternative propulsion method (see e.g., Rehmatulla et al. (2017), Ballnii et al. (2017), Talluri et al. (2018), Viola et al. (2015), van der Kolk et al. (2019)). Further, wind-assisted propulsion requires detailed modeling of aero- and hydrodynamic interaction effects for accurate prediction of the effects on a ship's fuel consumption and operation. Transport logistics and economics must be included to predict the impact of fuel-saving measures for ship owners and operators and to identify motivators to apply and install fuel-saving measures.

To quantify and increase the accuracy of the model's predictions, uncertainties should be identified and quantified. To increase the trustworthiness of the prediction, several questions must be investigated and answered. Questions of special interest in this thesis are:

(i) Is it necessary to model 4 DOF, i.e., surge, drift, yaw, and heel, and what is the difference in accuracy between 1 DOF and 4 DOF predictions?
(ii) Do aerodynamic interaction effects between Flettner rotors substantially affect the performance of wind-assisted propulsion?
(iii) How do simplified (Stage I) methods perform when validated against model and full-scale measurements and what is the prediction accuracy?

Apart from the model's development, a practical objective of this thesis is to investigate how wind-assisted propulsion can help reduce emissions from shipping and how ship design is influenced by wind-assisted propulsion.

1.4 Methodology, assumptions, and limitations

This thesis presents a summary of the development of a novel ship performance model called "ShipCLEAN". The model is an energy systems model including different methods to estimate ship dimensions, resistance, and propulsion coefficients, power increase as a result of environmental loads, drift, heel, and rudder angles, as well as wind-assisted propulsion including aerodynamic interaction effects. The model is programmed in MATLAB (Mathworks (2020)) and is component-based, i.e., alternative methods can easily be incorporated for each part of the energy system, e.g., if more detailed information becomes available. ShipCLEAN is foremost based on existing and validated methods in the literature instead of self-developed methods. The main developing work presented in this thesis is thus about evaluating, modifying, and extending those methods. In most modules, ShipCLEAN does not rely on only one method. Instead, several methods are (i) averaged or (ii) switched in between depending on the ship type, speed, dimensions, etc. Only if the existing methods prove to be inaccurate, insufficient, or simply not existing, are own methods developed. This is the case with: (i) the standard hull series to provide the wetted surface and the opportunity to perform CFD

calculations with limited information about the ship, (ii) the propeller standard series for a more modern design approach, (iii) the lift and drag for ships sailing at a drift angle, since existing methods proved inaccurate, and (iv) the method to evaluate the aerodynamic interactions on wind-assisted ships. A description of the model, the modules and the assumptions made for each module is presented in Section 2. Examples of limitations of the model and general assumptions in the model's development are presented below.

For a Stage I model such as ShipCLEAN, the main assumption is that the ship in question is a conventional ship, which can be evaluated with the underlying methods, especially concerning the resistance and propulsive efficiency. Special hull forms or special propulsors will require corrections to the used methods or the implementation of alternative methods. Special hulls (e.g., catamarans, swath, planning hulls) and propulsors (e.g., waterjets, surface-piercing propellers) have not been investigated, alternative methods to capture the hydrodynamics of such special designs have not been evaluated. However, as a result of the component-based architecture, it would be possible to incorporate special methods or use model test data for the prediction. The latter would, however, not qualify as a Stage I model.

Further, a Stage I model introduces some limitations owing to the nature of such a model. In general, only parameters that are an input to the model can influence the results. In this case, only the main dimensions and environmental conditions will influence the predicted power but not design features, e.g., bulbous bow form or special propellers. An exception is when other methods can alternatively be used, e.g., in ShipCLEAN, model test results can be used instead of the resistance and propulsion prediction with the empirical methods. However, concerning possible optimization studies, only the actual input data should be possible variables. The quasi-static nature of the model introduces the limitation that no maneuvering and acceleration/ deceleration are captured, which might lead to small deviations in predicting the fuel consumption over a full route.

As ShipCLEAN is based on several empirical, theoretical, and standard series methods, the model is only valid for the range of dimensions, ship types, and conditions for which the methods are valid. For ShipCLEAN, this means the model is assumed to be limited (and validated) for conventional cargo ships of any size traveling in normal service conditions, e.g., maximum wave heights of around 8 m. Exceeding such limitations will significantly decrease the prediction accuracy. Further, the engine model only includes fuel consumption curves for the standard fuel type for the selected engine types (e.g., heavy fuel oil for low rpm diesel engines). Alternative fuels require implementing special fuel consumption curves (see Section 2.8). The module for wind-assisted propulsion only considers Flettner rotors (see Section 2.7), methods for other sail types are under development, but not included in this thesis. Some methods are based on results (CFD or model tests) from one or a limited number of vessels, i.e., the decrease of propulsion efficiency in waves and the added resistance in ice. The accuracy of these methods when used for other ship designs or ship types is not tested individually. Especially, the validation of the performance loss in waves is complicated, as resistance and propulsive efficiency are difficult to separate in full-scale measurements. Additionally, accurate information about the wavelength and wave height is seldom available for full-scale measurements. In the study about zero-emission ships (see Section 4.4), modules for batteries, solar panels, wind turbines, and hydro turbines were developed. These modules have not been validated but are based on existing, validated methods, and data from manufacturers.

1.5 Outline of the thesis

This thesis is structured into six parts. The introduction in Section 1 is followed by a detailed description of the performance prediction model “ShipCLEAN” in Section 2. Section 3 presents an analysis of sources and quantification of uncertainties in the performance prediction, followed by a validation study using model- and full-scale measurement data. Finally, Section 4 presents applications of the model “ShipCLEAN” on wind-assisted propulsion, ship design, and speed optimizations. The conclusions and an outlook on future work are presented in sections 5 and 6, respectively.

2 The generic energy systems model – ShipCLEAN

As a Stage I model, ShipCLEAN was conceptualized following four criteria during the model's development:

- The input, i.e., required information about the ship, must be kept at a minimum, i.e., publicly available data such as the main dimensions.
- The model must be valid for a wide range of ships and environmental conditions (all commercial ships and normal operational conditions).
- The simulation and set-up time must be low, i.e., single point evaluations in real-life conditions must be provided in real time (less than 60 s).
- A prediction and operational simulation using a new ship shall not require any calibration or modification of the model.

To fulfill the above criteria, ShipCLEAN is a component-based model, divided into three parts: (i) a static power prediction part for calm water and trial conditions (see papers A and B), (ii) a dynamic operational analysis part, including added resistance and performance penalties as a result of e.g., fouling, wind, waves, drift, and ice, as well as analysis methods for wind-assisted propulsion (see papers C, D, E), and (iii) a transport economics part to evaluate the costs and income for a particular journey or over a longer time (see Paper D). ShipCLEAN requires only a few input parameters and no calibration to predict the propulsion power and fuel consumption of a ship at sea. With a simulation time per condition of about 10 seconds on a standard desktop computer for a full four degrees of freedom analysis of a wind-assisted propelled ship including rotor control and involuntary speed loss, ShipCLEAN offers fast predictions. An overview of the parts and modules of the model "ShipCLEAN" is provided in Figure 3. A summary of the details of the modules is presented in sections 2.2- 2.11.

In Table 2, the minimum required information for each part of ShipCLEAN is presented. In general, any available information more than the minimum required can be used to reduce uncertainties (see Section 3).

Table 2: Minimum required input for each part of ShipCLEAN.

		Minimum required input
I	Static part (power prediction)	L_{oa}, B, T_{des}, Δ_{des}, propeller rpm, ship type
IIa	Dynamic part (operational analysis)	Results from I, TWS, TWA, v_S, T or Δ, water depth, water temperature, fetch (for wave height computation)
IIb	Wind-assisted propulsion (Flettner rotors)	Same as IIa, number of rotors, size (18m x 3m, 25m x 5m, 30m x 6m), position on the ship (long. and transv.)
III	Economics model	Results from II, freight rate, fuel costs, utilization rate, cargo capacity, operational costs

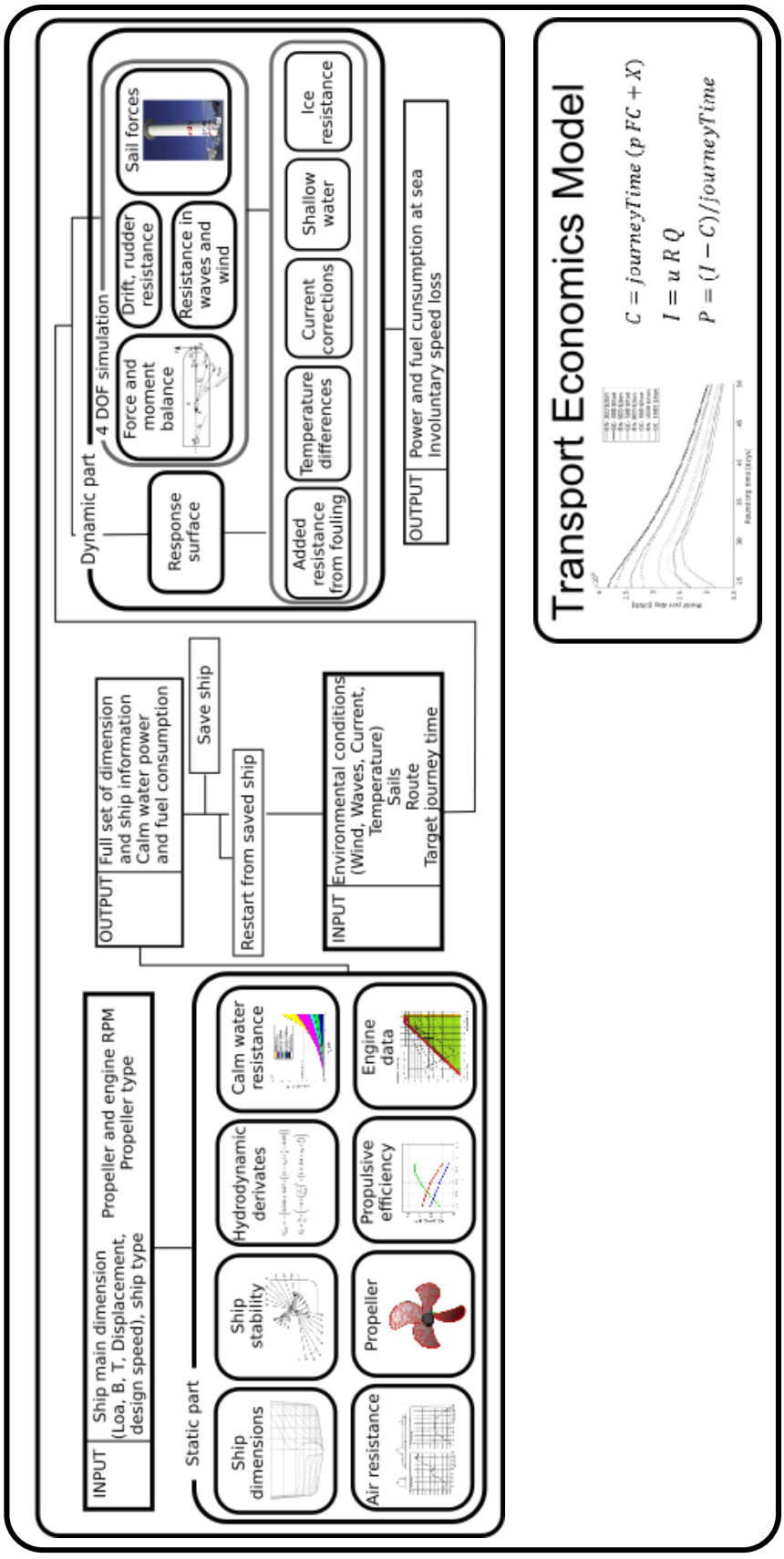

Figure 3: Overview of the parts and modules of the model “ShipCLEAN” (see Paper D).

The static performance prediction part (part I) follows the ITTC78 approach (ITTC (1999)) in the resistance and propulsive efficiency prediction, mainly because a Stage I model must rely on empirical methods. Such empirical methods are often based on model tests that follow the ITTC procedure. Details on the resistance and propulsion prediction are presented in Section 2.3, Tillig (2017), and in Paper A. To keep the required input at a minimum, numerous estimation formulas for ship dimensions are included in ShipCLEAN (see Section 2.2 and Tillig (2017) for details). The results of the static part are a full set of ship dimensions, a standard hull shape, a standard propeller matching the wake and rpm requirements, an engine diagram (including specific fuel oil consumption curves) and a design condition power prediction for calm water and typical contract conditions, i.e., 12 kn headwind, 2 m head waves (see Tillig (2017) and papers A and B).

The dynamic part (part IIa) and the wind-assisted propulsion part (part IIb) are built around the four degrees of freedom (4 DOF) module (see papers C-E), where the equilibrium of forces and moments is found in four directions (surge, drift, yaw, heel). Added resistance, decreased propulsion efficiency, and course deviations are evaluated as occurring as a result of waves, wind, currents, fouling, draft, shallow water, drift, rudder angle, and ice (see sections 2.4, 2.5 and 2.6). For the static case (which is evaluated in ShipCLEAN), all forces and moments acting on the ship must be in balance.

$$\sum F_X = \sum F_Y = \sum M_x = \sum M_z = 0 \tag{1}$$

As some forces and moments depend on each other, e.g., the rudder side force and drag on the propeller thrust (total resistance), the balance and solution of Equation (1) can only be found iteratively. Details on the 4 DOF method are presented in Section 2.6 and in papers C-E. The dynamic part also accounts for involuntary speed loss in case the torque/rpm combination is outside of the engine diagram (see Section 2.8). To provide the possibility to perform extensive studies using a large number of points with different environmental conditions, a response surface methodology is included in the model (see Section 2.10).

The results of the dynamic part are the required propeller power, main engine fuel consumption, drift angle, heel angle, rudder angle, and attained ship speed for each environmental and operational condition.

The third part, the transport economics model, is a cost-income analysis over some time using specified fuel prices, freight rates, and utilization rate (see Paper D and Section 2.11). The results of this part include the operational and fixed costs of the ship, as well as the income considering journey times and freight rates. From this, the journey and daily profit is computed.

2.1 Coordinate systems

In a 4 DOF model, the heading (HDG) and course through water (CTW) are not identical because the ship drifts. As some forces, e.g., the resistance, are acting along the ship's longitudinal axis (i.e., in HDG direction) and some in the direction or perpendicular to the CTW, e.g., the lift and drag because of drift, two coordinate systems are required. The coordinate systems, one ship (or HDG) fixed (x', y', z') and one flow-oriented (CTW) fixed (X, Y, Z), used in ShipCLEAN are shown in Figure 4. Both systems have their origins in the forward perpendicular, with the x-axis pointing aft, the y-axis to starboard, and the z-axis upwards.

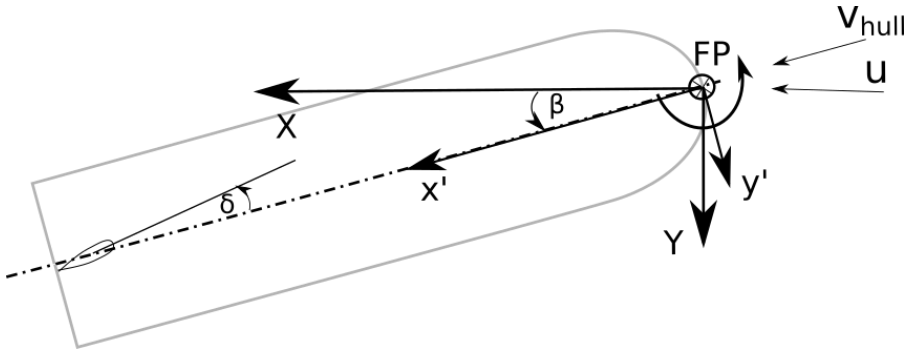

Figure 4: Coordinate systems in ShipCLEAN (see Paper E).

The force and moment balance in the 4 DOF part of ShipCLEAN is evaluated in the flow-oriented coordinate system, which requires the transfer of all forces and distances from the ship-fixed coordinate system to the flow-oriented coordinate system according to equations (2) to (4).

$$F_X = F_{x'} \cos\beta + F_{y'} \sin\beta \tag{2}$$

$$F_Y = F_{y'} \cos\beta - F_{x'} \sin\beta \tag{3}$$

$$F_Z = F_{z'} \tag{4}$$

2.2 Estimation of ship dimensions

The first fundamental module of ShipCLEAN calculates all ship dimensions that are required but not defined. The estimation formulas used in ShipCLEAN are compiled in Table 3. In Table 3, the estimation of ship dimensions is based on ships with a bulbous bow. However, typical cargo ships operate in a speed range where the performance of ships with and without a bulbous bow, but with identical wetted length (i.e., the length of the submerged hull), is expected to be similar (Schneekluth and Bertram (1998)). Thus, the power prediction is expected to be valid for straight stem ships, as well as ships with bulbous bow, although the L_{pp} is calculated assuming a bulbous bow.

Table 3: Estimation formulas for ship dimensions.

Estimation formula	Reference
Main dimensions	
$L_{pr} = 0.025\, L_{oa}\ [m]$ (Tanker/Bulker) $L_{pr} = 0.04\, L_{oa}\ [m]$ (Other)	(Estimation by the author of this thesis)
$L_{pp} = 0.98\, L_{oa} - L_{pr} [m]$	(Estimation by the author of this thesis)
$L_{wl} = L_{oa} - L_{pr}\ [m]$	-
$c_B = \frac{\Delta}{1.025\ (L_{pp}\ B\ T)} [-]$	-

$c_M = 0.93 + 0.08\, c_B[-]$		Schneekluth and Bertram (1998)
$c_P = \frac{c_B}{c_M}\ [-]$		-
$c_{WP} = 0.763\ (c_P + 0.34)[-]$		Bertram and Wobig (1999)
$L_E = 6.3\, Fn_{des}^2\, L_{pp}[m]$		Schneekluth and Bertram (1998)
$A_R = 0.036\, L_{pp}\, T_{des}[m^2]$		Schneekluth and Bertram (1998)
$D_h = 0.087\, L_{pp}\ [m]$		Bertram and Wobig (1999)
Propeller dimensions		
$D_P = 0.75\, T_{des}\ [m]$ (initial) $D_P = 1.524 \left(0.385662 \frac{\left(\frac{P_{E-des}}{0.7}\right)^2}{n^6} \right)^{0.1} (1.146 - 0.073)Z - 2) + 0.085\ (Z-2)(Z-4)\ [m]$ (final) $D_P \leq\ T_{des} - 1\ [m]$		MAN (2013) Kracht (2000)
$T_P = \frac{R_{des}}{(1-t)n_{propeller}}\ [kN]$		-
$\frac{A_e}{A_0} = \frac{(1.3 + 0.3\, Z)T_P}{(p_0 - p_v) * D_P^2} + 0.15\ [-]$		Holtrop (1977)
Superstructure dimensions		
$H_{super} = 24 + 2\ [m]$ $H_{super} = 15 + 2\ [m]$ $H_{super} = 12 + 2\ [m]$	($L_{pp} > 100$ m, PCTC) ($L_{pp} > 100$ m, other) ($L_{pp} \leq 100$ m)	(Estimation by the author of this thesis)
$B_s\ = B\ [m]$ $B_s = 30\ m$	 ($B > 30\ m$, Tanker, Bulker)	(Estimation by the author of this thesis)
$L_s = L_{pp}/2\ [m]$ $L_s = L_{pp}\ [m]$ $L_s = \frac{L_{pp}}{7}, L_s \leq 30\ [m]$	(RoRo) (Cruise ship, container, PCTC) (Other)	(Estimation by the author of this thesis)

2.3 Calm-water power prediction

In ShipCLEAN, the prediction of the calm water propulsion power follows the principles of model test evaluations described in ITTC (1999). The calm water propulsion power, P_D, of ships can be expressed by:

$$P_D = \frac{P_E}{\eta_D}\, v_S \tag{5}$$

with the effective power, P_E, as:

$$P_E = \frac{1}{2}\rho\, c_T\, S\, v_S^2 \tag{6}$$

The unknown propulsive efficiency η_D, total resistance coefficient c_T, and wetted surface S in equations (5) and (6) are estimated using empirical formulas, as well as hull and propeller standard series (see papers A and B for details). As discussed earlier, any information, e.g., hydrostatics or model test results, can be used if available because of the component-based approach.

The wetted surface is as standard computed using the numerical hull standard series, several fully parametric hull models, as described in Tillig (2017). Five different models, for different ship types, are available: (i) full block, single skeg ships, (ii) full block twin skeg ships (iii) slender single skeg ships, (iv) slender twin skeg ships, and (v) slender twin skrew (open shaft) ships. The transition between slender and full block ships is set around $c_B = 0.75$, depending on the ship type. It is found that the wetted surface from the standard series agrees well with actual data from existing ships. However, the boundaries of the standard series are narrower than those of empirical formulas as from Kristensen and Lützen (2012) or Hollenbach (1998). For full block ships, the average of the above methods shows good agreement with the standard series (less than 2% difference) while the wetted surface of slender ships is typically underestimated by 5%. For robustness and flexibility of the model, the adjusted and averaged results from the empirical formulas might as well be used instead of the (more accurate) computation using the standard hull series.

The resistance coefficient c_T is decomposed into two parts: the frictional resistance coefficient c_F and the residual resistance coefficient c_R. In ShipCLEAN, the three-dimensional viscous part, which is often estimated using a form factor k, is included in the residual resistance coefficient. As most empirical methods for calculating resistance are only valid for the design speed, the residual resistance coefficient is evaluated in two steps. At first the resistance coefficient at design speed is evaluated using an average of the results from the estimation methods presented in Kristensen and Lützen (2012) and in Hollenbach (1998). In the second step, the residual resistance in off-design speeds is estimated using generic curves related to the residual resistance coefficient at design speed, as presented in Figure 5. The curves presented in Figure 5 are based on CFD computations using the standard series hulls and modifications of those hulls with large gooseneck bulbous bows (see Tillig (2017) for details about the standard hull series).

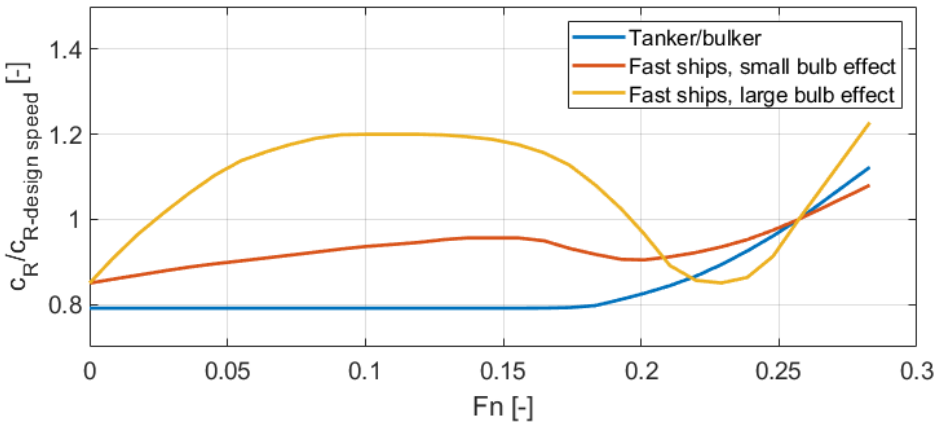

Figure 5: Different c_R curves for the resistance prediction.

For standard cases, two different c_R curves are used, one for slower ships without a bulb effect (blue curve in Figure 5) and one with a moderate bulb effect for faster ships (red curve in Figure 5). Additionally, a c_R curve with a large bulb effect is available in ShipCLEAN that can be used for ships with large bulbs, optimized for a single speed (yellow curve in Figure 5). The bulb effect describes the increase of the c_R at lower speeds as a result of unfavorable wave patterns created by the bulbous bow. Ships without bulbous bow are assumed to have no (tankers, bulkers) or small (faster ships) bulb effects.

The propulsive efficiency is divided into two parts, the propeller open water efficiency and the hull efficiency. To estimate the propeller thrust and advance ratio, the effective wake and thrust deduction must be evaluated. The average of five empirical methods is used to predict the efficient wake of single and twin skeg ships, i.e., the methods developed by Harvald (Kristensen and Lützen (2012)), Schneekluth, Krüger, Heckscher and Troost (Schneekluth and Bertram (1998)). All the methods deliver high values of the efficient wake, especially for slender ships. Thus, the recommendation given in Kristensen and Lützen (2012) to reduce the wake fraction by 30% is followed for slender ships. For high blockage ships, such as tankers and bulkers, the wake is reduced by 5%. Twin screw (open shaft) ships have a much lower wake fraction. In ShipCLEAN the effective wake of twin-screw ships is evaluated using the same methods as for single and twin skeg ships, but with a reduced block coefficient to the value:

$$c_{Bcorr} = 0.4 + (c_B - 0.4)/2 \tag{7}$$

Equation (7) is based on the author's experience and assumes the efficient wake of a ship with a block coefficient of 0.4 is similar for ships with open shafts and skegs and much slower increasing with the block coefficient. With this method, typical open shaft ships, such as ferries and RoRo ships with block coefficients of around 0.7, are estimated to have an effective wake of about 0.15 to 0.2, which is reasonable when compared to existing ships.

As the prediction of the thrust deduction is difficult, an estimation of the hull efficiency based on the ship type and block coefficient does reduce uncertainty. For open shaft ships, the hull efficiency is set constant to be equal to η_H=1.05 while the hull efficiency for all other ships is estimated according to Equation (8). Equation (8) is the author's estimation to provide hull efficiencies between 1.05 for slender ships and about 1.14 for high blockage ships.

$$\eta_H = 1.05 + 0.2\,(c_B - 0.4) \tag{8}$$

As the effective wake, w_e, is estimated using empirical formulas (see Paper B), the thrust deduction can be computed using Equation (9).

$$1 - t = \eta_H \, (1 - w_e) \tag{9}$$

For some ships with low effective wake, this method will result in low, unrealistic, thrust deduction numbers. Thus, a lower limit of the thrust deduction of 0.1 is ensured by lowering the hull efficiency accordingly for such ships.

The propeller open water efficiency is evaluated using the propeller standard series developed for ShipCLEAN (see Tillig (2017) for details) and the lifting line evaluation software OpenProp (Epps et al. (2009)).

With all information at hand, the propulsive performance is evaluated using the ITTC 78 method (ITTC (1999)). The same method is employed for off-design conditions, i.e., for conditions with increased or decreased propeller load, as described in the following sections.

2.4 Draft and trim influences

As cargo ships operate at different loading conditions (trim and draft), it is necessary to compensate for the power difference as a result of off-design loading conditions. Draft changes will not or only slightly affect the propulsive efficiency if the propeller is fully immersed in the water and not sucking air. Trim changes will most likely affect the propulsive coefficients; however, no general methods to evaluate these effects are available. In the design condition, the trim is often small (less than 0.1 m) and thus the influences on the propulsive efficiency and resistance will be small. Larger trim is often experienced in ballast drafts. However, in the ballast draft, the propeller is much less loaded, which will also influence the thrust deduction positively. Hence any negative effects from the trim can be (at least partly) compensated by higher hull efficiency. In fact, the propulsive efficiency in the ballast draft is often close to the propulsive efficiency in the design draft (Schneekluth and Bertram (1998)). Thus, it is assumed that only the resistance, but not the propulsive efficiency, is affected by draft and trim changes.

In Hollenbach (1998), a method for estimating the residual resistance at ballast drafts is presented. This method is used in ShipCLEAN for displacements of maximum 80% of the design displacement. In contrast to the evaluation of the resistance at the design draft, no averaging of results from different methods is performed for the ballast draft. However, many ships operate on intermediate drafts, sometimes combined with a trim. Effects from draft differences are captured in two ways, (i) the wetted surface is adjusted and (ii) the residual resistance coefficient is adjusted. The difference in wetted surface is estimated using the admiralty formula:

$$S = S_{design} \left(\frac{\nabla}{\nabla_{design}} \right)^{2/3} \tag{10}$$

The relationship between the residual resistance coefficient in design and off-design draft depends on the design of the bulbous bow. Two curves of the relative c_R are defined in ShipCLEAN, one for ships without or with moderate bulbs, e.g., tankers and bulkers, and one with normal designed bulbs, optimized for the design draft, e.g., ferries and RoRo ships. The curves are presented in Figure 6. It must be noted that these curves are adjusted to match the ballast c_R evaluated with the method from Hollenbach (1998). In Figure 6, it is assumed that the ballast c_R is equal to the design c_R. The curves show it is assumed that the c_R stays almost

constant for ships without bulbous bows but increases considerably with decreasing draft for ships with design draft-optimized bows. These curves are a general approximation based on CFD computations with the standard series hulls (see Tillig (2017)) as the real relationship between the c_R and the draft depends on the hull form features, e.g., bulb shape, as well as transom shape and height.

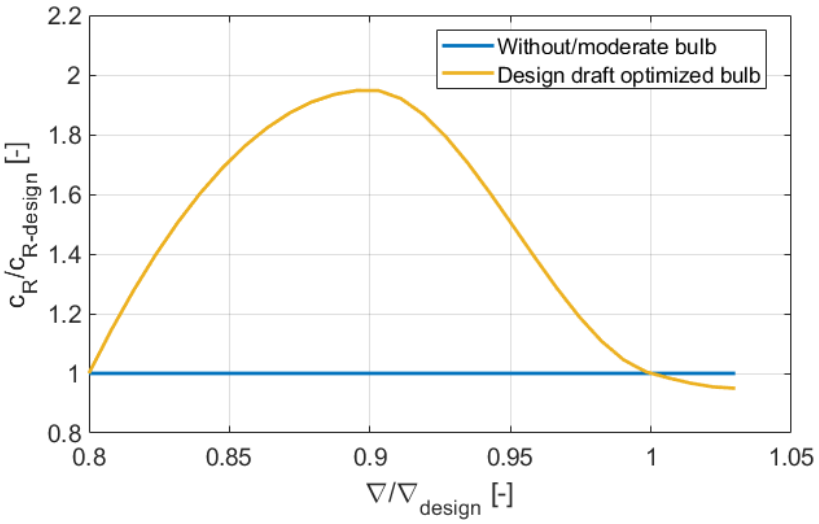

Figure 6: Relative c_R for off-design conditions.

Changes in the resistance because of trim are not considered in ShipCLEAN, as the influence on the resistance is difficult to capture in a generic model. One possibility to include trim in the model would be to combine the trim and draft changes and create c_R curves based on the forward and aft draft, thus considering influence from the bulbous bow and the transom immersion. However, specifying such curves will require more test data on trim optimization, which are seldom performed, or extensive CFD computations. Further, such influences are more of interest for detailed operational analysis, which can be performed with higher accuracy if Stage III or IV models are used where model tests or CFD computations at different trim angles and drafts could be included. For a Stage I or II model, it can be assumed that the ship is operated on a favorable trim for the actual draft and additional influence from the trim can be neglected.

2.5 Environmental loads

A ship at sea experiences increased resistance as a result of several environmental influences. In ShipCLEAN, the influences from wind, waves, fouling, water depth, ocean current, and ice are respected. Details on the different methods are presented in Paper B and the references presented in Table 4. While some environmental influences only create additional resistance, some others (especially the wind) create side forces for which the ship must compensate using a drift and rudder angle. Methods to include the impact from drifting and steering of the ship are described in detail in Section 2.6 and Paper E. An overview of the methods used to predict the impact of environmental conditions and hull fouling on the performance of a ship is provided in Table 4.

Table 4: Methods used in ShipCLEAN to estimate the impact of environmental influences on a ship's performance.

Environmental influence	**Method**
Fouling	SSPA roughness database (SSPA (2020))
Ice	Li et al. (2019)
Ocean current	Trigonometric correction of the heading and speed through water
Water depth	ITTC (2014)
Waves	Stawave2 (ITTC (2014)), Liu et al. (2016), Taskar et al. (2016)
Wind	Blendermann (1993)

Influences from fouling are only considered as increased resistance of the hull, but not decreased propeller performance. The effect of propeller fouling is much more complicated as it does not only affect the frictional section drag and thus torque of the propeller, but a rough blade surface also decreases the sectional lift and thus the thrust of the propeller (Abbot and Doenhoff (1959)). This would not only require a decrease of the propeller efficiency in the model but an adaption of both the torque and thrust curves of the propeller. To estimate propeller fouling from full-scale measurements, it is necessary to measure the rpm, torque, and thrust on the propeller shaft. As the thrust measurements are complicated and seldom performed, it is often not possible to accurately estimate propeller fouling from full-scale measurements. Fouling on the propeller is not included in ShipCLEAN, even though the thrust and torque curves of the propeller can easily be modified in ShipCLEAN if methods to evaluate the changes as a result of fouling become available. Additionally, it is not modeled how the hull fouls over time. Thus, input following the classification of fouling according to SSPA (2020) is required. In general, it could be questioned if Stage I models need to model fouling, as this is more a topic of performance analysis, i.e., more focus on Stage IV or digital twin models. However, as presented in Section 4.1, decreased performance because of fouling can influence the economics and thus lead to different results in optimization and variation studies, e.g., speed optimizations. Thus, hull fouling is a good feature of a Stage I model to run scenario-based simulations but does not have to be as sophisticated as it must be for performance analysis (i.e., Stage IV) models.

The influence of waves on the performance of a ship is that they not only increase the resistance but also decrease the propulsive efficiency. The resistance increase is accounted for using the average of the methods from ITTC (2014) and Liu et al. (2016) adjusted with an angular function to account for oblique waves according to results presented by Tsujimoto et al. (2008). A decrease of propulsion efficiency is observed on ships sailing in waves. This decrease can be divided into (i) an increase of the wake, (ii) decrease of the hull efficiency, and (iii) change of propeller open water efficiency as a result of the change in wake fraction (Taskar et al. (2016)). There are analytical/ empirical methods to determine the increased wake available (Faltinsen et al. (1980), Taskar et al. (2016)). However, all methods require the pitch motion of the ship, which is not estimated in ShipCLEAN. This is why such methods are not applicable. In Faltinsen et al. (1980), it is discussed that the thrust deduction follows the change in wake fraction, keeping the hull efficiency close to constant. However, the propeller will encounter

thrust losses when emerging out of the water and after re-entrance (Minsaas et al. (1983)), which can be reflected by a decrease in hull efficiency, as shown by Taskar et al. (2016). To include the effects of decreased propulsive efficiencies, the curves for different wave heights, wave lengths, and for wave angles of 0 degrees and 45 degrees presented in Taskar et al. (2016) are used in ShipCLEAN. In beam and following waves the effect was reported to be small (Taskar et al. (2016)) and thus assumed to be zero in ShipCLEAN. The values for the increase of the wake and decrease of the hull efficiency are presented in Table 5. As it is presented in Table 5, no changes in the propulsive coefficients are applied in waves shorter or equal to 0.6 L_{pp}. It must be noted that the values for higher or longer waves are not extrapolated, but the values for 5m wave height and a wavelength of 1.6 L_{pp} are used. Changes for smaller waves are linearly interpolated assuming no change at zero-meter wave height.

Table 5: Deviations of propulsive factors for a ship sailing in waves.

Wavelength over L_{pp}	[-]	0.6		1.1		1.6	
Encounter angle	[deg]	0	45	0	45	0	45
3 m wave height							
$w_e/w_{e\text{-calm water}}$	[-]	1	1	1.02	1.01	1.02	1.01
$\eta_h/\eta_{h\text{-calm water}}$	[-]	1	1	0.97	0.98	0.96	0.97
4 m wave height							
$w_e/w_{e\text{-calm water}}$	[-]	1	1	1.03	1.02	1.03	1.02
$\eta_h/\eta_{h\text{-calm water}}$	[-]	1	1	0.95	0.97	0.94	0.95
5 m wave height							
$w_e/w_{e\text{-calm water}}$	[-]	1	1	1.04	1.03	1.04	1.03
$\eta_h/\eta_{h\text{-calm water}}$	[-]	1	1	0.91	0.95	0.91	0.92

2.6 Drift, yaw, and heel

To compensate for the aerodynamic side forces, especially when applying wind-assisted propulsion, the ship drifts and heels, making it necessary for a performance prediction model to include 4 DOF. To respect 4 DOF, it is crucial to accurately predict the lift and drag forces of a hull sailing at a drift angle. Additionally, the center of the lateral resistance, i.e., the longitudinal position where the lift and drag forces act on the hull, is important for accurately predicting the rudder angle. In ShipCLEAN, low aspect ratio wing theory is employed to estimate the lift and drag forces. Details about the method can be found in Paper E.

The lift and drag coefficient (in the flow-oriented coordinate system) are evaluated by (see Paper E):

$$c_L = 0.8\, 0.5\, \pi\, AR \sin\beta + 0.6541 \sin\beta \sin|\beta| \cos\beta \tag{11}$$

$$c_{Di} = 0.66\, c_L |\beta|^{0.6} + 0.6541 \sin^3|\beta| \tag{12}$$

The center of effort is evaluated using the empirical method presented in Inoue and Hirano (1987):

$$CoE = \frac{N_h}{Y_h} L_{PP} = \left(\frac{N_v}{Y_v} \sin|\beta| + \frac{N_{vv}}{Y_{vv}} (sin\beta)^2\right) L_{PP} \tag{13}$$

$$N_v = 2\,\frac{T}{L_{pp}} \tag{14}$$

$$N_{vv} = 0.066 - 0.96\,(1 - c_B)\frac{T}{B} \tag{15}$$

$$Y_v = \pi\,\frac{T}{L_{pp}} + 1.4\,c_B\,\frac{B}{L_{pp}} \tag{16}$$

$$Y_{vv} = 0.244 + 6.67\,((1 - c_B)\frac{T}{B} - 0.05) \tag{17}$$

As the aero- and hydrodynamic force centers are normally not at the same longitudinal position, a yaw moment is introduced, which must be compensated by a rudder angle. The rudder lift and drag forces are evaluated according to the method presented in Schneekluth and Bertram (1998).

$$x'_R = c_D v_s^2 \frac{\rho}{2} A_R + T\left(1 + \frac{1}{\sqrt{1+c_{Th}}}\right)(1 - \cos\delta_R) \tag{18}$$

$$y'_R = c_L v_s^2 \frac{\rho}{2} A_R + T\left(1 + \frac{1}{\sqrt{1+c_{Th}}}\right) sin\delta_R \tag{19}$$

$$c_L = 2\pi \frac{AR\,(AR+0.7)}{(AR+1.7)^2} sin\delta_R + sin\delta_R|sin\delta_R|cos\delta_R \tag{20}$$

$$c_D = \frac{c_L^2}{\pi * AR} + |sin\delta_R|^3 \tag{21}$$

Owing to the ship's hull and aftbody skegs, the inflow to the rudder is not following the direction of the free inflow but is straightened towards the longitudinal axis of the ship. The inflow angle to the rudder can be evaluated by:

$$\delta_R = \delta - \gamma_R \beta \tag{22}$$

$$\gamma_R = -22.2\left(c_B \frac{B}{L_{PP}}\right)^2 + 0.02\left(c_B \frac{B}{L_{PP}}\right) + 0.68 \tag{23}$$

The proposed method showed significantly better agreement with CFD and model test results than other empirical methods developed for maneuvering prediction, see papers B and E. Further on, the method does not require more dimensions or input than available for a Stage I model, such as ShipCLEAN.

2.7 Wind-assisted propulsion

To reduce emissions from shipping significantly, alternative propulsion systems must be introduced. As it is discussed in Section 1.1, wind-assisted propulsion can be such an alternative. However, wind-assisted propulsion significantly changes how a ship's performance must be analyzed. While for conventional propulsion it is often enough to perform a force balance in longitudinal (surge) direction, it is necessary to perform a multi-dimensional force and moment balance for wind-assisted ships because sails introduce large side forces and yaw moments. The 4 DOF method is described in Section 2.6. Additionally, the aerodynamics become important as a result of interaction effects between the sails and between the sails and the superstructure. The method used to estimate the interaction effects between the sails and the sails and the ship structure is explained in detail in Paper E.

ShipCLEAN includes lift, drag and power consumption coefficients for Flettner rotors. Flettner rotors are chosen as a start for several reasons:

(i) Flettner rotors produce high lift forces that reduce the required sail area, i.e., the required deck area and sail height.
(ii) Flettner rotors are easy to operate and automize; thus, they are easy to operate for a small crew.
(iii) Flettner rotors are not sensible to the angle of attack (as other sails), thus periodic and dynamic effects from rolling, pitching and unsteady/turbulent inflow must not be considered.
(iv) Flettner rotors are well-investigated in literature.
(v) Full-scale measurements were available from a cruise ferry equipped with a Flettner rotor, offering validation possibilities, see Section 3.3.2.

The spinning rotors introduce circulation in the airflow, which, as a result of the air velocity difference, creates a pressure difference and lift force fulfilling the Kutta-Joukowski equation (see Paper E and Abbot and Doenhoff (1959)). In general, the lift generation of Flettner rotors is not different from other sail types other than that the circulation is initiated by the rotation of a cylinder instead of vortex separation at the trailing edge of a wing. This is why the sail module may be extended to other sail types. However, theoretically evaluating the lift force of the three-dimensional wings or rotors is complex and time-consuming. Thus, ShipCLEAN uses lift and drag relations presented in the literature. The basis to evaluate the performance of sails are curves of the lift and drag coefficients based on the angle of attack (conventional sails) or the spin ratio (SR) (Flettner rotor). With the apparent wind angle (AWA) the lift and drag coefficients can be translated into thrust and side force coefficients. As Flettner rotors consume energy, curves for the power coefficient must be included and the consumed power is added to the propeller thrust to be delivered from the main engine. This procedure assumes the use of shaft generators to provide the power to rotate the rotors. The definition of the lift (c_L), drag (c_D), thrust (c_T), side force (c_S), and power coefficients (c_P) are shown in Equation (23).

$$c_i = \frac{F_i}{0.5\ \rho\ A\ AWS^2}, i = L, D, T, S; c_P = \frac{P_{rotor}}{0.5\ \rho\ A\ AWS^2} \tag{24}$$

For Flettner rotors, the spin ratio, lift, drag, and power coefficients are estimated by (see Paper E):

$$SR = \frac{v_T}{AWS} = \frac{\omega\ R_R}{AWS} \tag{25}$$

$$c_L = -0.0046\,\mathrm{SR}^5 + 0.1145\,\mathrm{SR}^4 - 0.9817\,\mathrm{SR}^3 + 3.1309\,\mathrm{SR}^2 - 0.1039\,\mathrm{SR} \quad (26)$$

$$c_D = -0.0017\,SR^5 + 0.046\,SR^4 - 0.44\,SR^3 + 0.724\,SR^2 - 1.64\,SR + 0.638 \quad (27)$$

$$c_P = 0.0001\,SR^5 - 0.0004\,SR^4 + 0.0143\,SR^3 - 0.0168\,SR^2 - 0.0234\,SR \quad (28)$$

The true wind speed (TWS) profile over the height above the water surface and the deck is captured by (see Paper E):

$$TWS(h) = TWS_{10}\left(\frac{h}{h_{10}}\right)^{0.27} \quad (29)$$

Equation (29) assumes that a boundary layer is developed above the ship deck. To evaluate the wind speeds above the deck, the speed at deck height is assumed to be zero. At 10 m above the deck, the wind speed is assumed to be equal to the wind speed at a corresponding height (10 m + deck height) above the sea surface. The lift, drag, and power consumption are evaluated at different heights (10 as a standard in ShipCLEAN) and different rpm. The optimal rpm is found as the maximum net power (propulsion power – consumed power) summed up over all heights. The Hellman coefficient of 0.27 corresponds to stable air above the sea surface and unstable air above the deck (see Paper E for a more detailed discussion and a verification of the force and power coefficients using model test, CFD, and full-scale measurement results).

Aerodynamic interaction effects are divided into potential and viscous effects. Potential flow interaction caused by the bound vortex is captured by analytically solving the Navier-Stokes equation for potential flow, assuming that (i) the induced velocity from the sails at infinity is equal to zero, and (ii) the induced angular speed at the sails surface is equal to the angular speed caused by the circulation (Γ) creating the lift of the sail. The inducted velocity (v_T) can be computed by (see Paper E):

$$v_x(x,y) = \frac{v_T R_R}{\sqrt{x^2+y^2}}\cos\left(\arctan\left({}^{y}/_{x}\right)\right) \quad (30)$$

$$v_y(x,y) = \frac{v_T R_R}{\sqrt{x^2+y^2}}\sin\left(\arctan\left({}^{y}/_{x}\right)\right) \quad (31)$$

$$\Gamma = 2\,\pi\,\mathrm{R_C}\,v_T, R_C = R_R \quad (32)$$

In Paper E, this method is described in detail, and it is shown how the circulation of the bound vortex can be estimated for Flettner rotors. As an example, the induced velocities in an array of four Flettner rotors, including the resulting wind speed and angles at the positions of the rotors, are shown in Figure 7. A polar plot of the rotor thrust for a similar arrangement with and without considering the interaction effect caused by the bound circulation is presented in Figure 8. The combined thrust delivered by all four rotors differs less than 1% if evaluated with or without interaction effects considering the bound vortex.

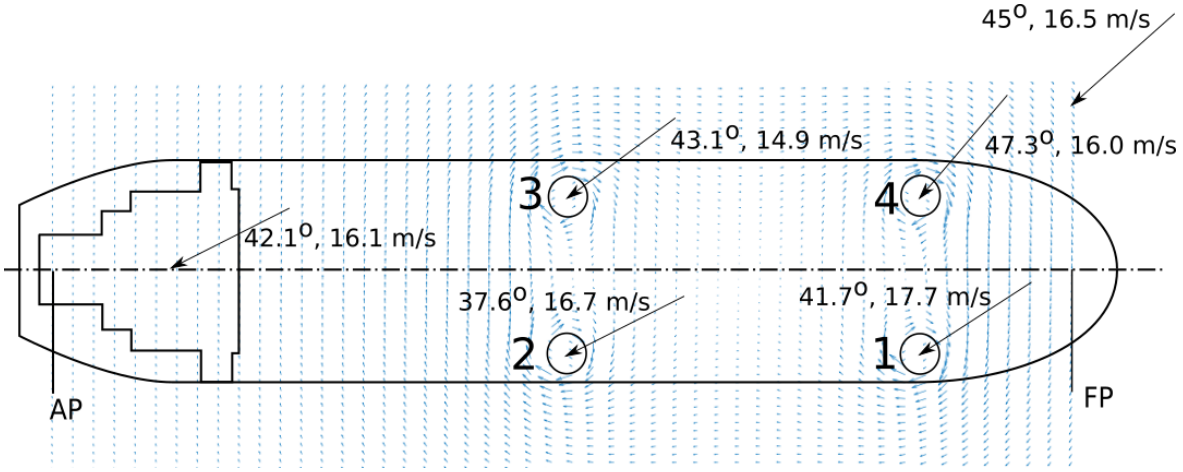

Figure 7: Induced velocities in an array of four Flettner rotors (see Paper E).

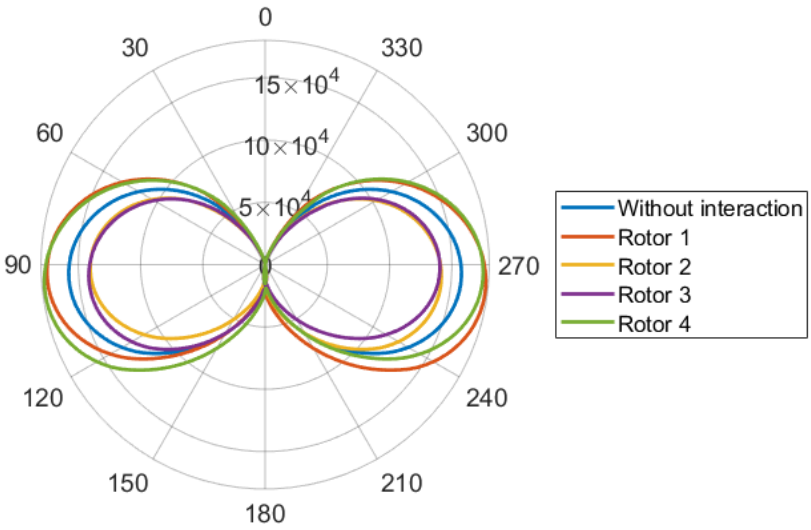

Figure 8: Thrust per rotor with and without interaction effects from the bound vortex, v_S = 12 kn, TWS = 12 m/s (see Paper E).

Additionally, tip vortices will be created at the top and the root of the sail. The influences from tip vortices can be included similarly to the influences from the bound vortex. To solve the Navier-Stokes equation it is assumed that (i) the induced velocities from the tip vortices at infinity are zero, and (ii) the induced angular speed at a given radius of the vortex R_C is equal to the angular speed caused by the circulation of the tip vortex at the radius R_C. In contrast to the bound vortex, which is created in a horizontal plane, the tip vortices are created in a vertical plane, normal to the inflow, i.e., the apparent wind direction (Zuhal (2001)). Thus, the height must be included when calculating the distance to the center of the vortex and the induced velocities must be divided into horizontal and vertical parts before being divided into the x- and y-velocities. The tangential induced velocity (v_T) from the tip vortices can be calculated using Equation (33), where Δh represents the difference between the analysed height and the root or top of the rotor.

$$v_T(x, y, h) = \frac{v_T R_C}{\sqrt{x^2+y^2+\Delta h^2}} \tag{33}$$

The horizontal (v_h), longitudinal (v_x) and transversal (v_y) induced speeds can be calculated by:

$$v_h(x, y, h) = v_T \cos\left(\arctan\left(\sqrt{x^2 + y^2}\Big/_{\Delta h}\right)\right) \quad (34)$$

$$v_x(x, y, h) = v_h \sin(AWA) \quad (35)$$

$$v_y(x, y, h) = -v_h \cos(AWA) \quad (36)$$

To evaluate the induced velocities, Equation (32) can be used. However, to use Equation (32), the circulation (Γ) and the radius of the vortex (R_C), i.e., the radius on which the circulation reaches its maximum, must be defined. Unfortunately, there are no empirical formulations, systematic model test or CFD results for the circulation and the radius of the tip vortices available in the literature. Some studies, e.g. Zuhal (2001), investigate the structure of the wing tip vortex for a single wing with different angle of attacks. Zuhal (2001) presents results from model tests, showing that the tip vortex has a circulation of about 80-90% of the circulation of the bound vortex and that the radius at which the circulation reaches its maximum is about equal to the profile thickness. It must be noted that these results were obtained for one three-dimensional wing, with only one free end without any winglet or endplate. A Flettner rotor (or any other sail on a ship) has two open ends, one at the root and one at the top, at each of them tip vortices are created. Further on, Flettner rotors have endplates that decrease the strength of the tip vortex. It is thus not possible to estimate the circulation and size of the tip vortices of a Flettner rotor from the measurements available in the literature. However, to simulate the effect that the tip vortices could have, it is assumed that the tip vortices created at the top and the root of a Flettner rotor have a total circulation of 80% of the circulation of the bound vortex and a radius (R_C) equal to the rotor's radius. Since a ship's deck represents a large endplate, it is assumed that the vortex created at the root of the rotor has less circulation, 30% of the circulation of the bound vortex and the vortex at the top has a circulation of 50% of the circulation of the bound vortex. It could be argued that the created vortices should have lower circulation, because of the endplate at the top. However, the assumed values should represent a maximum level for the influences. In ShipCLEAN, the tip vortices are assumed to follow the direction of the inflow (AWA), not to lose in height and have constant circulation and radius downwind of the sails.

Figure 9 presents the induced speeds from the tip vortices created at the top and the root of the rotors analysed at a height of one rotor radius above the root of the rotors, i.e., at the point of maximum circulation of the vortices created at the root. Only the horizontal parts of the induced velocities are respected. Figure 10 presents the same analysis for a height of half the rotor height over the base of the rotors. The influences are focused at the area straight downstream of the rotors at heights close to the root (or tip) of the rotors, but influence much wider areas when analysed at heights further away from the top and root of the rotors, as shown in figures 9 and 10. Figure 11 presents a comparison of the thrust per rotor with and without the influence form the tip vortices, assuming the circulations and radii as discussed above. It is shown, that the thrust of the rotors downwind of other rotors is reduced due to the tip vortices. The difference of the total thrust over all wind angles was found to be about 2%.

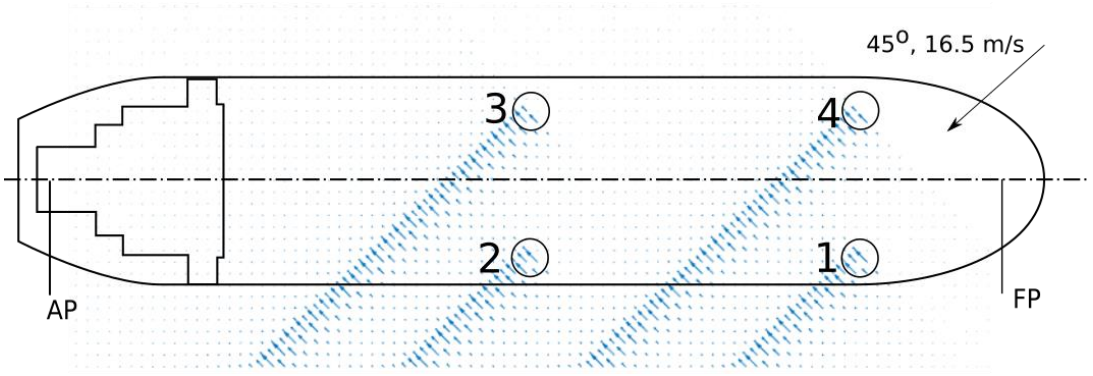

Figure 9: Induced speeds from the tip vortices created at the root and the top at h=R_R over the base of the rotors.

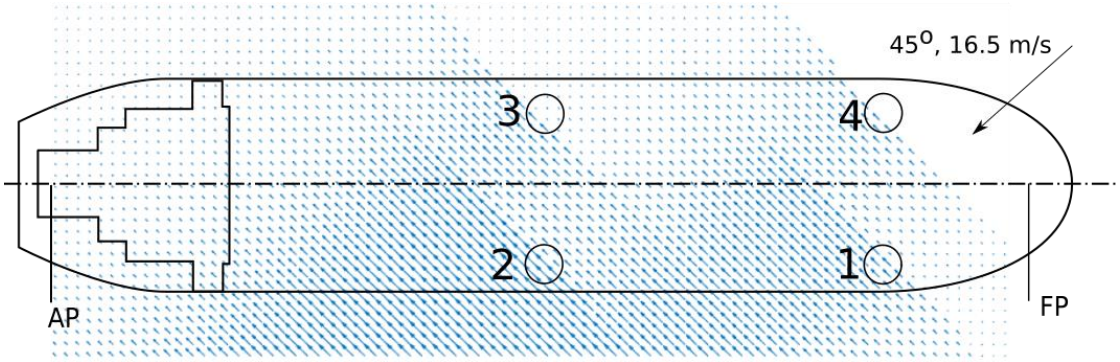

Figure 10: Induced speeds from the tip vortices created at the root and the top at half the rotor height over the base of the rotors.

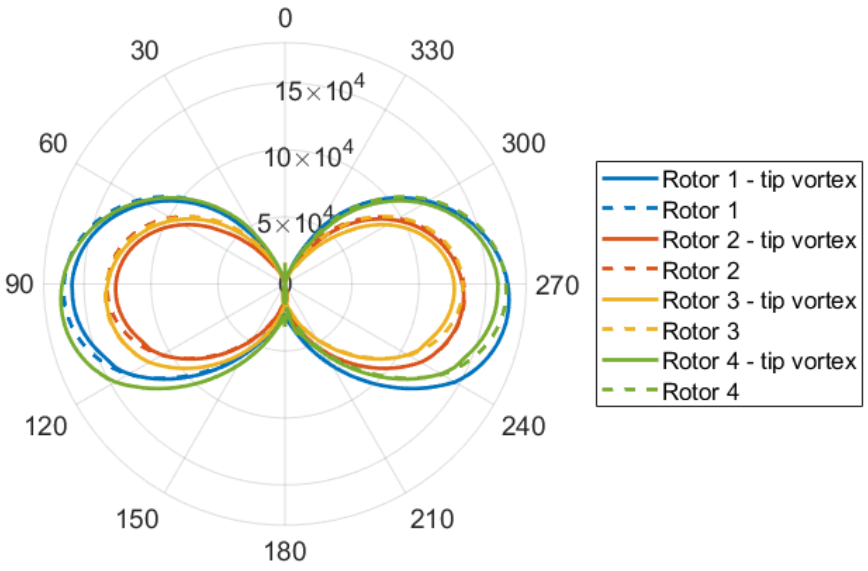

Figure 11: Thrust per rotor with and without interaction effects from the tip vortices, v_S = 12 kn, TWS = 12 m/s

It must be noted that, as discussed above, the values of the circulation and the radius of the tip vortices are not evaluated based on any measurements or estimation formulas but only assumed values. Thus, these results are only exemplary. Further investigations must be performed to better model the tip vortices. Thus, the results presented in Paper E do not include any influence from tip vortices, but only from the bound vortex.

The viscous interaction effects are caused by vortex shedding from the sails, which propagate along the potential streamlines downwind of a sail. These vortices create two effects, a decrease of the local wind speed and a periodic fluctuation of the wind direction, with the mean direction equal to the local wind direction considering only the potential flow interaction. In ShipCLEAN, the viscous effects are captured with a decrease of the wind speed in a corridor following the potential streamlines downwind of sails with a width equal to the sail's chord length. In the center of this corridor, the wind speed is defined to 95% of the local wind speed considering only the potential interaction effects. The resulting flow field for a rotor arrangement as in Figure 7 is presented in Figure 12. In Figure 12, the wind speed reduction in the vortex path is exaggerated to 20% of the local wind speed, for better visualization.

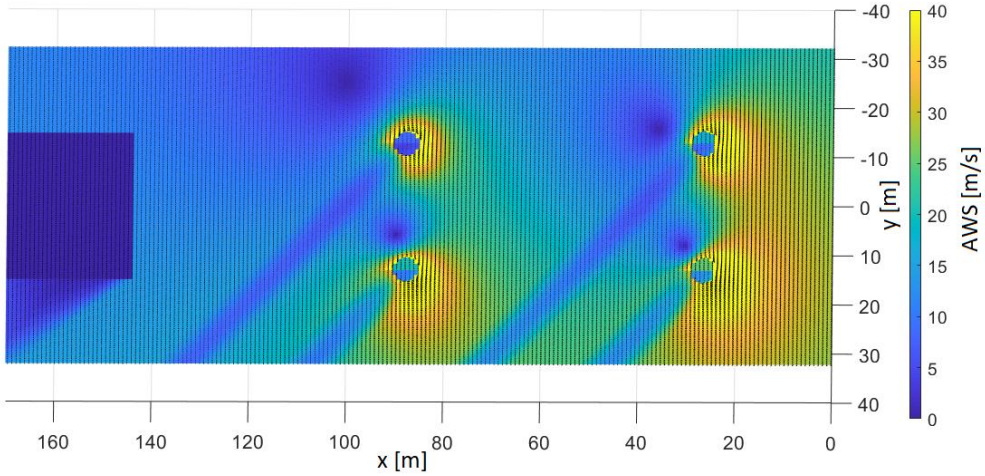

Figure 12: Flow velocities in an array of four Flettner rotors, including potential (bound vortex) and viscous interaction effects (see Paper E).

The method to only reduce the local flow velocity to account for viscous effects was developed for Flettner rotors (see Paper E). In contrast to wing sails, the lift and drag coefficients of Flettner rotors are not dependent on the angle of attack. Thus, the lift and drag coefficients in a flow with fluctuating directions but constant mean velocity will be constant, given that the spin ratio is constant. The thrust and side force coefficients in the vortex path will thus be equal to thrust coefficients in conditions with the same wind speeds but constant direction. However, other sail types, e.g., wing sails, are dependent on the angle of attack and will thus experience different lift and drag coefficients in the vortex path than in flows with stable direction. If the sails are in an area of the angle of attack well below stall angle, the lift coefficient will depend linearly on the angle of attack (Abbot and Doenhoff (1959)) and the losses will be equal to the Flettner rotor case. However, if the sail experiences angles of attacks larger than the stall angle, or below zero, the lift coefficient will drastically decrease and the drag coefficient will increase, reducing the sail's performance. Such cases are not captured by the method in ShipCLEAN.

On typical arrangements, such as those shown above, it only happens at three areas of apparent wind angles and only for a span of about five degrees that one sail is in the vortex path of another. Thus, these conditions could easily be avoided if it is provided that the prediction model penalizes the performance enough.

In Paper E, the performance of an array of four Flettner rotors is compared with and without interaction effects. It was found that the thrust forces do not differ significantly for the whole array. However, the aft rotors contribute much less, which moves the center of effort forward. The method developed for ShipCLEAN is verified against model test results for a two-rotor arrangement, see Paper E for details.

Further on, it is shown in Paper E that rpm optimizations of each rotor considering the local wind speed and direction, as well as the drift and rudder angles, are important and increase the performance of sail-assisted ships, especially in beating conditions. The rpm optimization is performed using a scoring system to reef the rotors contributing the least to the forward thrust while optimizing the center of effort of the sail force to achieve an optimal rudder angle and minimize the propeller thrust by balancing rotor loading and drift resistance (see Section 2.6). The optimal rpm of each rotor on a RoRo ship with four Flettner rotors is presented in Figure 13a and a comparison of the relative fuel consumption ($FC_{withSail}/FC_{withoutSail}$) is provided in Figure 13b. Exemplary results of applying wind-assisted propulsion to different ships on several routes are presented in Section 4.3.

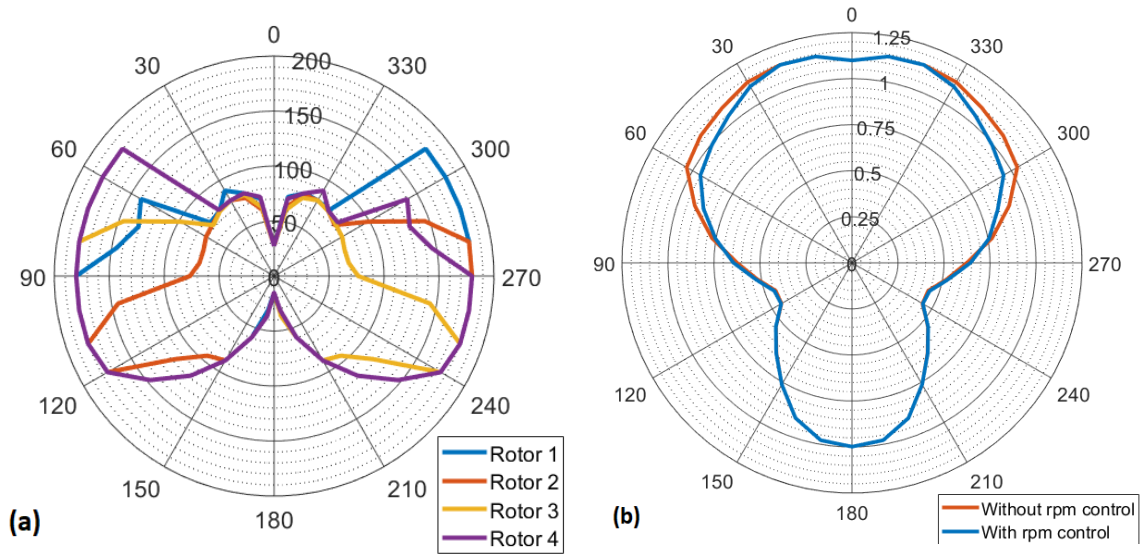

Figure 13: Results from rpm optimization for a RoRo ship with four Flettner rotors (TWS = 20kn, v_S = 18kn): (a) rotor rpm, (b) fuel consumption relative to the fuel consumption without sails (see Paper E).

2.8 Engine and involuntary speed loss

In ShipCLEAN, engines are modeled using the engine limits, as shown in Figure 14, i.e., limits for the maximum power (3), maximum rpm (4), maximum torque (2), and the limit for minimum air supply (1). Details about the engine model are presented in Paper A. Engine limits and fuel consumption curves are based on MAN (2015). The limit curves are defined relative to the design rpm and design engine power. An extract of the definition is shown in Table 6.

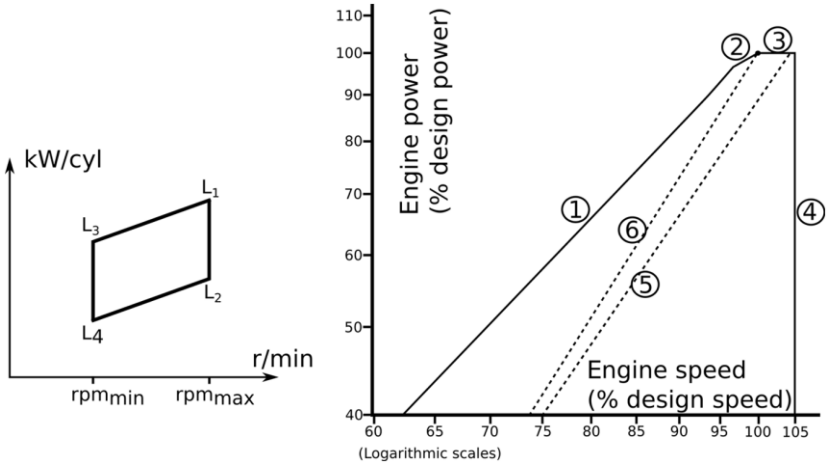

Figure 14: Illustration of engine limits (right) and engine layout points (left) (see Paper A).

Table 6: Engine limit curves.

rpm/rpm_{Design}	0	0.2	0.4	0.6	0.8	0.9	0.95	1	1.05
P/P_{Design}	0.020	0.041	0.165	0.371	0.660	0.835	0.930	1	1

The fuel consumption is based on the mean effective pressure (MEP) concerning the MEP and reference fuel consumption at the maximum engine power design point (L1). The MEP and the specific fuel oil consumption (sfoc) are calculated with (see Paper A):

$$MEP = smcr \;/\; (V_H n_z rps) \tag{37}$$

$$sfoc = sfoc_{L1}\,(0.1775\, MEP \;/\; MEP_{L1} \; + 0.82235) \tag{38}$$

The cylinder volume (V_H) is estimated using the stroke-to-bore ratio and bore for different engine types. Accordingly, the sfoc and MEP at the L1 point are specified based on the engine type. As an example, large low-speed, two-stroke engines are estimated with a stroke-to-bore ratio of four, a bore of 600 mm, sfoc at L1 of 200 g/kWh, and a MEP at L1 of 20 bar. The specific fuel oil consumption according to Equation (38) is valid for fuel oil. If alternative fuels should be used, other fuel consumption curves (if available) can easily be included. During journey simulations, auxiliary loads (e.g., hotel loads) are modelled as a constant power increase of the main engine. This assumes that 100% of the auxiliary load is on a shaft generator. This will slightly underestimate the fuel consumption, since auxiliary engines with higher specific fuel oil consumption are normally used on ships in operation.

2.9 Weather conditions for realistic journey predictions

To perform fuel consumption predictions and studies on potential fuel-saving measures, reliable information about the environmental conditions is crucial. As ShipCLEAN is designed to be a Stage I model (see Section 1.2) hindcast data and weather statistics are of interest rather than weather predictions.

The environmental conditions can be taken from: (i) on-board measurements from ships operating in the area of interest, (ii) hindcast data from the geographic area or, (iii) long-term statistics. Option (i) and (iii) often lack information about the wave height (as discussed in Paper E); thus, it must be evaluated based on the wind speed.

$$H_S = 0.01616\, U_A \sqrt{fetch}\ ;\ U_A = 0.71\, TWS^{1.23},\ \text{TWS in [m/s]} \tag{39}$$

The maximum wave height is computed by:

$$H_{S-max} = \frac{0.2433}{9.81}\, U_A^2 \tag{40}$$

While option (ii), hindcast data, probably offers the highest accuracy for the grid points, option (i), onboard measurements, provides data for an actual route, including local effects, e.g., close to coasts. However, to predict payback times of investments to increase ships' energy efficiency, it is necessary to perform predictions of potential savings based on various possible weather scenarios. For these cases, option (iii), long-term statistics, are the obvious choice, as presented in Paper D. All options can be used in ShipCLEAN; however, option (iii) meets the model's main purpose.

2.10 Response surface methods

To predict long-term fuel savings accurately, many conditions, i.e., many journeys, must be simulated. In Section 4.2 and Paper D, the use of statistical weather to predict the expected fuel saving and the variability between different journeys with the help of Monte Carlo simulations is discussed. In Paper D, the method is used to predict long-term fuel savings and economics for speed reduction and wind-assisted propulsion. For the study in Paper D, 10 000 runs were performed per route with about 70 waypoints per route. This added up to 700 000 simulated points per route. A direct simulation using the 4 DOF method in ShipCLEAN takes about 5-10 seconds on a standard desktop PC, which would result in a simulation time of over 40 days for all 700 000 points. By using response surface methods (RSM), the computation time for all points was reduced to 60 seconds.

To define the response surface and minimize the required number of simulations to build up the response surface, all environmental factors were sorted by their influence on the ship, i.e., if they require a 4 DOF simulation or if it is enough to respect the thrust direction only. Influences requiring a 4 DOF simulation are those that introduce side forces, i.e., the wind, and those that are dependent on the heading of the ship, i.e., the waves. All other environmental influences, e.g., shallow water, ice, and fouling are only dependent on the longitudinal speed through water and only affect the longitudinal thrust and can thus be added to the thrust after the 4 DOF analysis. With this categorization, the response surface becomes 5 dimensional (i.e., 4 variables and a response parameter), with the TWA, TWS, wave encounter angle, and Hs as input variables and the required propeller thrust as the output parameter. Considering the methodology used in Paper D (see also Section 2.9), i.e., the wave heights evaluated based on the wind speeds, the response surface reduces to be 3 dimensional with only the TWS and TWA

as input variables. With an increase in dimensions (i.e., input variables) the number of necessary simulations increases. As the used method requires the input data in grid format, each variable must have the same resolution. Thus, if 18 different TWA should be simulated as a base, the 3-dimensional RSM would require 324 simulations and the 5-dimensional almost 105 000.

The RSM in ShipCLEAN is an interpolation method built into MATLAB (Mathworks, 2020) called the gridded interpolation. The used interpolation method is a modified Akima formulation, i.e., a piecewise polynomial interpolation that gives the exact value at the sample points and avoids overshooting (Mathworks (2020), Akima (1974)). For example, using a grid of 324 sample points for a tanker (Ship 4 in Section 3) and a 3-dimensional response surface (TWA from 0 to 180 degrees in steps of 10 degrees, 18 different TWS from 0 to 52 kn, symmetric arrangement of sails) the difference of the required propeller thrust between the RSM output and the direct computation (in random conditions) was less than 0.1% (see Paper D for details).

2.11 Transport economics analysis

A transport economics model is integrated in ShipCLEAN. The model is based on a cost-income analysis respecting running and operational costs (see Paper D and Psaraftis et al. (2019)).

The costs (C) of a ship in operation can be evaluated using the fuel price p, the fuel consumption FC, and the operational costs (OPEX) X.

$$C = journeyTime\ (p\ FC + X) \tag{41}$$

For payback time studies, the costs must be evaluated for (i) the original ship, with the fuel consumption without the energy-saving measures, and (ii) the modified ship with the new fuel consumption but with the installation and running costs of the installed energy-saving measures added to the costs. The income I is a function of the load factor u, the cargo capacity Q, and the freight rate R.

$$I = u\ R\ Q \tag{42}$$

With the income and the costs defined, the profit per day P can be evaluated, which can later be used for optimization studies.

$$P = \frac{(I-C)}{journeyTime} \tag{43}$$

3 Uncertainties and validation

This section presents a validation of the power prediction and a prediction of uncertainties using the ShipCLEAN model. The uncertainties are identified in Section 3.1 and estimated in Section 3.2. The validation is performed using model- and full-scale measurement data and is presented in Section 3.3. For the model validation and quantification of uncertainties, five example ships are used. Their dimensions and the available measurement results (model and full scale) are presented in Table 7.

Table 7: Dimensions and available measurements of the example ships.

	1	2	3	4	5
Ship type	Cruise ferry	RoRo	Container	Tanker	RoRo
L_{oa} [m]	210	190	350	183	212
B [m]	31.8	26.4	45.6	32.2	26.7
T [m]	6.8	7.8	13.0	11.0	6.0
Δ [t]	28504	24050	128000	50610	21000
c_B [-]	0.652	0.637	0.640	0.798	0.642
D_P [m]	5.2	5.5	8.8	7.0	4.5
rpm_P [min^{-1}]	130	130	102	130	120
Z [-]	5	4	6	4	5
n_P [-]	2	1	1	1	1
Model scale meas.	x	x	x	x	x
Full scale meas.	x	x	x	-	-

3.1 Identification and categorization of uncertainties

In a Stage I model, such as ShipCLEAN, uncertainties originate from two sources, (i) uncertainties in the estimation of missing ship design parameters and (ii) uncertainties in the employed methods for predicting the different components. As explained in Paper B, the first group is referred to as design uncertainties (D) while the second group is referred to as method uncertainties (M). Design uncertainties are caused by the unknown design of the ships, e.g., unknown dimensions, hull shape, or propeller design. Method uncertainties originate from inaccuracies in prediction methods, including measurement uncertainties in, e.g., model tests. Design uncertainties can be fully eliminated once all parameters of a ship are known and available. Contrarily, method uncertainties can be reduced, but never eliminated, even if model tests, full-scale trials, or CFD computations are available. Details on the categorization of uncertainties are presented in Paper B.

3.2 Estimation of design and method uncertainties

This section presents the estimation of design and method uncertainties in ShipCLEAN. The analysis is divided into five parts. Section 3.2.1 presents an analysis of the static part, i.e., the calm water and 1 DOF power prediction, Section 3.2.2 presents an analysis of the dynamic (4 DOF) part, Section 3.2.3 presents an analysis of the wind-assisted propulsion module, Section 3.2.4 presents the analysis of the transport economics model, and Section 3.2.5 presents the analysis of the methods used to predict the environmental loads. To estimate design

uncertainties, the design of a ship must be varied in a way that it does not affect the predicted power with the methods used. As an example, the hull form can be varied without changing the main dimensions, which will affect the actual resistance of the ship, but not the predicted resistance with empirical formulas. Method uncertainties are estimated using published statistics and comparing different methods for the empirical methods and analyzing measurement uncertainties for model tests.

3.2.1 One degree of freedom model

Uncertainties in the 1 DOF part of ShipCLEAN are estimated in Paper B. Design and method uncertainties are estimated based on two example ships: a tanker (Ship 4) and a RoRo (Ship 2). Detailed results for the RoRo are presented in Table 8. The design phases defined in Paper B are quite like the model stages introduced in Section 2 but focused on the design process of a ship. Design phase I represents an early design phase, i.e., only the main dimensions are defined. In phase II, the hull design is defined, and model test results are available in phase III. Phase IV represents the end of the design project, i.e., the whole design of the ship, including the superstructure, is finished. However, full-scale measurements are not available. As a result of the available input parameters in the different design phases, in phase I, only Stage I models can be used and similar to phases II, III, and IV where Stage II, III, and IV models could be applied, respectively.

Table 8: Estimation uncertainties in the propulsion power prediction for Ship 2 (see Paper B).

	Design phase							
	I		II		III		IV	
	D	M	D	M	D	M	D	M
S_W	1%	-	-	-	-	-	-	-
$k^*c_F + c_R$	3.1%	6.4%	-	6.4%	-	4.1%	-	4.1%
w_e	10.0%	7.1%	-	7.1%	-	2.0%	-	2.0%
η_H	-	6.0%	-	6.0%	-	-	-	-
t	-	-	-	-	-	5.0%	-	5.0%
η_0	2.0%	1.5%	-	1.5%	-	1.2%	-	1.2%
A_T	6.0%	-	6.0%	-	6.0%	-	-	-
A_L	3.1%	-	3.1%	-	3.1%	-	-	-
c_X	3.0%	2.0%	3.0%	2.0%	3.0%	2.0%	-	2.0%
R_{AWaves}	2.2%	12.6%	-	12.6%	-	12.6%	-	12.6%
SFOC	-	3.0%	-	3.0%	-	3.0%	-	3.0%
P_D *(CW)*	10.0%		8.9%		2.1%		2.1%	
FC (CW)	10.4%		9.4%		3.7%		3.7%	
P_D *(sea)*	10.5%		9.0%		3.2%		3.2%	
FC (sea)	10.2%		9.5%		4.3%		4.2%	

The results in Paper B showed slightly higher uncertainties for the tanker in phase I, caused by larger uncertainties in the prediction of the effective wake compared to the RoRo. The expected standard deviation of the propulsion power was estimated to be about 10% for the RoRo and 12% for the tanker (phase I), which could be reduced to 3% for the RoRo and 2% for the tanker by eliminating the design uncertainties and performing model tests (phase IV). This analysis also shows the achievable accuracy for models of different stages, as discussed in Section 1.2.

In Paper B, how uncertainties are reduced in ShipCLEAN was also discussed. Huge reductions could be achieved by introducing the standard hull series to obtain the wetted surface, as all methods showed insufficient results compared to actual hulls. In other areas, such as the added wave resistance or resistance prediction, multiple methods were combined to reduce uncertainties. Even though the model has been further developed when compared between Paper B and E, the uncertainties will not be affected significantly as most of the development work was focused on extending the range of validity and the model's functionality.

It must be stressed that all power prediction methods, even model tests, do have uncertainties, as presented in Table 8. Thus, any power prediction will not be completely accurate if compared to full-scale measurements, which will have measurement uncertainties as well. From the results presented here and in Paper B it must be concluded that the largest modeling uncertainties appear in the estimation of the propulsive factors, i.e., the effective wake and hull efficiency and the added wave resistance.

3.2.2 Four degrees of freedom model

Uncertainties in the 4 DOF part of ShipCLEAN originate from prediction of the lift and drag of a ship sailing at a drift angle, from prediction of the center of lateral resistance (CLR), and from prediction of the rudder force. If only small side forces are introduced, for example, for a ship with low windage area (e.g., tankers) without sails, the accuracy of the 4 DOF method is equal to the 1 DOF method. Once the side forces become higher (e.g., when sails are introduced), the accuracy of the 4 DOF method increases compared to the 1 DOF method because added drag from drifting and steering is included. However, the methods to calculate the added drag introduce new uncertainties.

As a result of the limited model test and CFD results available in the literature, it is impossible to quantify design uncertainties for the lift, drag, and CLR of the ship hull. In Paper E, it is discussed that hull form features, especially the waterline shape in the bow region, the transom shape/immersion, and the bilge radius must influence the lift, drag, and CLR of the hull; however, without systematic CFD computations or model tests, these influences are not quantifiable. Method uncertainties are discussed in Paper E. Uncertainties in predicting the lift force result in inaccurate predictions of the drift angle. It was found in Paper E that the deviation of the predicted drift angles from measured/CFD computed values was up to 3 degrees at a drift angle of 10 degrees. However, this inaccuracy mainly affects the thrust from sails, which can be reduced by about 1% because of this inaccuracy. Larger uncertainties are found in the drag (or lift/drag) prediction where differences of up to 15% were found. In the study presented in Paper E and Section 4.3, the average drag from drifting (for the long-term prediction) was found to be 8% (for Ship 5) of the total resistance. This would result in an uncertainty for the fuel consumption prediction of about 1.2%. In the variation study in Paper E, the highest added drag as a result of drift was found to be 20% (for both ships 4 and 5) of the total resistance, which would result in uncertainty of about 3%. However, it must be noted that the drift angle and added resistance are dependent on the TWA. Generally, in beating and downwind conditions, the side forces and thus the drift angles, are higher, which results in higher percentages of the added drag compared to the total resistance. However, with the rpm control of the Flettner rotors, the added drag is limited because the rpm of one or several rotors, if beneficial for the balance of side force, added drag and sail thrust.

As discussed in Paper E, the CLR is difficult to predict, both theoretically, with CFD and in model tests. Thus, it must be assumed that the uncertainties are high, even though it is difficult to quantify because of the limited data available and large uncertainties in all methods.

Additionally, the impact of an inaccurate CLR on the performance of a wind-assisted ship is complex. The CLR influences the necessary rudder angle and with this, the side force delivered from the rudder and thus even the drift angle and drag from drifting. Additionally, the rpm control aims to optimize the rudder angle. Thus, an inaccurate CLR will even affect the delivered thrust from the sails. However, it must also be stated that the absolute position of the CLR is not important but only the relative position between the CLR and the center of the aerodynamic side forces. It can thus be assumed that the relationship between the final CLR (evaluated by CFD or model tests) and the center of the aerodynamic side forces can be adjusted to be equal to the relationship during simulations by moving the sails in a longitudinal direction. Thus, even though the uncertainties in the prediction of the CLR are large, the effect on the resulting fuel savings is small or even zero if the final sail arrangement is adjusted once more sophisticated methods to predict the CLR (e.g., CFD or model tests) become available.

The rudder model consists mainly of the evaluation of the lift and the drag coefficients. Uncertainties in the prediction of the lift and drag coefficients must be categorized as design uncertainties, because the coefficients are based on airfoil theory, which is a well-validated theory. However, design details, such as the exact planform, the sectional profile, and eventual skegs in front of the rudder influence the lift and drag coefficients. Even the rudder area can differ from the area assumed in ShipCLEAN. A difference in the lift force between the actual design and the values in ShipCLEAN would mainly influence the optimal rotor position, comparable to the CLR. Additionally, there is an influence on the drift angle, and added resistance as a rudder with lower lift forces contributes less to the total hydrodynamic lift and the hull must create more lift. As the lift-to-drag ratio of a rudder is much better than that of a ship hull, rudders with less lift force (e.g., through less area or lower lift coefficients) would decrease the ship's performance. In most conditions, this influence is small; however, especially in beating conditions, wind-assisted propelled ships require large rudder forces. Uncertainties in the rudder lift force will, comparable to the CLR, influence the balance of the ship and rpm optimization of the rotors. As for the CLR, the effects are difficult to quantify and for most conditions, differences in rudder lift forces can be balanced with re-arrangement of the sails. However, in beating conditions, the rudder design is important, especially for the TWA where the sails become effective as de-powering of the sails often happens as a result of large rudder angles.

In conclusion, the largest uncertainties are caused by the estimation of the lift-to-drag ratio of the ship hull. Uncertainties in the estimation of the CLR, the rudder area, and rudder lift and drag coefficients can be balanced with re-arranged sails and the effect on the fuel consumption prediction is thus considered negligible. Only in some conditions, especially beating, the exact location of the CLR and the lift force from the rudder become important. However, because of the complexity of the system, including the rpm control, it is not possible to quantify these uncertainties exactly without extensive variation studies. The uncertainties in the CLR estimation and the rudder lift force show that it is crucial to re-evaluate the sail arrangement once the final design of the ship is available.

3.2.3 Wind-assisted propulsion module

In ShipCLEAN, three different Flettner rotors with defined heights, end plate, diameter, and maximum rpm are available. These are the only design parameters that influence the performance of Flettner rotors, according to literature. Thus, the design uncertainties are zero.

Method uncertainties are found in the lift, drag, and power coefficients, as well as in the evaluation of the aerodynamic interactions. The lift, drag, and power coefficients are corrected

using full-scale measurement data (see Paper E). Thus, assuming similar build quality and motor efficiencies for all rotors, the method uncertainties for the lift, drag, and power coefficients are small. In Paper E, the uncertainty in predicting the forces of a single rotor is evaluated to be well below 4%, with the predicted lift and drag forces being within 1% of the full-scale measurements for the test case. The evaluation of the aerodynamic interactions is based on the potential flow Navier-Stokes equation (see Paper E) and shows results that are comparable to results from simulations of fleets of sailboats and model tests with two rotors (see Paper E). The main uncertainty in this approach is in evaluating the circulation caused by the rotors, see Paper E for details. However, the results in Paper E show that the main effect of the potential flow interactions is a difference in the location of the center of the aerodynamic force as the aft rotors become less and the front rotors more efficient. As for the CLR and the rudder in Section 3.2.2, the effect of this difference is complex but can be compensated in the detailed design of a ship or the sail arrangement once more sophisticated methods (CFD or model tests) are applied.

The viscous interaction effects are much more difficult to model and cause higher uncertainties. However, viscous interaction effects do only occur in narrow TWA ranges, i.e., when one rotor is downstream of another rotor. To overcome these uncertainties, ShipCLEAN introduces performance decreases by reducing the local wind speed downstream of the rotors. These performance decreases are much larger than they would be, to avoid the ship sailing in those TWA ranges once routing algorithms are applied. Thus, the uncertainties are large but do not affect the fuel consumption predictions since the TWA ranges where the uncertainties occur are avoided.

3.2.4 Transport economics model

The validation and uncertainty quantification of the logistics model are not part of this thesis. However, it must be mentioned that all factors, the fuel price, the operational costs, the freight rate, and the utilization rate are linear factors in the model. Thus, any uncertainties in the evaluation of the input to the economics model will directly influence the resulting profit. This shows the importance of well-investigated economic factors as input for this model.

3.2.5 Environmental conditions

For the studies presented in this thesis, the TWA and TWS are either based on global weather statistics or on measurements from ships. It must be noted that any source of weather data, especially on-board measurements, will have uncertainties. However, such measurement and prediction uncertainties are not quantified in this thesis. For all studies presented, the wave heights are based on a defined fetch and the TWS, see Section 2.9. This introduces uncertainties since geographical effects, such as sheltered water, water depth or regions close to coastlines are disregarded. In this thesis, the uncertainties of the predicted wave heights are not quantified. However, in Table 9, the influence of differences in the wave height on the propulsion power of the 5 example ships is presented. The results show the importance of predicting the correct wave height and the magnitude of the uncertainties caused by uncertainties in predicting the wave heights using the method presented in this thesis.

Table 9: Relative propulsion power at design speed compared to the reference power at 3 m wave height ($P_D/P_{D\ 3m}$), TWS = 20 kn.

	Ship 1	Ship 2	Ship 3	Ship 4	Ship 5
Hs = 1 m	0.89	0.77	0.90	0.76	0.87
Hs = 2 m	0.93	0.84	0.95	0.83	0.92
Hs = 3 m	1.00	1.00	1.00	1.00	1.00
Hs = 4 m	1.16	1.34	1.13	1.34	1.19
Hs = 5 m	1.45	1.84	1.32	1.81	1.51

3.3 Validation of the power prediction

Model validation is comparing a model's prediction with real-life measurement data, where the results from the measurements are unknown at the time the model predictions are performed. To consider a model validated, the maximum allowable difference between the prediction and the measurement must be defined before the comparison is made and sources of uncertainty and their magnitudes should also have been identified.

The validation of ShipCLEAN is performed in two steps: (i) using calm water model test results from five ships to validate the static part (see Figure 3) and (ii) using full-scale measurement data from three of the five ships to validate the dynamic part. During the validation study, the input to the ShipCLEAN model was limited to the ship's dimensions and information given in Table 7, which is the minimum required input. However, for this study, the propeller diameter was included as input because it increases the accuracy of the prediction and is often available, even for Stage I models. Thus, ShipCLEAN was run as a pure Stage I model in the validation study. All predictions are performed before receiving measurement data. Following the results from Paper B, the model's prediction of both, the calm water propulsion power/fuel consumption and the propulsion power/fuel consumption at sea shall not deviate more than 10-12% (depending on the ship type) from the measured values, which is equal to the estimated standard deviation for a design phase I prediction (see Paper B and Section 3.2). As ShipCLEAN only predicts the full-scale values, only the full-scale prediction from model tests was used for validation. The focus of ShipCLEAN is predicting long-term fuel consumption instead of instantaneous predictions. To consider the model validated, it is required that the averaged difference between predicted power and power measured in full-scale tests (moving average over 10 days) stays within the defined standard deviation of 10-12%. As a result of limited input data (e.g., no wave height information), it is expected that individual measurement points show higher differences.

3.3.1 Validation against model test results

Results from model tests consisting of resistance, propeller open water, and self-propulsion tests are available for the five example ships. As ShipCLEAN follows an approach for the power prediction, which is like the scaling procedure of model tests, it is possible to compare individual parts of the prediction, e.g., the resistance or open water efficiency. It must be remembered that model test results are also affected by uncertainties caused by inaccuracies in the measurements but also human influence in the evaluation process, especially connected to the estimation of the form factor (ITTC (1999)). As the model tests are performed in calm water, only the static part of ShipCLEAN is used, i.e., the simulations are 1 DOF.

In Figure 15, the predicted power from ShipCLEAN is compared to the predicted power from model test results. The solid lines represent the standard prediction, dashed lines show the prediction with the high bulb effect c_R curve (see Section 2.3), and the asterisk mark the design condition for each ship. The differences between the predicted power from ShipCLEAN and model test results are less than 2% for the design condition for ships 1, 3, and 4, i.e., for the cruise ferry, the container ship, and the tanker. The predicted power at design speed from ShipCLEAN for the two RoRo ships is 6% lower (Ship 2) and 8% higher (Ship 5) than the predicted power from model tests. All deviations are significantly lower than the 10% deviation defined as allowable for the validation, which is a good result.

For Ship 2, the difference originates from a low propulsive efficiency (η_D about 0.595) during the model tests, which is caused by both a low hull efficiency of less than 1.02 and a propeller open water efficiency of less than 0.6, both considered much lower than usual. The propulsive efficiency predicted by ShipCLEAN for Ship 2 is 0.625. It must be noted that Ship 2 is the only ship in this study that has a controllable pitch propeller (CPP). In ShipCLEAN, CPPs are evaluated as fixed pitch propellers, which will cause large differences in propeller efficiency in off-design condition if the CPP is operated on a combinator curve or with fixed rpm, i.e., with variable pitch over the speed range.

The available model test results for Ship 5 are limited to the propulsion power, with no intermediate results, such as the propulsive efficiency or the resistance available. Thus, a detailed investigation about the cause of the overprediction from ShipCLEAN cannot be performed. However, according to reports by the owner of the built ship, the fuel consumption is about 5% higher than when it is computed from the propulsion power from model test results. This could indicate an underpredicted power from model tests but might also be because of a higher specific fuel oil consumption of the main engine.

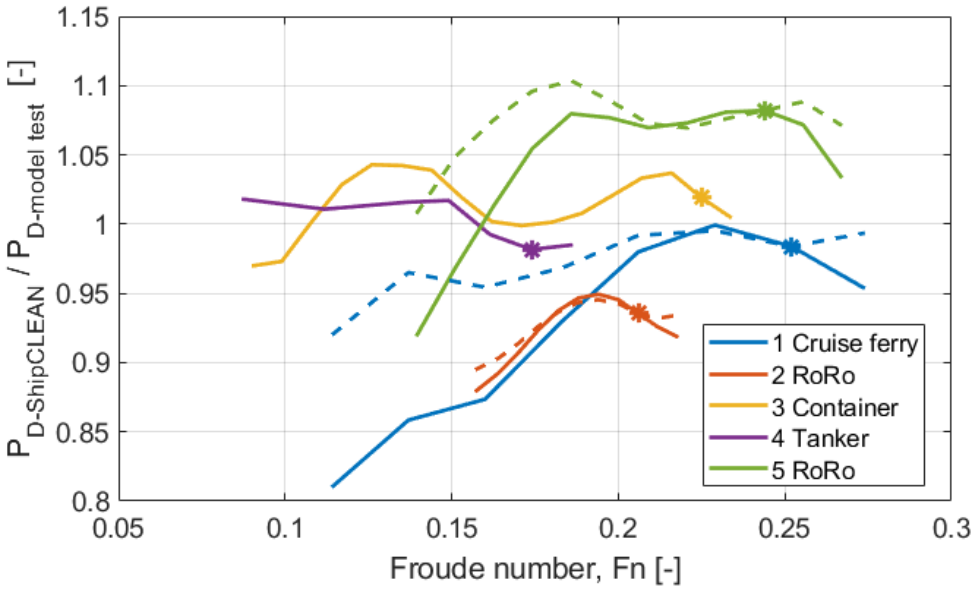

Figure 15: Predicted propulsion power from ShipCLEAN over the propulsion power from model tests for five sample ships. Solid lines: prediction with standard c_R curves; dashed lines: prediction with c_R curve for high bulb effect.

In the off-design condition, i.e., at lower or higher speeds, the predictions differ more, except for the container ship and the tanker (ships 3 and 4). For all other ships, the prediction from ShipCLEAN shows lower power consumptions at low speeds than the predictions from model test results. This difference can be explained with the different bulb effects. As described in Section 2.3, three curves for c_R over the ship speed are used in ShipCLEAN: one with almost no bulb effect for full block ships such as tankers, one with a moderate bulb effect for faster ships, and one with a significant bulb effect. Ship 4, the tanker, and Ship 3, the container ship, obviously have no or only small bulb effects at lower speeds. The container ship has, in fact, been rebuilt with a new bulbous bow to increase the performance at lower speeds. Ships 1, 2, and 5 are ships optimized for one speed, i.e., design speed, featuring large bulbous bows, resulting in higher resistance at lower speeds than predicted from ShipCLEAN. The cruise ferry (Ship 1) does not operate in off-design conditions. Thus, this resistance increases and difference in prediction does not influence the ship's performance or the model's prediction accuracy. However, ships 2 and 5 operate at different speeds, which will cause the ShipCLEAN prediction to be less accurate at lower speeds and the ship to be less efficient at lower speeds. It is shown in Figure 15 that the c_R curve, which models a high bulb effect, gives better results for the RoRos and, especially, the cruise ferry. Thus, this curve should be used if it is known that the bulbous bow is optimized for a single speed and of large size, maybe even goose-neck shaped.

From the results of this validation study, it can be concluded that the prediction accuracy of ShipCLEAN for calm water conditions is better than expected compared to the results presented in Paper B. The differences between the ShipCLEAN prediction and the model's test results are less than 10% for all ships, which is less than the previously defined accepted difference. Thus, the calm water prediction can be considered validated. However, the modeling of the bulb effect for ships with large and single speed optimized bulbous bows is challenging and not accurate for all ships.

3.3.2 Validation against full scale measurements

To validate the dynamic part of ShipCLEAN, the measured power on-board ships in operation is compared to the predicted power from ShipCLEAN for similar environmental and operational conditions. Thus, additional to the propulsion power, the environmental loads, i.e., wind speed and angle, wave height and encounter angle, water temperature, water depth, current speed and direction, and the operational condition, i.e., ship speed, draft and trim, must be known. ShipCLEAN is run as the Stage I model it is designed to be, i.e., only the dimensions given in Table 7 are used. However, to increase the value of the study and reduce uncertainties caused by unknown environmental loads, on-board measurements of the wind speed and angles and other available measurements as presented in Table 10 are used for the prediction.. For all ships and all conditions, the 4 DOF method is used in ShipCLEAN.

Full-scale measurements are available for three ships, as shown in Table 7. Ships 1 and 2 operate on liner routes on the Baltic Sea while Ship 3 operates on a worldwide liner route. On-board measurements were taken once every hour (Ship 1 and 3) or once every four hours (Ship 2), regardless of the operational mode. Thanks to the coarse measurement intervals, maneuvering and acceleration could not be filtered out. An exception is Ship 1, where the on-board measurements include longitudinal accelerations. With this data, only data points with an absolute value of longitudinal acceleration of less than 0.0003 m/s^2 are used. It must be mentioned that measurement uncertainties are not quantified in this thesis. Table 10 presents an overview of the available measurement data for the three sample ships.

Table 10: Available measurement data.

	Ship 1	Ship 2	Ship 3
AWA, AWS	x	x	x
Speed over ground (SOG)	x	x	x
Speed through water (STW)	x	x	x
Draft, trim	x	x	x
Water depth	x	-	-
Water temperature	x	-	-
Position	-	-	x
Engine power	x	x	x
Rpm	x	x	x
Accelerations	x	-	-

The wave height is not measured on any of the ships but instead computed using the relationship shown in Section 2.9. This assumption does, of course, add uncertainties as the wave height does not necessarily follow the wind speed, especially in confined waters such as the Baltic Sea. However, reliable wave height measurements are close to impossible from on-board a ship. To increase the accuracy of the validation using full-scale measurements, hindcast data of the wave heights together with the ship's positions should be used. All ships are assumed to be clean, i.e., no fouling is included in the predictions.

For validation, all measurements with ship speeds higher than 5 kn are used. No limits on the wind speed or loading condition are implied. Table 11 presents the intervals of wind speed, draft, trim, and ship speed during full-scale measurements.

Table 11: Wind, speed, and loading condition intervals during full-scale measurements.

	Ship 1	Ship 2	Ship 3
TWS [kn]	1.1 – 38.6	0.3 – 47.8	1.6 – 48.2
Draft [m]	6.25 – 7.05	5.6 – 8.7	8.3 – 14.7
Trim [m]	-0.7 – 0.2	-1.3 – 0.3	-3.2 – 0.2
v_S [kn]	16.9 – 22.1	5 – 20	5 – 22.5

The presented conditions are far from trial conditions. However, the goal of ShipCLEAN is that the model shall be applicable in all types of typical operational conditions. Thus, it is required that the model gives results with the expected accuracy (see sections 3.2 and 3.3), at least averaged over a longer period, e.g., a full journey or year. The results from the comparison of measured and predicted propulsion power are presented in Figure 16.

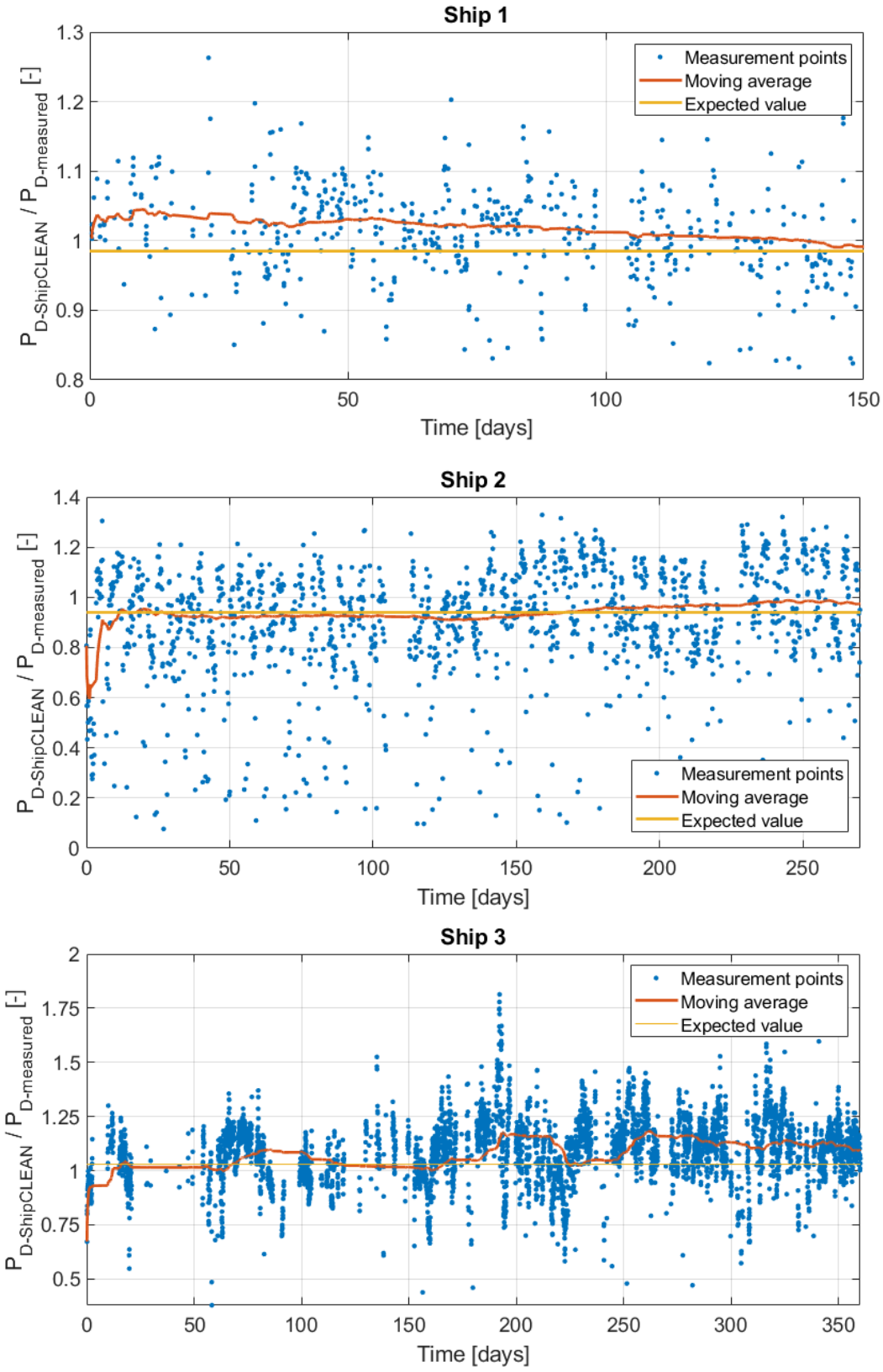

Figure 16: Comparison of propulsion power from full-scale measurement and ShipCLEAN prediction for three ships.

The results of all ships show variations in the power relation. However, for all ships, the moving average stays close to one and the expected value from validation with model test results, i.e., the relation between the propulsion power in model tests and according to the ShipCLEAN prediction (see Section 3.3.1). The moving average for Ship 1 shows a clear trend of decreasing performance over time, with the relative power being about 5% higher after 150 days, i.e., comparing the end of the measurement period with the beginning. This almost linear decrease in performance is most likely caused by fouling.

Over the whole measurement period, the averaged power relation (prediction from ShipCLEAN divided by measured power) was 1.02 for Ship 1, 0.95 for Ship 2, and 1.03 for Ship 3. All these values were well within the expected deviation (see Section 3.2 and Paper B). In Section 3.3.1, the relationship between model tests and the calm water power prediction from ShipCLEAN (at design speed) was found to be 0.99 for Ship 1, 0.94 for Ship 2, and 1.02 for Ship 3. The largest deviation from the results from the model scale validation was found for Ship 1, which performed better in full scale than in model scale, compared to the ShipCLEAN prediction. From the above numbers, it must be concluded that ShipCLEAN gives accurate performance prediction for ships in operation, if seen over a long time, which is the focus of ShipCLEAN. However, the individual measurements showed large scatter. The reasons for this scatter are further analyzed in Section 3.3.3.

3.3.3 Discussion of the validation using full-scale measurements

The results for all three ships show a large variation in the power relations, between 0.8 to 1.25 for Ship 1, 0.1 to 1.35 (with most points between 0.75 and 1.2) for Ship 2, and 0.5 to 1.8 (most points between 0.8 and 1.3) for Ship 3. Ship 1 is the only case that could be filtered for low acceleration and shows the smallest difference between the maximum and minimum power relations. This leads to the conclusion that most of the outliers for ships 2 and 3 are caused by de- or acceleration of the ship. Still, the analysis varies from an underprediction of the power by 25% to an overprediction by about 20% for Ship 1. To further investigate the source of the deviation, two pairs of neighboring measurement points with different power relations are picked for Ship 1. The data for TWS, TWA, water depth, draft, and roll and pitch motion together with the power relation is presented in Table 12.

Table 12: Four distinct measurement points for Ship 1, including ship motions.

IDX	TWS [m/s]	TWA [deg]	T_{water} [°C]	Depth [m]	T_m [m]	Roll [deg]	Pitch [m]	$P_{ShipCLEAN}/P_{measured}$ [-]
7	3.7	3	18	54	6.7	0.15	0.0113	0.95
8	1.5	157	18	52	6.7	0.02	0.006	1.03
66	10.7	13	9	63	6.6	0.009	0.0093	1.01
67	10.0	92	9	52	6.5	0.03	0.0294	0.91

The wind speeds for the measurements in both pairs are almost identical, low wind (1.5 and 3.7 m/s) for pair one and quite fresh wind (10.7 and 10.0 m/s) for pair 2. Even the TWA and the water depth are comparable. Comparing the measurements of the first pair, i.e., IDX 7 and 8, shows the ship is moving (both pitch and roll) for measurement 7 but is almost still for measurement 8. Obviously, the ship experiences waves in the time of measurement number 7 but almost calm water for measurement number 8. This results in an underprediction (5%) of the power for measurement 7 and an overprediction (3%) for measurement 8. The same can be

seen for measurement 66 and 67, where the ship is rolling and pitching during measurement 67 but much calmer in measurement 66. This shows that the ship experiences different wave heights, despite the similar wind speeds, most likely as a result of the ship's route, which leads partially through protected waters. As the wave height for the ShipCLEAN prediction is based on the TWS (see Section 2.9), the wave height in the prediction will be constant for constant TWS.

A similar study can be performed for Ship 3, where the ship's positions are available. The power relation and the positions during two days with almost constant TWS (around 12 m/s) are presented in Figure 17.

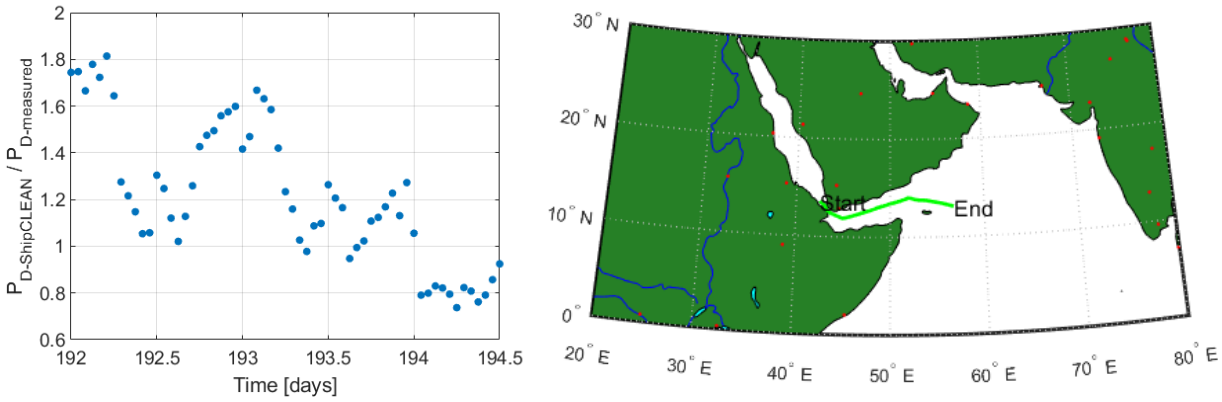

Figure 17: Position and power relation during two days for Ship 3.

During the two days, the power relation reduces from 1.8 (80% overprediction from ShipCLEAN) to about 0.8 (20% underprediction from ShipCLEAN). From the positions during the first period of the two days, the ship is sailing in protected waters, i.e., exiting the Red Sea, while it is on the open Indian Ocean at the end of the two days. It can be assumed that, despite the high wind, the ship sails on calm seas during the beginning of the period but experiences high waves during the end. As for the case of Ship 1, this can explain some of the variations in the power relations.

From the examples shown above it can be concluded the problem of predicting the correct wave height is a main cause for the variation in power relation. However, during some periods, it was found that, for Ship 3, the ship speed changed over time (both, STW and SOG), but the measured propulsion power did not change even though all measured environmental influences were constant. An example is presented in Figure 18. This effect cannot be explained with the measurements available.

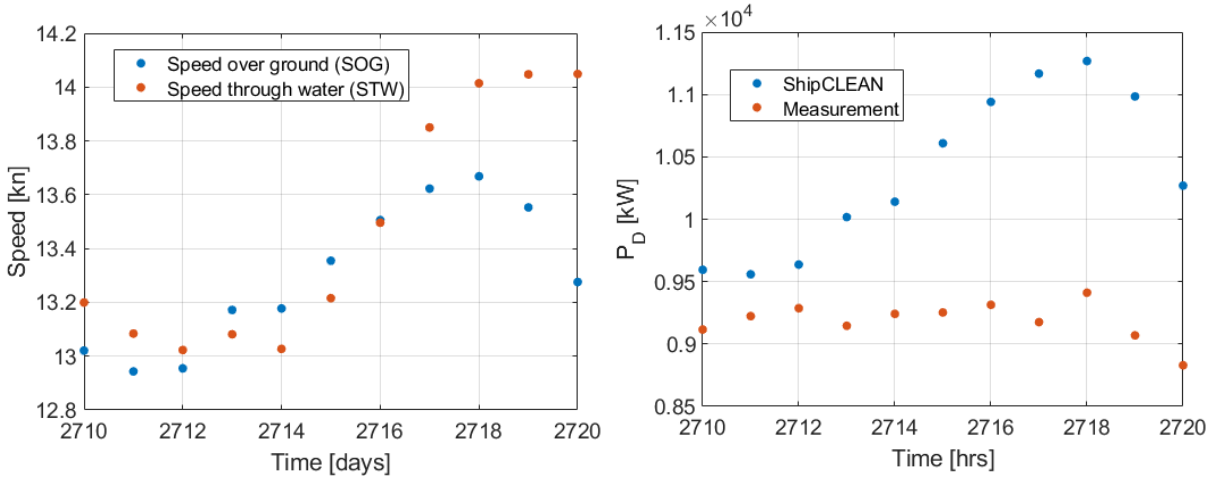

Figure 18: Measured speed through water and speed over ground and predicted and measured power over 10 hours for Ship 3.

For Ship 2, a further difficulty is that the ship has a controllable pitch propeller (CPP), which is treated like a fixed pitch propeller (FPP) in ShipCLEAN. In Figure 19, the propeller rpm over the ship speed is presented. The ship is operated at two distinct propeller rpms (governed by the ship's engine arrangement), which requires adjustments of the propeller pitch when the ship speed is varied. Variations in propeller and propulsive efficiencies attributable to the pitch variations are not captured by ShipCLEAN because of the difficulties when evaluating CPP without model test data or extensive computational effort (see Paper A for a discussion).

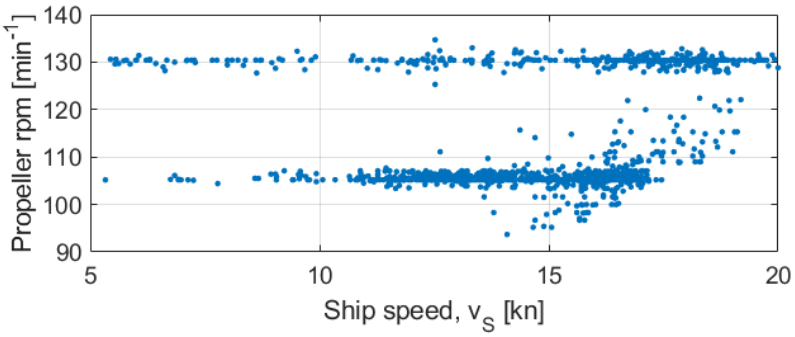

Figure 19: Propeller rpm over ship speed for Ship 2.

Further to the abovementioned influences, the variation of the draft and trim will influence the accuracy of the prediction from ShipCLEAN. As discussed in Section 2.4, the influence from draft changes is modelled with a resistance prediction at ballast draft and generic c_R curves in between the ballast and the design draft. The influences from trim are not modelled in ShipCLEAN. Since Ship 3 experienced the largest differences in draft and trim during the measurement period, the analysis is done for Ship 3. Figure 20 presents the relation of the predicted and the measured propulsion power over the trim. An almost linear relation between the power relation and the trim of the ship can be observed. Thus, it must be concluded that the influences of trim on the propulsion power are significant and must be included in future versions of ShipCLEAN, even though these influences are difficult to model. However, it must also be noted that the trend could be different for ship types that are commonly model tested at large trim for ballast conditions, e.g., tankers and bulk carriers. It is possible that the method

used to predict the resistance coefficients at ballast draft (which is based on model test results, see Section 2.4) includes the trim effects and that the inaccuracies shown in Figure 20 are smaller for such ships.

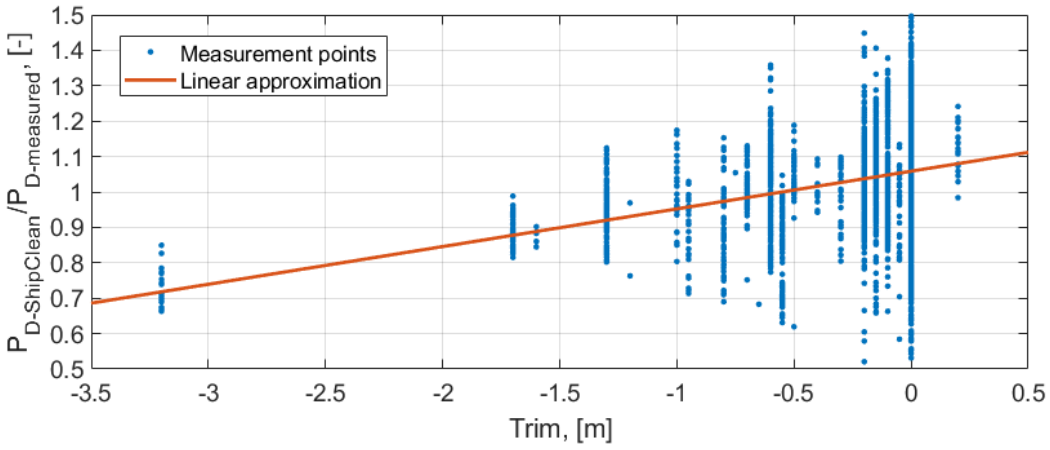

Figure 20: Relation between predicted and measured power over the trim (Ship3).

To evaluate the influence of the mean draft on the prediction accuracy, conditions with less than 0.1 m of trim (to bow or stern) are analysed. Figure 21 presents the power relation over the draft for all conditions with less than 0.1 m trim. A slight increasing trend can be seen with decreasing draft, i.e., ShipCLEAN overpredicts the power at smaller drafts compared to the prediction around design draft. Additionally, a hump can be found just below the design draft of 14 m. This is most likely due to more unfavourable wave patterns created by the bulbous bow which might be just above the water surface for these conditions. From the results presented in Figure 21 it can be concluded that the effect of draft changes is well modelled, considering that ShipCLEAN is a generic model without any information about the hull form required for the prediction. However, it must be noted that almost no measurements at even keel are available for drafts between 9 m and 11.5 m.

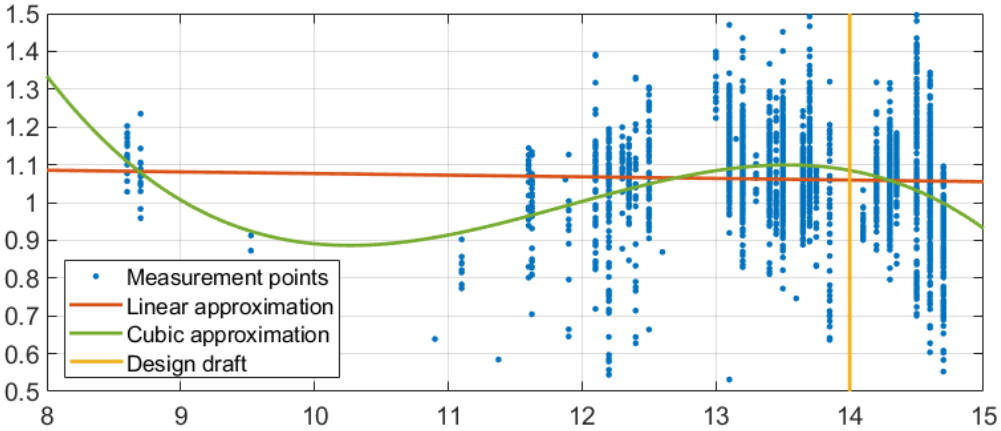

Figure 21: Relation between predicted and measured power over the draft for even keel conditions (Ship 3).

Additionally, in Norsepower (2019), a study analyzing the fuel-saving potential with Flettner rotors on a cruise ferry was presented. ShipCLEAN was used to predict the fuel savings based on the collected weather data while measurement data was used to analyze the actual fuel savings in operation. The difference between the predicted fuel savings from ShipCLEAN and the measured fuel savings was found to be as low as 1.7% (Norsepower (2019)).

In conclusion, despite the few input parameters and no filtering of the measurement data for calm weather or design draft, ShipCLEAN can provide accurate predictions of the propulsion power, when averaged over a longer period. Significant variations in the power relations of single measurement points during a short period were observed for all three ships. One important cause for these variations was identified to be the wave height, which was estimated based on the TWS instead of measurements or hindcast data. Additionally, trim highly influences the prediction accuracy. Apart from the wave heights and the trim, other factors, which were not measured, seem to influence the propulsion power. Such factors could be, e.g., the water depth. It must further be noted that sensor accuracy and measurement uncertainty was not part of this study.

4 Examples of applications and results

This section presents selected applications of the ShipCLEAN model and results obtained to reduce emissions generated from shipping. In Section 4.1 two different ways of speed optimization, one speed profile optimization during a journey and one journey time optimization, are presented. Speed optimization is a simple and economically motivated method of reducing a ship's fuel consumption. Section 4.1 presents how ShipCLEAN can be used to do such study for any cargo ship, existing or newbuild. Section 4.2 presents two approaches for long-term predictions of expected fuel consumption on specified routes with the use of weather statistics. These approaches help quantify the effects of fuel-saving measures, e.g., wind-assisted propulsion or speed optimization, for more than one journey but a full year or lifetime of a ship. The application of wind-assisted propulsion to two ships on three different routes is presented in Section 4.3. Further the design and operation of wind-assisted ships is discussed. Wind-assisted propulsion is widely seen as a suitable measure to reduce fuel consumption. However, sophisticated methods (as included in ShipCLEAN) are necessary to evaluate the potential and challenges of wind-assisted propulsion fully (see Section 1). Finally, Section 4.3 discusses two approaches to design zero-emission ships—one relying fully on wind propulsion and renewable energies and the other focusing on batteries and electrical propulsion. All studies (except the zero-emission ships) are presented in more detail in the appended articles (Paper A-E) and will only be summarized below.

4.1 Speed optimization

The ship speed is the single most important factor for a ship's fuel consumption. Thus, it is important to (i) choose the optimal mode of operation to ensure optimal speeds throughout the journey, and (ii) choose the optimal average speed for a journey. With the help of ShipCLEAN, the speed profile over a journey can be analyzed and optimized concerning the defined weather along the route and a fixed journey time. However, even choosing the correct journey time is important. Naturally, lower speeds (and longer journey times) will reduce fuel consumption; however, the operational costs increase, and the income decreases with longer journey times. Through the unique coupling of a performance prediction model and an economic model, ShipCLEAN can be used to optimize the journey time for maximum profit, i.e., balancing fuel consumption, costs, and income.

Paper A presents a study comparing the fuel consumption of an MR tanker (Ship 4 from Section 3) on a Baltic Sea route with four different modes of operation, i.e., constant propeller torque, constant target speed, constant average speed, and constant rpm. All operational modes resulted in the same journey time and identical routes were used for all modes of operation (no weather routing). The analysis was done using realistic weather conditions (see Paper A for details). The results of the study are shown in Figure 22. The difference between the best (constant target speed) and worst (constant torque) operational mode was found to be about 3%. Certainly, this is not a huge fuel saving but one that is without any economic risk because it does not involve any investments or schedule changes. In analyzing the accumulated fuel consumption and speed profile over the route, it is obvious the best alternative is to operate the ship on as constant a speed as possible. Times with high ship speeds especially lead to high fuel consumption.

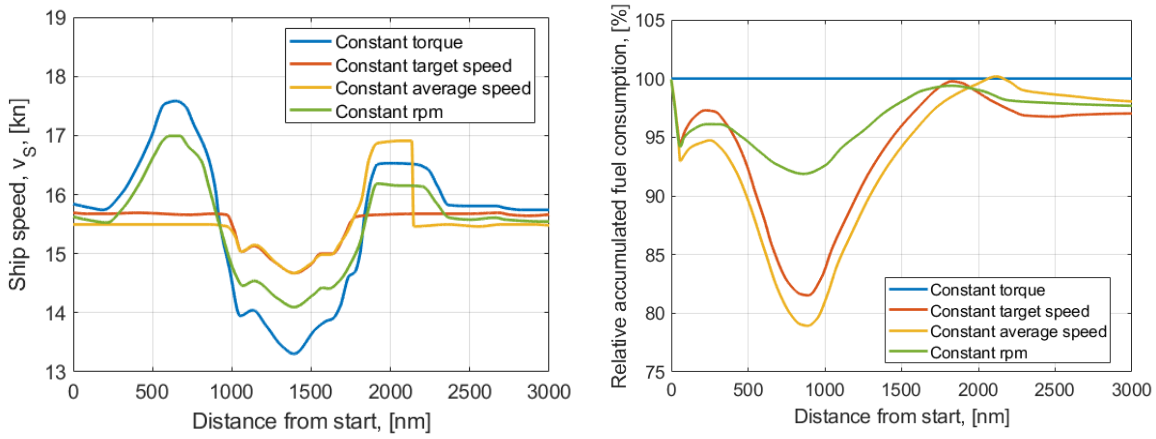

Figure 22: Comparison of different operational modes: (left) ship speed and (right) accumulated fuel consumption (see Paper A).

It can be concluded that it is important to choose the optimal operational mode to minimize fuel consumption. From the results obtained from the study in Paper A, it is concluded that high speeds must be avoided in favor of a constant target speed. Using routing or simulation models (as ShipCLEAN) and weather forecasts, a target speed can be obtained that compensates for areas of rough weather and possible speed loss by choosing a target speed slightly higher than the necessary average speed.

A journey time optimization is presented in Paper D, were the speed of a container ship (Ship 3 from Section 3) is optimized with regards to best profit. Journey time optimizations try to find the best trade-off between reduced fuel consumption as a result of reduced speed with increased operational costs because of longer journey times, which requires the coupling of sophisticated power prediction models with logistical models, as it is available in ShipCLEAN. During the study, a Pacific Ocean crossing was simulated using statistical weather in Monte Carlo simulations to provide reliable long-term predictions of the fuel savings. Journey time optimizations were performed for different fuel prices and two possible route options: the rhumbline, i.e., a constant heading, and the great circle route, i.e., the shortest route. Results from the study are shown in Figure 23 and Figure 24.

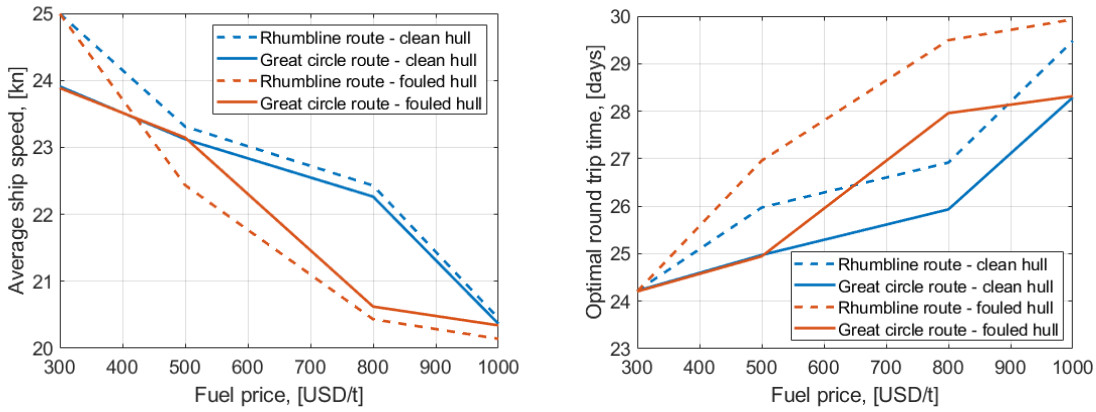

Figure 23: (Left) optimal average speed and (right) optimal round-trip time (right) for two route alternatives, with and without fouling (see Paper D).

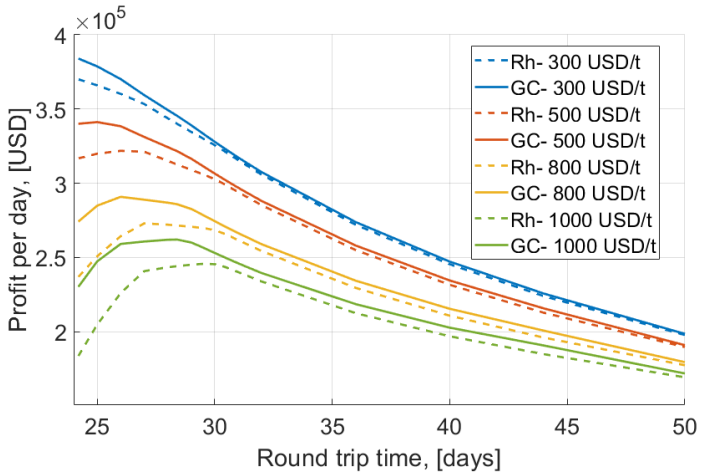

Figure 24: Profit per day for different fuel prices and round- trip times (see Paper D).

As the fuel consumption of ships is roughly proportional to the cube of the ship speed, but operational costs only increase linearly with the journey time, the optimal journey speed naturally decreases with increased fuel prices. The optimal round-trip times increase from about 24 days for both routes with a fuel price of 300 USD/t to about 28 days for the great circle and 29.5 days for the rhumbline route, with a fuel price of 1 000 USD/t. In Figure 24, it is presented that the curves of the daily profits over the round-trip time show wide and flat maxima, meaning there is no distinct optima of journey times but rather a region of favorable journey time. The reduction of the optimal ship speed from about 24 kn to about 20.5 kn with increasing fuel prices (for the great circle route) results in a reduction of emissions by about 6.015 t of CO_2 (about 34%).

The results of this study show the importance of optimizing the ship speed and journey time using a coupled power prediction and transport economics model. It can be concluded that increased fuel prices, e.g., by implementing a bunker levy, lead to reduced ship speeds and thus a considerable reduction of CO_2 emissions.

4.2 Prediction of fuel consumption using statistical weather

To predict long-term fuel savings, it is necessary to simulate many journeys in varying, realistic environmental conditions. Varying environmental conditions can be simulated using statistical distributions and Monte Carlo simulations, as done in papers D and E. To provide the statistical distributions of environmental conditions, two possibilities are discussed in papers D and E: (i) using on-board measurements to estimate statistical distributions and weighting curves for different conditions and (ii) using long-term mean values and standard deviations (i.e., probability density functions) for each waypoint.

The first option, using on-board measurements, is discussed in detail in Paper E on the example of two routes: one Pacific Ocean and one Baltic Sea route. The wind rose plots, i.e., the combination of measured TWA and TWS, are presented in Figure 25.

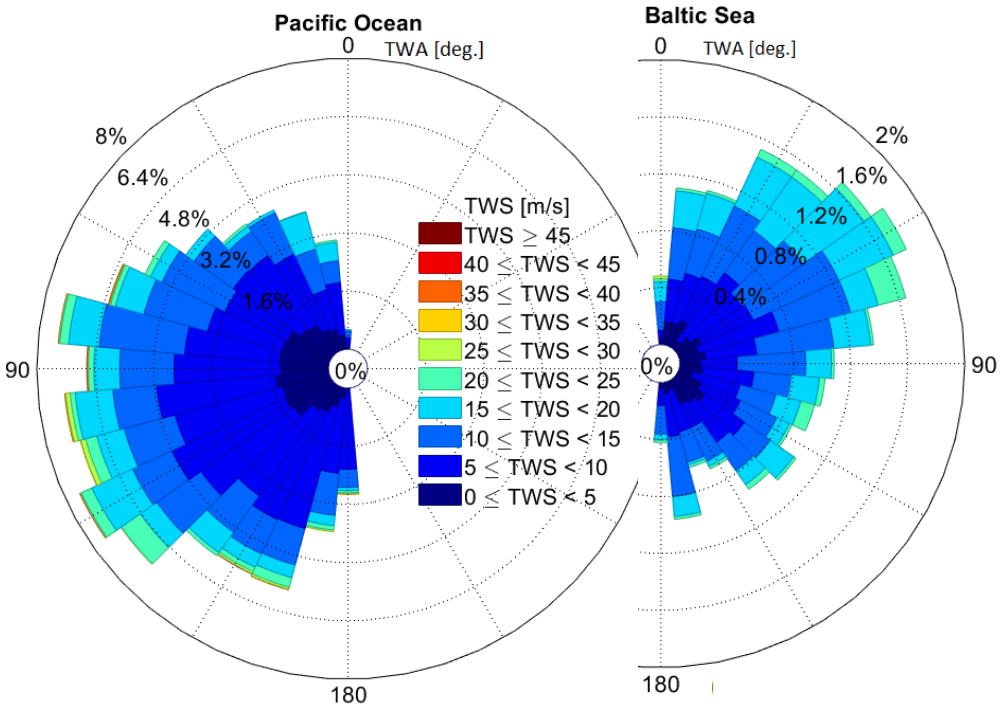

Figure 25: Wind rose plots of the measured TWA and TWS: (left) Pacific Ocean and (right) Baltic Sea (see Paper E).

An important pre-requisite for this method is that the TWS and TWA are not correlated, i.e., that the wind speed is not dependent on the wind direction. For the examples shown in Figure 25, this is the case since the TWS distribution is similar for each TWA region. With this prerequisite fulfilled, probability density functions (pdf) are fitted to the measured TWA and TWS, as presented in Figure 26 and Figure 27. In Paper E, Weibull distributions are chosen for the TWS while the TWA was found to be best represented by Kernel distributions.

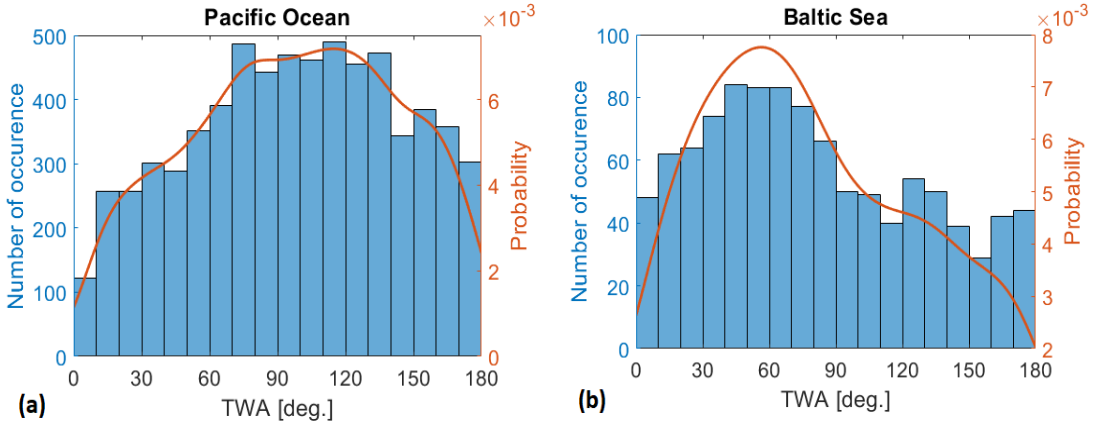

Figure 26: Distribution of the measured TWA: (a) Pacific Ocean, (b) Baltic Sea (see Paper E).

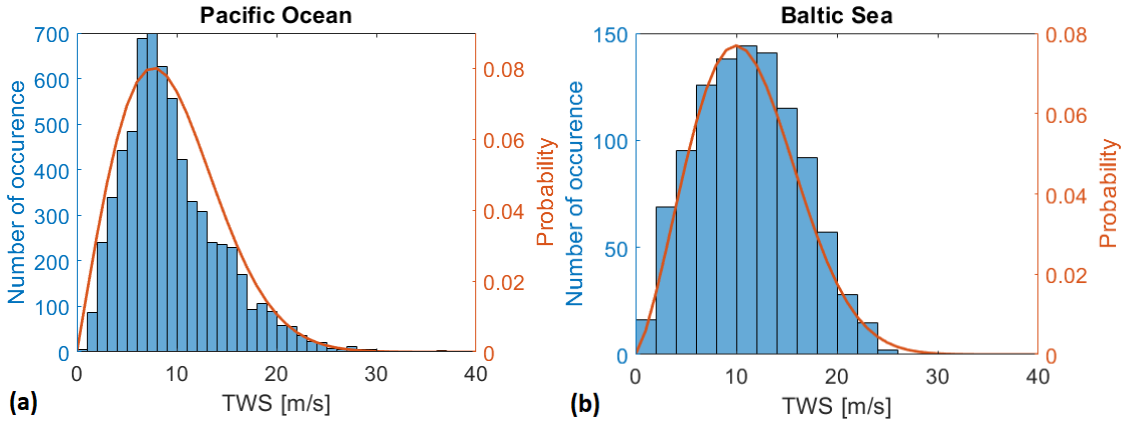

Figure 27: Distribution of the measured TWS: (a) Pacific Ocean, (b) Baltic Sea (see Paper E).

Using the pdf, weights for specified TWA and TWS ranges can be calculated by (with x_1 and x_2 as the boundaries of the specified ranges):

$$w = \int_{x_1}^{x_2} pdf\ dx \,/\, \int_0^{x_{max}} pdf\ dx. \tag{40}$$

The long-term mean value of the fuel consumption can then be evaluated by summing up the estimated fuel consumption for all TWA and TWS combinations that were selected to be representative (i.e., mean values of the specified ranges) multiplied with the weight for the range. As an example, in Paper E, 10 TWA ranges (for a symmetrical case) and five TWS ranges were defined. Thus, only 50 conditions must be simulated, instead of all the 6,000 measurement points that were available from full-scale measurements for one year. The difference between the statistically obtained fuel consumption and the directly evaluated was found to be about 3%. As this method was used to predict the fuel savings from Flettner rotors, this was sufficiently accurate. If the accuracy needs to be higher, more TWA and TWS intervals could be defined, which will increase the accuracy but also the computational effort.

In summary, the presented method gives fast and accurate results for long-term fuel consumption predictions and is based on real, experienced weather on the route. However, one drawback of the method is that only the mean value of the long-term fuel consumption is evaluated. Thus, it is not possible to predict how much the actual consumption might differ

between journeys. A second drawback is that the statistics are only available for journeys where weather observations are available for a long period and not globally.

To also evaluate the standard deviation of fuel savings, it is necessary to evaluate the variation of the weather at each waypoint and to simulate many journeys, which is done in the second option, i.e., long-term mean values and standard deviations for each waypoint. Using global weather statistics, this option can also be used for any arbitrary route. This method is described in detail in Paper D, where the mean value and standard deviation of the TWA and TWS were taken from Onogi et al. (2007). Examples of values are presented in Figure 28 for an Atlantic triangular route (Rotterdam – New York – Houston – Rotterdam).

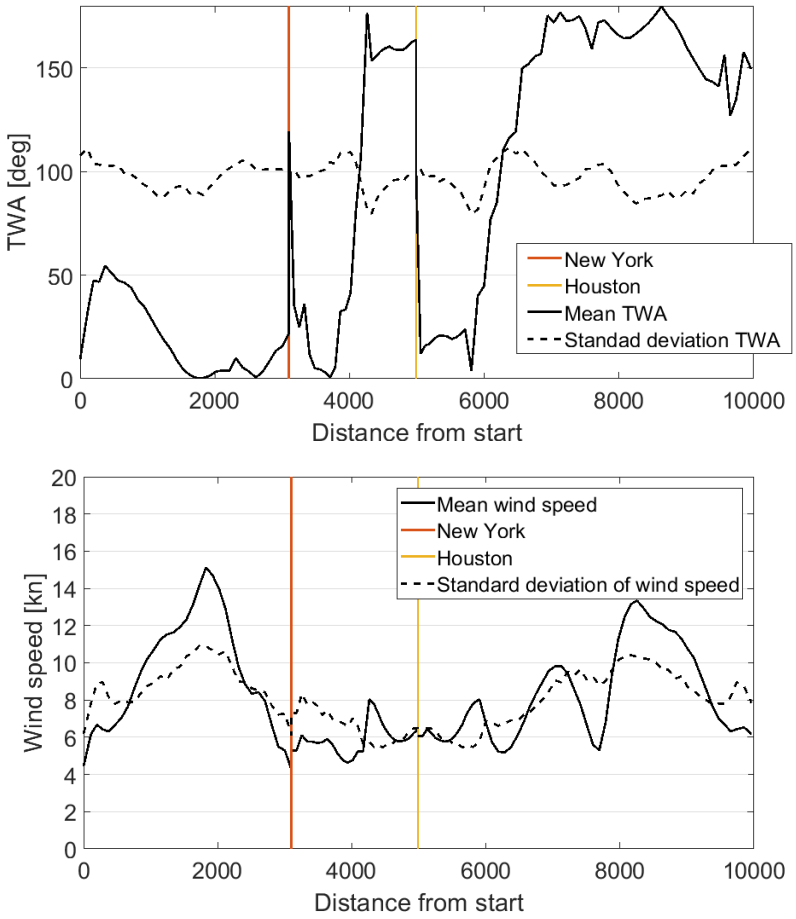

Figure 28: Mean value and standard deviation, (top) TWA, and (bottom) TWS (see Paper D).

If long-term measurement data is available, it could also be used to provide the mean value and standard deviation. However, this would require a measurement campaign stretching over several years on a ship traveling similar routes during the time or on stationary weather buoys on or close to each waypoint. Using the mean values and standard deviations, a pdf for each, the TWA and TWS for every waypoint can be obtained. For this study, Weibull distributions are assumed for the TWS and normal distributions are assumed for the TWA. The distributions for the whole route are presented in Figure 29.

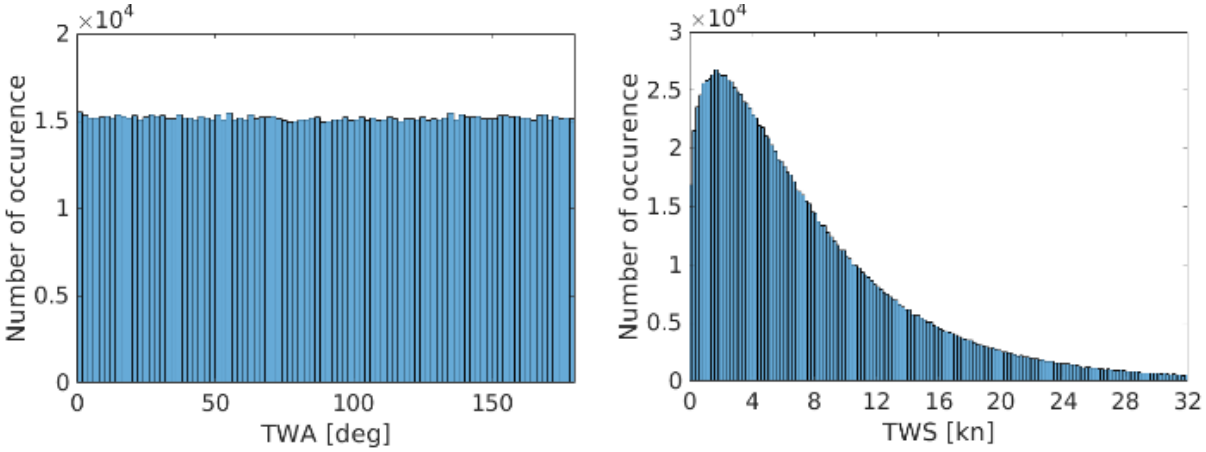

Figure 29: Pdf of the (left) TWA and the (right) TWS for the Atlantic route (see Paper D).

With a pdf for TWA and TWS on each waypoint, Monte Carlo simulations can be performed. In Paper D, 10 000 runs were performed for the whole route using the response surface method presented in Section 2.10. The results of the Monte Carlo simulations are a mean value and a standard deviation, indicating the expected fuel consumption and variation between journeys. Especially the latter, the variation in fuel consumption, is a huge advantage of this method compared to the one presented before. However, the computational effort is significantly higher for this method.

In conclusion, two methods to estimate and use statistical distributions of realistic weather condition are presented. The first, using measurement data and a weighting system, provides low computational effort and thus a quick prediction of the expected fuel consumption while the second, Monte Carlo simulations using distributions at each waypoint, require more computational time but also provide the standard deviation of the fuel consumption.

4.3 Operation, design and analysis of wind-assisted propelled ships

Wind-assisted propulsion is one possible and promising alternative to reducing the emissions from shipping, as discussed in sections 1.2 and 2.7. Using ShipCLEAN, the fuel-saving potential of Flettner rotors were analyzed in two studies: (i) in Paper D, an MR tanker operating in the Atlantic Ocean is equipped with several Flettner rotor arrangements, and (ii) the design and operation of wind-assisted cargo ships, using improved analysis methods, is discussed in Paper E considering a RoRo on the Baltic Sea and an MR tanker on the Pacific Ocean as examples. All examples are evaluated using fixed routes and speeds, i.e., no voyage or speed optimizations were performed.

The first study, presented in Paper D, aims to predict fuel savings from the installation of Flettner rotors on an MR tanker (Ship 4 from Section 3) operating on an Atlantic Ocean trade route (Rotterdam - New York - Houston - Rotterdam), as shown in Figure 30. As a result of the westerly winds on the North Atlantic, this route is not favorable for wind-assisted propulsion, as the Atlantic crossings are in headwind or dead-downwind conditions. Thus, an additional aim was to investigate how much the fuel savings (or penalties) could vary in between journeys. Thus, the second approach from Section 4.2 was used, i.e., Monte Carlo simulations with probability distributions for every waypoint.

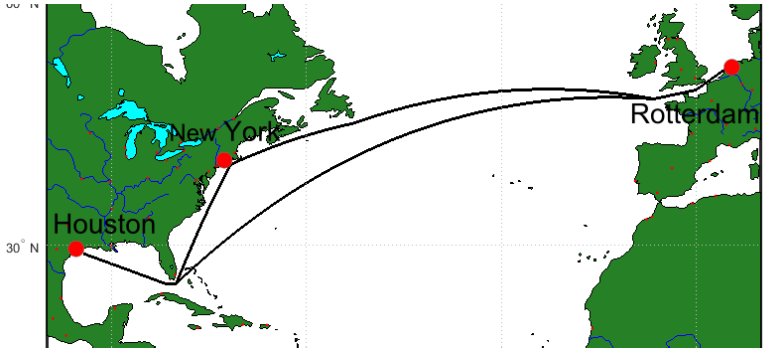

Figure 30: North Atlantic triangular route (see Paper D).

The fuel savings achieved with 1, 2, 4 and 6 Flettner rotors of three different sizes (3m x 18m, 4m x 24m and 5m x 30m) were analyzed. The analyses were done with an earlier version of the wind-assisted propulsion module in ShipCLEAN, which did not account for the interaction in between the sails and the sails and the superstructure. This means the force of the Flettner rotors acts in the geometrical center of the arrangement and that the rpm of the Flettner rotors is not controlled individually. Further, the lift and drag coefficients of the ship sailing at a drift angle were improved, as presented in Paper E. However, the employed methods are already considering 4 DOF, i.e., the additional resistance from drift and rudder angles are accounted for and the heel angle is evaluated to not exceed 10 degrees. In addition to the fuel savings, the payback times assuming three different fuel price scenarios (500 USD/t, 800 USD/t, 1 000 USD/t) were estimated including installation and operational/ maintenance costs (see Paper D for details). Resulting fuel savings and payback times are presented in Figure 31.

Results show that, even on a route with much headwind, fuel savings of more than 12% are achievable with wind-assisted propulsion. As presented in Section 2.7, these results include the propulsion thrust from the sails but also the added power as a result of drift and rudder angles, as well as the added power to rotate the Flettner rotors. With the chosen statistical approach, it is also possible to conclude that the standard deviation of the fuel saving is less than the total fuel saving, meaning that it is not expected that the Flettner rotors increase the fuel consumption of a full journey. Naturally, the payback times of the investment to install Flettner rotors are coupled to the fuel prices. It is also obvious that the payback time is shortest for the arrangements with only one rotor, even though the fuel savings increase with the number of rotors. This occurs because the costs of the Flettner rotors increase linearly with the number. However, the savings do not because of headwind regions and necessary reefing at times.

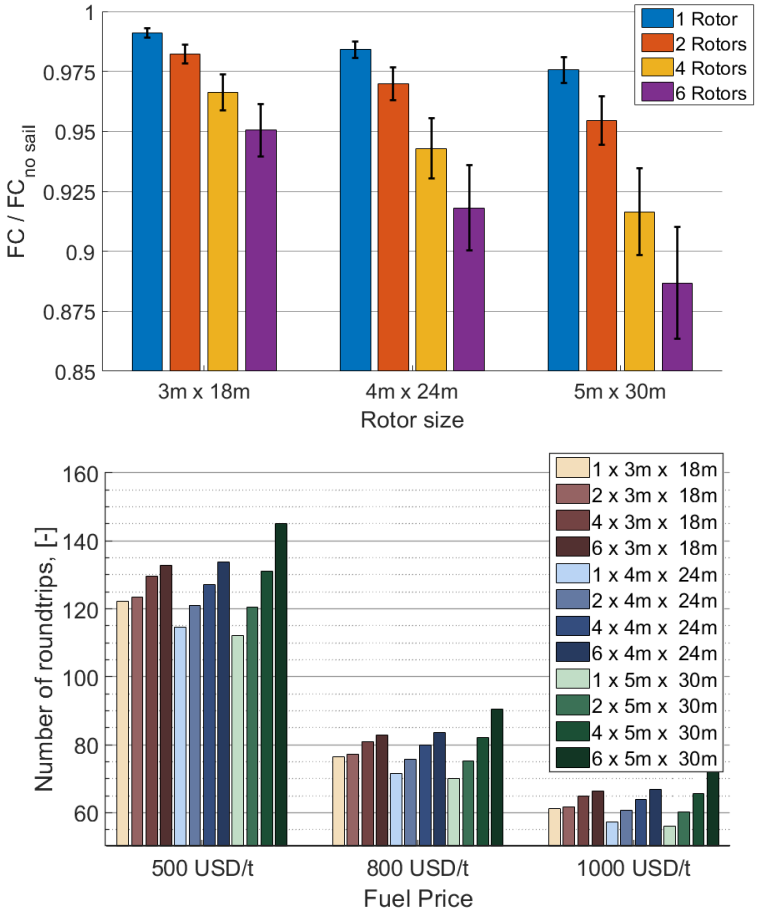

Figure 31: Results from Monte Carlo simulations: (top) fuel savings (including standard deviation) and (bottom) payback times with different arrangements of Flettner rotors on a MR tanker on the Atlantic Ocean (see Paper D).

In Paper E, the wind-assisted propulsion module in ShipCLEAN was extended and improved by improving the lift and drag formulations for a ship sailing at a drift angle, adding sail-sail and sail-superstructure interaction effects, adding the vertical wind speed profile and adding an individual rpm control for the Flettner rotors, see Section 2.7. The rpm control improves the overall performance of the Flettner rotors as it balances the provided propulsion force and the added power to drive the rotors plus added resistance from drift and rudder drag. Additionally, the rpm control aims to achieve the optimal rudder angle by moving the center of the sail force (see Section 2.7 and Paper E for details). As presented in Paper E, the lift, drag and power coefficients were adjusted with the use of full-scale force and power measurements on a Flettner rotor. The versatility of the new wind-assisted propulsion module was, in Paper E, presented on two example ships under realistic environmental conditions: a RoRo (Ship 5 from Section 3) on the Baltic Sea and an MR tanker (Ship 4 from Section 3) on the Pacific Ocean. Details about the ships can be found in Paper E. Figure 32 presents polar plots of the relative fuel consumption ($FC_{with\ sails}/FC_{without\ sails}$) for both ships with four Flettner rotors sailing in 20 kn TWS. The ship speed is defined as 12 kn for the tanker and 18 kn for the RoRo.

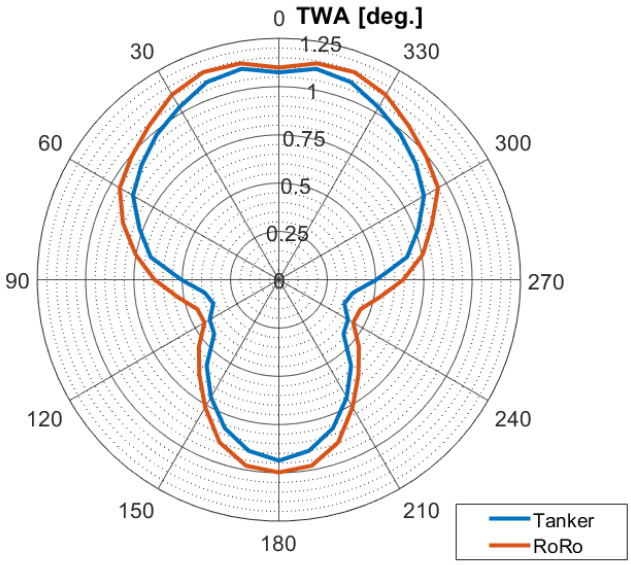

Figure 32: Polar plots of the relative fuel consumption, TWS = 20kn, v_S= 12kn (Tanker), 18kn (RoRo) (see Paper E).

Both ships experience increased fuel consumption with the Flettner rotors when sailing in headwinds up to a TWA of about 30 degrees (tanker) and about 45 degrees (RoRo). The maximum of the fuel consumption increase is about 10% for the RoRo at 15 degrees TWA. However, sailing at a TWA of around 110 degrees, the fuel consumption is decreased by about 65% (tanker) and 55% for the RoRo. With higher wind speeds or more Flettner rotors, both ships could be fully propelled by the Flettner rotors. However, fuel consumption will not become zero because of the required power to rotate the Flettner rotors.

Both ships were tested with different Flettner rotor arrangements, as presented in Figure 33. Arrangements with an identical number of rotors have similar geometrical centers of the rotors. However, because of the interaction effect, the actual center of the side and thrust force will be different for each arrangement. The aim of the study was to investigate the influence of changes of the rotor arrangements and the ship design on the expected fuel savings in realistic weather conditions. As the variation of the fuel saving in between journeys was not relevant for this study and because a lot of different arrangements and designs were investigated, the first option, as presented in Section 4.2, was chosen. In this method, the weighting function for different TWA and TWS ranges are established based on measured weather along the routes. The expected fuel saving is then the weighted sum of fuel savings estimated at the reference wind speeds and directions. The predicted fuel savings are presented in Figure 34 and the payback times assuming different fuel prices are shown in Figure 35.

For the tanker, fuel savings of up to 32% are achievable with six Flettner rotors while three Flettner rotors can give fuel savings of more than 20%. The faster RoRo ship can experience up to 15% fuel saving with four Flettner rotors. The differences between the arrangements with identical numbers of rotors are small and mainly as a result of different rudder loadings. As observed before, the fuel savings do not increase linearly with the number of rotors but the costs do. Thus, the payback times are shortest for the arrangements with the fewest number of rotors. The payback times for the RoRo and the tanker are comparable, between 7-10 years for a fuel price of 325 USD/t, which decreases to 2.5-4 years assuming a fuel price of 760 USD/t.

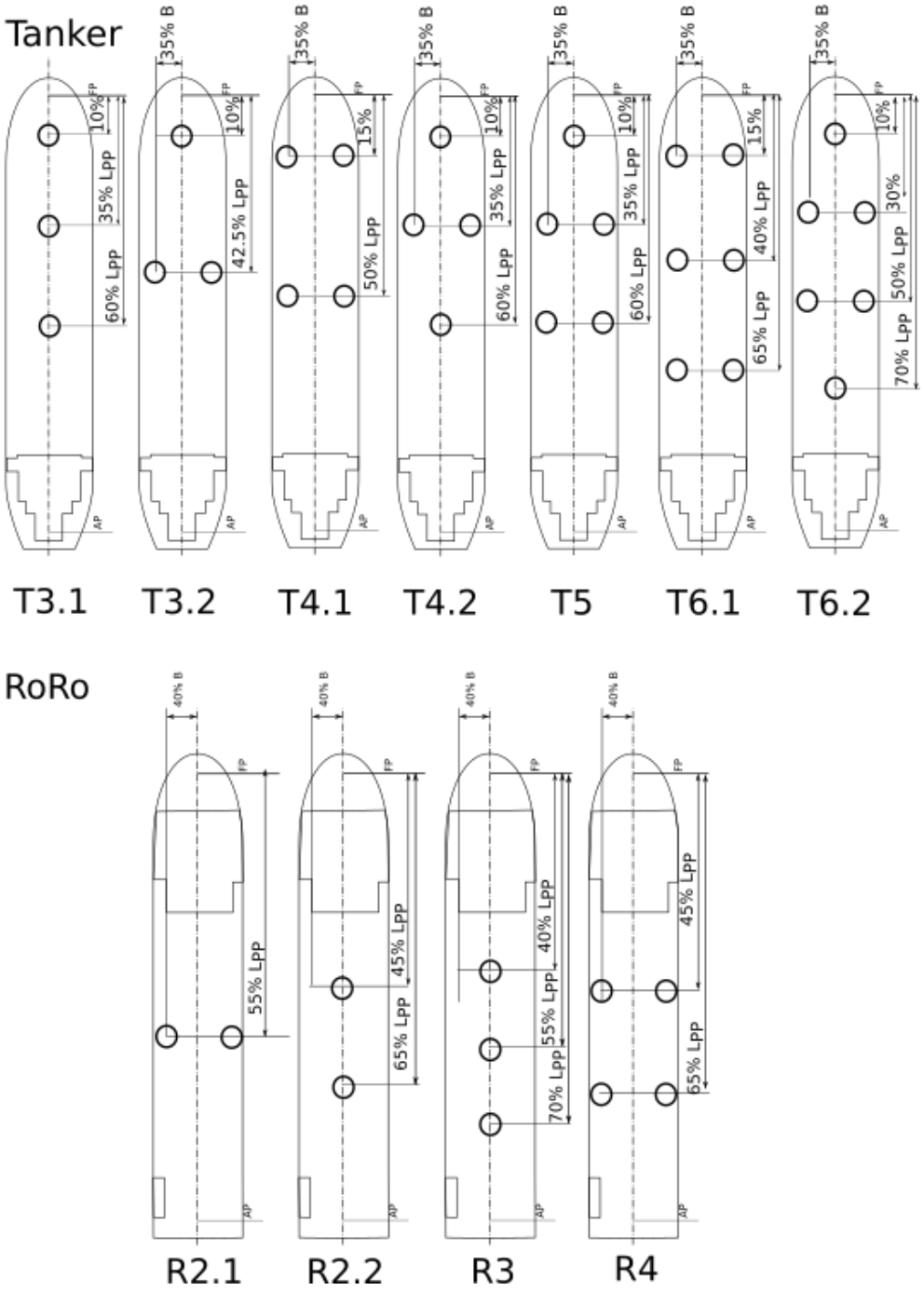

Figure 33: Arrangements of Flettner rotors on (top) the tanker, and (bottom) the RoRo (see Paper E).

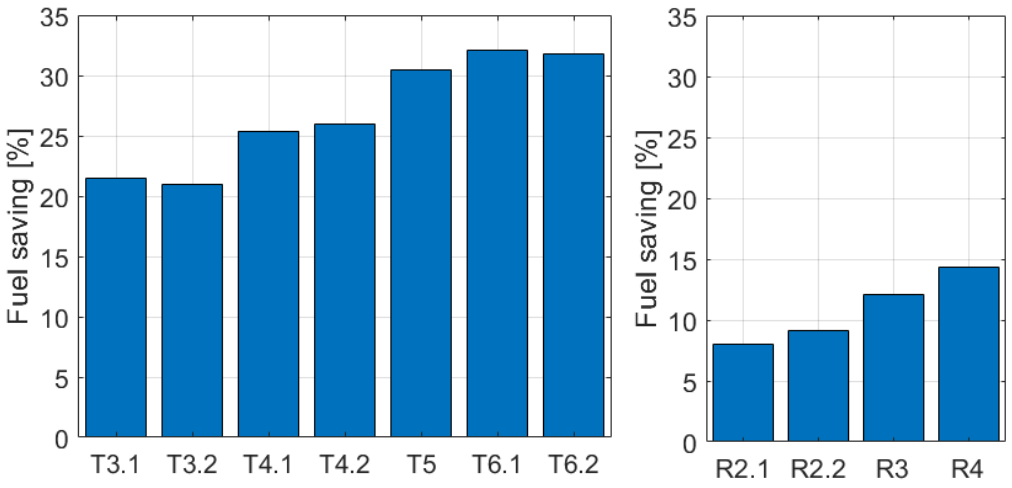

Figure 34: Fuel savings with different sail arrangements: (left) tanker and (right) RoRo (see Paper E).

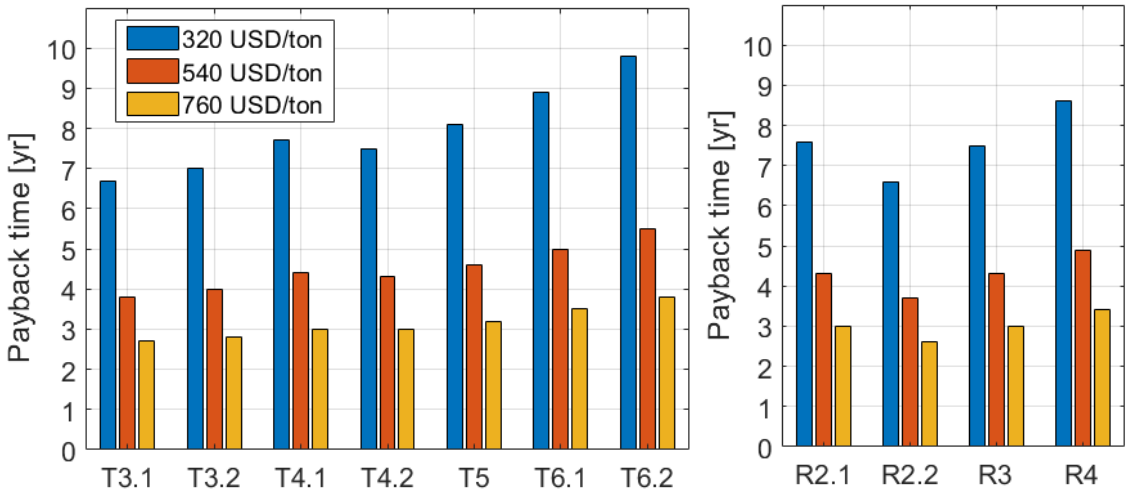

Figure 35: Payback times for different fuel prices, (left) tanker, and (right) RoRo (see Paper E).

In Paper E, it is further discussed how to improve the arrangement of Flettner rotors and ship design in general. It is shown that the optimal positioning of the rotors can increase the fuel savings from 32% to 36% for the tanker (arrangement T6.1) and from 14% to 21% for the RoRo (arrangement R4). Further, it was investigated how adding a keel to both ships and a second rudder to the tanker would influence the fuel savings. For the tanker, the savings increased from 32% to 36% (T6.1). For the RoRo, the increase was from 14% to 17% (R4).

From the studies presented in Paper D and Paper E, it can be concluded that Flettner rotors can provide huge fuel savings under realistic conditions. It was shown in Paper E that the position of the rotors is crucial to maximize the benefits and that special design features like keels and double rudders can further increase the potential fuel savings. It must be noticed that such studies require a flexible white-box model, preferably a Stage I model, such as ShipCLEAN.

4.4 Zero-emission ships

As discussed in Section 1.1, the IMO goals of emission reduction in shipping are only achievable with radical action in ship design and operation. During this thesis work, two studies took emission reduction of ships some steps further and aimed at designing ships with zero emission under operation: (i) the design of a fossil-free operated ship with unlimited range and (ii) the design of a fully electric RoPax ferry. In both studies, ShipCLEAN was used as the design and prediction tool.

In the first study, the development of a fossil-free operated ship is presented in detail by Luis et al. (2020), aiming to design a ship that is powered and operated purely on renewable energy. A sketch of the design that consists of a full block hull shape, six Flettner rotors, two vertical wind axis turbines, 1 780 solar panels (480W each) on the weather deck, a dual-mode propeller for propulsion and power generation, and batteries is provided in Figure 36.

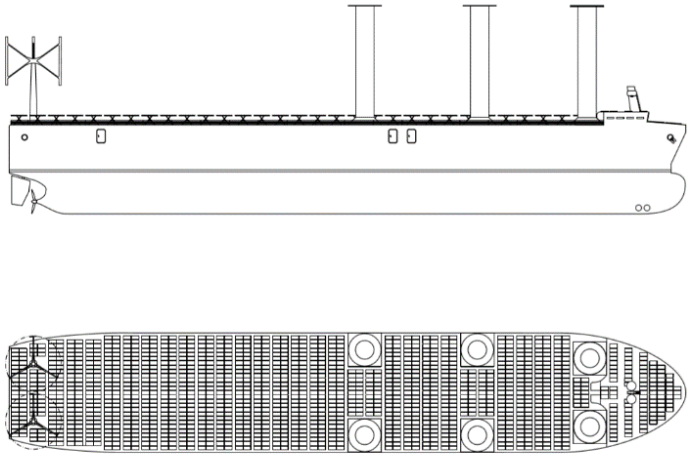

Figure 36: Sketch of the fossil-free operated cargo ship.

In the design and prediction process, ShipCLEAN provides the attained speed and power consumption for all conditions: (i) pure sailing, (ii) in hybrid propulsion, i.e., sailing and electric propulsion, (iii) sailing and hydropower generation, i.e., dual-mode propeller in turbine mode, and (iv) when operated in pure electric propulsion. A detailed description of the operational modes and detailed results are presented in Luis et al. (2020). Generally, results show that, for a route in the Mediterranean Sea, average speeds of up to 7 kn are achievable. However, it was also found that renewable energy production on-board a ship cannot cover the energy consumption of the ship as a result of hoteling and navigational/operational loads.

A conclusion of the study is that fossil-free operation of cargo ships is possible, even for long journeys, but not for unlimited range as a result of on-board consumption, which requires charged batteries at the start of the journey. Considering the advances made in unmanned shipping, the hotel load and other consumption of ships might be reduced in the future, which will possibly lead to reaching the target of developing fuel-free operated ships with unlimited range. A versatile performance prediction model that can model wind-assisted and pure wind-propelled ships is crucial to predict the ship speed, power generation, and power consumption of such ship.

The second study aimed to design a zero-emission, fully electric ferry by using only batteries as energy storage. ShipCLEAN was used in the initial design investigation of the project. Two problems were investigated: (i) what is the achievable range with electric propulsion for different speeds, considering that the deadweight and main dimensions (except the displacement) are kept constant), and (ii) variation of the ship speed considering average weather, turnaround times and speed regulations. For both investigations a quick and accurate Stage I power prediction model is crucial.

The first part is an investigation of the necessary battery weight to achieve a specified range with different ship speeds while considering the increase in propulsion power as a result of the increase in displacement. The main dimensions were kept constant at a length overall of 212 m, beam of 26.7 m, draft of 6.3 m, and a displacement without batteries of 17 400 t. In Figure 37, curves of the power consumption over the displacement are presented for a range of 300 nm together with the installed battery capacity using the battery weight and the initial displacement. The feasible displacements are found at the intersections of the curve for the installed battery capacity and power consumption. It can be seen in Figure 37 that the range of 300 nm is not achievable with a ship speed of 21 kn but is feasible for all other investigated ship speeds.

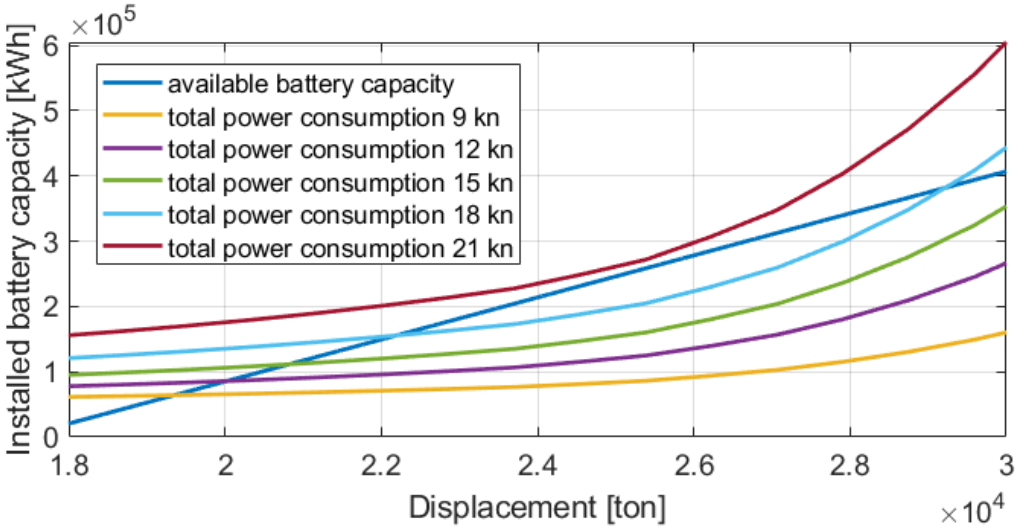

Figure 37: Power consumption over displacement for a 300 nm range and different ship speeds.

In the second study, the ship speed at the open sea leg (speed restrictions were respected at the start and end of the journey) was varied to visualize the effect of the ship speed on the energy consumption and the required charging power. The turnaround time was kept constant at two roundtrips per day during this investigation. Thus, a higher ship speed will lead to longer harbor times. The resulting energy consumption and required charging power are presented in Figure 38.

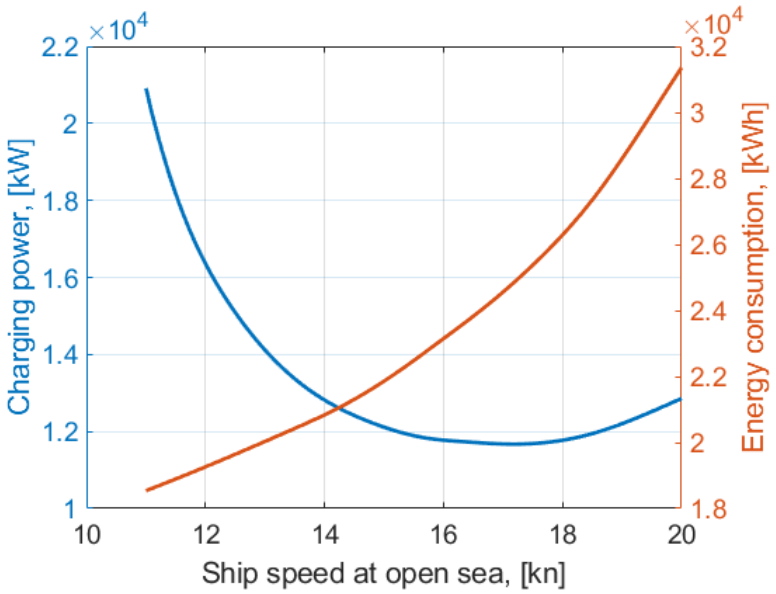

Figure 38: Required charging power and energy consumption over the ship speed on the open sea leg.

From the charging power curve, it can be concluded there is an optimum (about 17 kn) where the best trade-off between low power consumption and long harbor times is obtained. Additionally, with the results presented in Figure 38, it is possible to obtain the minimal ship speed and energy consumption if a maximum charging power limit is introduced, as it would be in reality as a result of power system limitations.

From the two presented studies, it can be concluded that (i) it is possible to design emission-free operated ships, but only for a limited range and (ii) a quick and accurate Stage I power prediction model is crucial for early design simulations and investigations. These early investigations will significantly increase knowledge of the potentials and limitations in a phase of design projects when most of the decisions are made. It is, therefore, crucial to integrate Stage I models, such as ShipCLEAN, in the design process of ships.

5 Conclusions

This thesis presented the development of a novel ship energy systems model, ShipCLEAN, which can predict the propulsion power and fuel consumption of ships under realistic conditions while requiring few input parameters, i.e., main dimensions, ship type, propeller rpm, design speed, and environmental conditions. It was developed to be a pure white box, modularized model, which makes it easy to introduce changes or alternative methods to increase the accuracy or predict the performance of unconventional ships. The model is quick and easy to use, i.e., low computation and set-up times and no calibration of the model is required.

Validation against model- and full-scale measurements showed the prediction accuracy is good, especially considering the few input parameters. It was proven that the predicted propulsion power at design condition is well within 8% from model test results and from long-term averages from full-scale measurements. During the validation study, full-scale measurements included off-design conditions (speed and draft) as well as rough weather (wind speeds above 40 kn), proving that ShipCLEAN can predict the propulsion power in all kinds of service conditions. However, the full-scale validation showed a huge variation in the relationship between measured and predicted power in short times for all ships. The detailed analysis concluded that the origin of these variations arose mainly from ship and environmental data that were not measured but estimated, especially the wave height. A systematic dependency of the prediction accuracy on the trim of the ship was found. Thus, it must be concluded that the influences from trim on the propulsion power must be included in future versions, despite the difficulties discussed in Section 2.4.

It was shown in comparison studies that 4 DOF analysis is necessary once large side forces are introduced into the ship. This is the case for wind-assisted propelled ships and for ships with high windage area, such as PCTC or container ships. As shown in Paper C, the difference between power predictions 1 DOF and 4 DOF methods for a wind-assisted tanker can be as large as 10%.

From a detailed uncertainty analysis, it is concluded that the power prediction from ShipCLEAN is well within 10% from model and full-scale measurement results, which is an accurate prediction considering the limited required input. From the analysis it is concluded that the highest method uncertainties are caused by the prediction of the propulsive coefficients (especially the effective wake) and the added resistance and decreased propulsive efficiency of a ship in waves. Further, it is concluded that to achieve high prediction accuracy, reliable and complete information of the wind speed and direction, wave height and direction, current speed and direction, water temperature, and water depth are more important than detailed information about the ship, e.g., hull form, etc.

A sail module to evaluate the effect of sail-assisted propulsion is included in ShipCLEAN. From application and development, it is concluded that it is crucial to respect 4 DOF for wind-assisted ships and ships with high superstructure areas (e.g., PCTC, container), as well as to model aerodynamic interactions in between the sails and the sails and the superstructure. For power predictions of low windage ships without sails, it is enough to perform 1 DOF simulations, which require substantially less computational time, i.e., about 1/5 of the time for a 4 DOF simulation. Regardless that the interaction effects do not significantly affect the delivered thrust of the sails, they highly affect the longitudinal center of the sail force. From example applications, it is concluded that an individual rpm control of Flettner rotors, considering the local wind speed and angle, is crucial to maximize the effect, especially in beating (around 30-

60 degrees TWA) conditions. Results from applications of Flettner rotors on a tanker and a RoRo show potential long-term fuel saving of up to 30% (tanker) and 15% (RoRo) in realistic weather conditions for routes on the Pacific Ocean (tanker) and the Baltic Sea (RoRo).

The unique coupling of a performance model to an economic model proved to be crucial to identify motivators to reduce the environmental impact. The coupled model also provides the opportunity to easily evaluate payback times of fuel-saving investments. For ship owners and operators, the ultimate motivator for investments is cost savings, with ShipCLEAN it is possible to identify measures to motivate lower speeds and investments in fuel-saving techniques by presenting that the costs for the owners and operators will decrease. In conclusion, the coupling of an economic model and a performance model makes ShipCLEAN a unique workbench to perform new design and retrofitting studies, as well as logistics planning studies, e.g., journey time optimization and route planning.

Several application studies were presented. Generally, it is concluded that a variable Stage I model, as ShipCLEAN, can significantly contribute to reducing the emissions from shipping through improved ship design, improved ship operation, alternative propulsion, and better maritime logistics. It was shown that the correct ship speed, both the average speed over the journey and the instantaneous speed, are crucial to lower fuel consumption and decrease the emissions. Wind assisted propulsion was shown to provide up to 30% fuel consumption reduction for a tanker on a Pacific Ocean trade, with payback times of less than eight years. From the studies, it is concluded that higher fuel prices significantly increase the motivation to decrease the ship speed and invest in alternative propulsion. Finally, studies on zero-emission ships proved that it is possible to design ships that are operated at reasonable speeds and with reasonable operational range without the use of fossil fuels.

6 Future work

As this thesis is about model development, there are many areas where more work and investigations are needed. ShipCLEAN is defined as a pure white-box model, thus no calibration will be done in the model. As shown in Section 3, the prediction accuracy is good with the methods used today. Validation studies show that the predicted power, averaged over a longer time (a journey or a year) in realistic environmental conditions, is well within 10% of full-scale measurements. However, the uncertainty analysis showed there are still some modules and methods in ShipCLEAN that can be improved and modified to further increase the accuracy. Naturally, the functionality of the model can be widened by implementing more couplings and more options to model fuel-saving techniques. This section gives an overview of possible areas for improvement and future extensions/couplings of the model.

Method improvements

Method improvements are always targeted to reduce uncertainties; thus, improvements should be done in modules and methods where high uncertainty was identified (see Section 3). Areas where improvements and further investigations are more impending are the added wave resistance in combination with the reduction in propulsion efficiency and the lift, drag, and CLR of a ship sailing at a drift angle. Performance decrease in waves is a complicated matter not only because there are many effects but also because validation and full-scale measurement is difficult. The development of own methods is naturally not part of the model development of ShipCLEAN, but newly developed methods should be continuously evaluated and integrated. The method to estimate the lift and drag of a ship sailing at a drift angle is based on wing theory. However, with the little data available, some dependencies that should exist in theory, as a dependency on the beam and the block coefficient, could not be established (see Paper E). Particularly, the uncertainties introduced from the prediction of the CLR are potentially large but cannot be quantified exactly (see Section 3). More model test or CFD data is required to further develop today's methods or to develop alternative methods. Further, the ice resistance method is simplified and could be improved, possibly by coupling a more sophisticated model.

The full-scale validation showed the importance of including the influence of trim on the propulsion power. However, the influence from the trim on the resistance and propulsion power is complicated to capture in a generic way since it highly depends on hull form features, e.g. bulb shape and transom immersion. One approach could be to model the bulb effect and the effect from transom immersion individually using the forward and aft draft. A second approach could be to use CFD computations with the standard series hulls.

Wind-assisted propulsion

An important part of ShipCLEAN is the prediction of fuel saving from wind-assisted propulsion. One important step forward would be to extend the sail module to include more sail types than only Flettner rotors. A possible challenge with this development is the fact, that, in contrast to the Flettner rotors, other sail techniques are sensitive to the angle of attack to the sail. This requires analysis of the dynamic effects from ship motions, i.e., rolling and pitching, and thus periodically changing wind angles on the achieved thrust from the sails.

To better model the aerodynamic interactions, methods to predict the circulation and the radius of the tip vortices created by sails (including Flettner rotors) must be included. Such methods could be based on systematic model tests or CFD results.

Couplings

ShipCLEAN is the coupling of a performance prediction model to a transportation economics model. To further increase the model's applicability, more integrations could be realized. There are some obvious areas were specialized model could increase the applicability. ShipCLEAN provides accurate performance and economic predictions in realistic conditions but does not offer the opportunity to perform route optimization. The integration of a specialized routing model would increase the applicability of ShipCLEAN for ship owners and operators.

The integration of a more sophisticated, possibly dynamic, engine model would increase the accuracy and variability of the fuel consumption prediction by, e.g., respecting more environmental conditions for the engine, respecting aging of the engine, modeling alternative fuels, and possibly model engine dynamics.

One focus area during the development of ShipCLEAN was wind-assisted propulsion. Sails introduce large external forces into the ship, which are captured hydrodynamically by performing (static) 4 DOF analyses and aerodynamically by respecting the interaction of the sails. Further areas of interest would be to investigate the ship's structural response because of the side forces acting on the ship from the sail foundation. Coupling ShipCLEAN to structural analysis software, e.g., FEM software, would provide the opportunity to investigate these interactions. External forces will also influence the ship's motions (especially rolling) and the ship's motions will, in turn, influence the sails' performance as the apparent wind angle will fluctuate periodically, especially as a result of rolling. Thus, the coupling of ShipCLEAN to a ship motion model/software would offer opportunities to interesting studies for wind-assisted propulsion in real-life conditions.

Prediction of the environmental conditions

As discussed in Paper E and Section 3.2, the largest uncertainties in the performance prediction with ShipCLEAN are in the prediction of the environmental conditions the ship is operating in, especially the waves. The weather data available from the full-scale measurements, and in the study presented in Paper E, lack information about the wave height and direction. Wave statistics cosupled to the wind direction and strength or hindcast data of the wave height and direction must be included in the model (apart from the wind data available now) to increase the accuracy. Alternatively, the wave height estimation must be coupled to more parameters than only the wind speed, e.g., the geographical position of the ship, the water depth, the wind speed profiles over time, and more.

Application

Further, as for any model development, the model's application is important. Both for validation and development purposes but also to contribute and make an impact on the way towards greener shipping, better ships, and fewer emissions.

7 References

Abbot, I.H., Von Doenhoff, A.E. (1959). Theory of Wing Sections. Mineola, N.Y.: Dover Publications.

Akima, H. (1974). A method of bivariate interpolation and smooth surface fitting based on local procedures. *Communications of the ACM, 17(1)*: 18–20.

Aldous, L. (2015). Ship operational efficiency: performance models and uncertainty analysis [Dissertation]. London, UK: University College London.

Ballnii, F., Ölcer, A. I., Brandt, J., Neumann, D. (2017). Health costs and economic impact of wind assisted ship propulsion. *Ocean Engineering, 146(1)*: 477-485, DOI: 10.1016/j.oceaneng.2017.09.014.

Bertram, V., Wobig, M. (1999). Simple empirical formulae to estimate main form parameter. *Schiff Hafen. 11(1)*:118–121.

Bialystocki, N., Konovessis, D. (2016). On the estimation of ship's fuel consumption and speed curve: a statistical approach. *Journal of Ocean Engineering and Science, 1(1)*: 157-166.

Blendermann, W. (1994). Parameter identification of wind loads on ships. *Journal of Wind Engineering & Industrial Aerodynamics, 51(1)*: 339-351.

Bøckmann, E. (2015). Wave Propulsion of Ships [Dissertation]. Trondheim, Norway: NTNU, 2015:16, ISSN 1503-8181.

Calleya, J. (2014). Ship Design Decision Support for a Carbon Dioxide Constrained Future [Dissertation]. London, UK: University College London.

Epps, B.P., Stanway, M.J., Kimball, R.W. (2009). OpenProp: an open-source design tool for propellers and turbines. Proceedings of Propellers and Shafting 2009, Sept 15th – Sept 16th, Williamsburg, VA: Crown Plaza.

Faltinsen, O.M., Minsaas, K.J., Liapis, N., Skjordal, S.O. (1980). Prediction of resistance and propulsion of a ship in a seaway. *Proceedings of the 13th Symposium on Naval hydrodynamics.*

Hansson, J., Månsson, S., Brynolf, S., Grahn, M. (2019). Alternative marine fuels: Prospects based on multi-criteria decision analysis involving Swedish stakeholders. *Biomass and Bioenergy, 126(1):* 159-173, DOI: 10.1016/j.biombioe.2019.05.008.

Hollenbach, K.U. (1998). Estimating resistance and propulsion for single-screw and twin-screw ships. *Ship Technology Research. 45(2)*: 72-76.

Holtrop, J. (1977). A statistical analysis of performance test results. *ISP, 24(270)*: 23-28, DOI: 10.3233/ISP-1977-2427001.

IMO (2018). [Online]. Available: http://www.imo.org/en/OurWork/Environment/PollutionPrevention/AirPollution/Pages/GHG-Emissions.aspx. [Assessed 2020-03-02].

Inoue, S., Hirano, M. (1987). A practical calculation method of ship maneuvering motion. *International Shipbuilding Progress, 28(325)*, DOI: 10.3233/ISP-1981-2832502.

ITTC (1999). 1978 ITTC Performance Prediction Method. ITTC recommended procedure, Procedure Number 7.5-02-03-01.4.

ITTC (2014). Speed and Power Trials, Part 2, Analysis of Speed/Power Trial Data. ITTC-Recommended Procedures and Guidelines, 7.5-04-01-01.2 Appendix D2. Available from: http://ittc.info/media/1936/75-04-01-012.pdf.

van der Kolk, N., Bordogna, G., Mason, J., Desprairies, P., Vrijdag, A. (2019). Case study: Wind-assisted ship propulsion performance prediction, routing, and economic modelling. *In Power&Propulsion Alternatives for Ships*, London, UK, 22-23 January 2019.

Kracht, A.M. (2000). Gegenläufige Propeller (german*). Handbuch der Werften 25(1)*: 115–145.

Kristensen, H.O., Lützen, M. (2012). Prediction of resistance and propulsion power of ships. Project no. 2010-56, Report No. 04. Copenhagen: Technical University of Denmark.

Li, Z., Ringsberg, J.W., Rita, F. (2019). A voyage planning tool for ships sailing between Europe and Asia via the Arctic. *Proceedings of the International Conference on Ships and Offshore Structures ICSOS 2019*, Melbourne, Flordia, USA, 04-07 November.

Liu, S., Shang, B., Papanikolaou, A., Bolbot, V. (2016). Improved formula for estimating added resistance of ships in engineering applications. *Journal of Marine Science and Application. 15(1)*: 442–451.

Lu, R., Turan, O., Boulougouris, E., Banks, C., Incecik, A. (2015). A semi-empirical ship operational performance prediction model for voyage optimization towards efficient shipping. *Ocean Engineering, 110(1)*: 18-28.

Luis, E., Tillig, F., Ringsberg, J.W. (2020). Concept design and performance evaluation of a fossil free operated cargo ship with unlimited range. Accepted for the *International INNOV'SAIL2020* conference, 15-17 June, Gothenburg, Sweden.

MAN (2015). CEAS Engine Calculations. Available at: http://marine.man.eu/two-stroke/ceas [Accessed: 2015-12-10].

MAN (2013). Basic Principles of Ship Propulsion. Report, MAN, Denmark, 2013.

Mathworks (2020). Matlab Documentations. [Online]. Available at: https://www.mathworks.com/help/matlab/. [Accessed: 2020-03-01].

Mermeris, D., Vassalos, D., Dodworth, K., Sfakianakis, D. (2011). Dynamic energy modeling - a new approach to energy efficiency and cost effectiveness in shipping operations. Low Carbon Shipping Conference, London, UK, 22-24 June 2011.

Minsaas, K., Falkinsen, O.M., Persson, B. (1983). On the importance of added resistance, propeller immersion and propeller ventilation for large ships in a seaway. *Proceedings of the 2nd international symposium on practical design in shipbuilding.*

Norsepower (2019). Viking Grace Rotor Sail Performance analysis results. Norsepower, Helsinki, Finland, Available: https://7c859085-dddb-4d30-8667-a689091113a8.filesusr.com/ugd/cea95e_a721091625ee452db73c9fb69804268e.pdf.

van Os, J. (2018). The Digital Twin throughout the Lifecycle. SNAME Maritime Convention, 24-27 October 2018, Providence, Rhode Island, USA.

Psaraftis, H.N. (2019). Speed Optimization for sustainable shipping. In: Sustainable shipping: a cross-disciplinary view, H.N. Psaraftis, Ed., Springer.

Rehmatulla, N., Parker, S., Smith, T., Stulgis, V. (2015). Wind technologies: Opportunities and barriers to a low carbon shipping industry. *Marine Policy, 75(1)*: 217–226, DOI: 10.1016/j.marpol.2015.12.021.

Schneekluth, H., Bertram, V. (1998). Ship Design for Efficiency and Economy. Oxford: Butterworth-Heinemann.

SSPA (2020). "Skin Friction Database". [Online]. Available at: https://www.sspa.se/tools-and-methods/skin-friction-database. [Accessed: 2020-03-10].

Talluri, L., Nalianda, D., Giuliani, E. (2018). Techno economic and environmental assessment of Flettner rotors for marine propulsion. *Ocean Engineering, 154(1)*: 1-15, DOI: 10.1016/j.oceaneng.2018.02.020.

Taskar, B., Koosup Yum, K., Steen, S., Pedersen, E. (2016). The effect of waves on engine-propeller dynamics and propulsion performance of ships. *Ocean Engineering, 122(1)*: 262-277, DOI: 10.1016/j.oceaneng.2016.06.034.

Tillig, F. (2017). A Generic Model for Simulation of the Energy Performance of Ships- from Early Design to Operational Conditions [Licentiate thesis]. Gothenburg, Sweden: Chalmers University. Report No. 2017:02.

UNCTAD (2019). Review of maritime transport. United Nations, Geneva, ISSN 0566-7682.

Varelas, T., Archontaki, S., Dimotikalis, J., Turan, O., Lazakis, I., Varelas, O. (2013). Optimizing Ship Routing to Maximize Fleet Revenue at Danaos. *Informs Journal on Applied Analytics, 43(1),* 37-47, DOI: 10.1287/inte.1120.0668.

Vinther Hansen, S. (2011). Performance Monitoring of Ships [Dissertation]. Copenhagen, Denmark: Technical University of Denmark.

Viola, I. M., Sacher, M., Xu, J., Wang, F. (2015). A numerical method for the design of ships with wind-assisted propulsion, *Ocean Engineering, 105(1),* 33-42, DOI: 10.1016/j.oceaneng.2015.06.009.

Zuhal, L. R. (2001). Formation and Near-field Dynamics of a Wing Tip Vortex [Dissertation]. Pasadena, California: California Institute of Technology.